Dissimilar joining of Carbon/Carbon composites to Ti6Al4V and copper by reactive resistance spot welding

by

Ali Akbar Shokati

A thesis
presented to the University of Waterloo
in fulfillment of the
thesis requirement for the degree of
Master of Applied Science
in
Mechanical and Mechatronics Engineering

Waterloo, Ontario, Canada, 2017

AUTHOR'S DECLARATION

I hereby declare that I am the sole author of this thesis. This is a true copy of the thesis, including any required final revisions, as accepted by my examiners.

I understand that my thesis may be made electronically available to the public.

Abstract

This study aims to develop an innovative and user-friendly method for dissimilar joining of the carbon/carbon (C/C) composites to Ti6Al4V and copper through reactive resistance spot welding to form the hybrid structures. The C/C composites used in this study were a 2D C/C composite with high porosity (low strength) and a 3D C/C composite with low porosity content (high strength). It was found that the infiltration of Ti into the C/C composite and formation of a continuous thin TiC layer at the interface of the joints are the dominant mechanisms of the joining. The 2D C/C composite with the flat surface was successfully joined to Ti6Al4V due to the infiltration of the melted Ti6Al4V into the porosity of the 2D C/C composite. On the other hand, it was required to drill the rectangular grooves on the surface of the 3D C/C composite to facilitate the infiltration of the melted Ti into the 3D C/C composite and consequently obtain high strength joints. The strength of 2D C/C composite-Ti6Al4V joints was 7 MPa due to failure of the joints within the low strength 2D C/C composite. By contrast, the maximum strength of the joints using the groove-patterned high-strength 3D C/C composite was 46.14 ± 3.92 MPa. In the case of joining between the 2D C/C composite and copper, the Ti thin sheet and Ti powder interlayers were used. Regarding the joints with the Ti sheet interlayer, some defects and cracks were formed at the interface of the joints, which decreased the strength of the joints, whereas in the case of using the Ti powder interlayer, defect-free joints were obtained.

Acknowledgements

I would like to express my greatest appreciation to my supervisors, Prof. John Z. Wen and Prof. Norman Y. Zhou for their consistent support, guidance and immense knowledge.

I would like to express my gratitude to the examining committee members, Prof. Adrian Gerlich and Prof. Hossein Sojoudi for their thoughtful questions and precious comments on my thesis.

I am really grateful to Dr. Ehsan Marzbanrad for his invaluable support, suggestion and recommendation.

I am thankful to my friends and colleagues in Centre for Advanced Materials Joining (CAMJ) and Laboratory for Emerging Energy Research (LEER) for their friendship and support.

Many of the activities involved in this work required the assistance of some technical staff in the Mechanical and Mechatronics Engineering Department, and I am indeed grateful to Mark Griffith in the Materials Testing Laboratory and Phil Laycock and Andrew Urschel in the Engineering Student Machine Shop.
The financial support from the Natural Sciences and Engineering Research Council (NSERC) is highly appreciated.

Words are definitely inadequate in offering my thanks to my beloved Parents, for their unconditional love, support and motivation. My very special thanks go to, my brothers Mostafa and Mohammad, and my sister Maryam for their love and continuous encouragement from miles away.

Dedicated to

My beloved parents, my sister and my brothers

Table of Contents

List of Figures

List of Tables

List of Abbreviations

Abbreviations	Explanation
2D C/C composite	2 Dimensional Carbon/Carbon composite
3D C/C composite	3 Dimensional Carbon/Carbon composite
C/C composite	Carbon/Carbon composite
CNTs	Carbon Nanotubes
CTE	Coefficient of Thermal Expansion
CVI	Chemical Vapor Infiltration
EDS	Energy Dispersive X-ray Spectroscopy
GIXRD	Grazing Incidence X-Ray Diffraction
MWCNTs	Multiwall Carbon Nanotubes
PIP	Polymer Infiltration and Pyrolysis
PVD	Physical Vapor Depositions
RRW	Reaction Resistance Welding
SEM	Scanning Electron Microscope
SEM-BSE	Scanning Electron Microscope-BackScattered Electron
SHS	Self-Propagated High-Temperature Synthesis
VCS	Volume Combustion Synthesis
XRD	X-Ray Diffraction

Chapter 1
Introduction

C/C composites are well known as a promising material for high temperature applications due to a number of factors including their low density, small coefficient of thermal expansion (CTE), high thermal stability, good ablation and thermal shock resistances, and high strength-to-weight ratio at elevated temperatures [1-6]. As a result, C/C composites are expected to be widely used in automotive, aerospace and other high temperature operation fields to manufacture turbine engine components, heat shields, brakes, nozzles, hot press dies, light weight heat rejection systems, and high temperature furnaces [2, 7-16]. One of the most essential requirements for implementing C/C composites at high temperatures is to join them with other materials such as TiAl, copper, and Ti6Al4V [8, 14, 17-23]. In many advanced applications, C/C composites must be joined to Ti6Al4V that is extensively used to construct high temperature components due to its low density, special strength, and excellent high temperature chemical and physical properties [17, 19-21, 24]. In lightweight heat rejection system applications, C/C composites, as a plasma facing components, are required to be joined to structural metallic heat sink materials, like Cu [14-16, 25].

1.1 Motivation

In recent years, a variety of procedures such as mechanical fastening, adhesive bonding, diffusion bonding, and brazing have been utilized for the integration of C/C composites [2, 9, 11, 17, 24, 26]. In the case of joining C/C composites by brazing and adhesive bonding, the joints cannot withstand high temperature applications [2, 10, 24]. For instance, brazing materials normally have low melting points and cannot withstand high operation temperatures [2, 24]. Diffusion bonding, on the other hand, requires a long procedure time, high pressure, and high temperature up to 1700 °C. However, treatment of C/C composites in such a situation causes the deterioration of their properties [2, 24]. Regarding mechanical fastening, the integration of C/C composites by mechanical bolts negatively affects the mechanical properties of the C/C composites as a result of stress concentration in the area close to the holes of the bolts [2, 10].

To avoid the shortcomings of the aforementioned techniques, joining of the C/C composite to metals without using a low-melting-point braze interlayer is considered to be preferable. In the first place, joining of C/C composites to other components by conventional fusion welding techniques seems to be impossible for three reasons. First, C/C composites are not melted at the welding temperature due to

the high melting point of carbon. Second, some materials like copper have a high wetting angle on the C/C composite, which does not allow direct joining of the C/C composites to Cu. Third, a high residual thermal stress is induced at the interface of the joint caused by the difference in the coefficients of thermal expansion (CTE) of the joint components. Therefore, the joints have a strong tendency to crack along the interface of the joints, which consequently leads to deterioration of the joints [11, 27-30]. However, the literature on reactive brazing of C/C composites reveals that, while the braze alloys contain Ti as the reactive element, the reaction between Ti and solid carbon results in a robust bonding between braze material and the C/C composite [2, 10, 31-39]. Moreover, formation of the carbide layer at the interface can decrease the interfacial tension, and consequently improve the wettability of the molten phase on the C/C composite [33-37]. Regarding the residual stress at the interface of the joint, it has been reported that infiltration of the melted metal phase into the pores of the C/C composite is beneficial to increase the mechanical strength of the joints via pinning effect [10, 11, 28, 40, 41]. Furthermore, previous investigations on the joining of dissimilar materials have shown that using surface patterned structures such as surface puncturing and wave pattern interface are promising approaches to regulate the thermal residual stress at the interface of the joint [11, 27-30, 42-44]. The patterned interface decreases the residual shear stress, as well as induces the compressive normal stress at the interface of the joints. This kind of stress field is beneficial to suppressing interfacial cracks. In addition, the patterned surface causes enlarging of the joining area as well as pins the interface of the joints, which are favorable to the mechanical strength of the joints [11, 27-30, 42-44]. The same approach can be employed for dissimilar joining of the C/C composite to Ti6Al4V and copper using the reactive resistance spot welding technique. The solid-liquid reaction between melted titanium and solid carbon can form a chemical bonding at the interface of the joint. Lastly, the infiltration of melted metal into the porosity or groove-patterned surface of the C/C composites can form a mechanical occlusion between the joining components, which tightly pins the interface of the joint.

1.2 Objectives and novelties

According to the literature, dissimilar joining of the C/C composites to other metals by using the reactive resistance spot welding has not been investigated. The major aim of this study is to introduce the reactive resistance spot welding technique and develop an innovative and user-friendly method for dissimilar joining of C/C composites to Ti6Al4V and Cu. This process has been found to be incredibly feasible, cost-effective, very fast (in millisecond range), and easy to scale up for industrial applications and mass production. The two different C/C composites used in this study were an inexpensive multi-

ply 2D woven C/C composite with high porosity content (low strength) and 3D C/C composite with low porosity content (high strength). The joining of the 2D and 3D C/C composites to Ti6Al4V and joining of the 2D C/C composite to Cu were studied. In the case of using the 2D C/C composite, feasibility of direct joining of the flat 2D C/C composite to Ti6Al4V and Cu were investigated. Regarding the joining of 3D C/C composite to Ti6Al4V, four rectangular grooves were machined on the surface of 3D C/C composites to facilitate the infiltration of the melted Ti into the 3D C/C composite. The obtained joints in the study can be considered as appropriate candidates for many advanced high temperature application such as heat shields, nozzles, turbine engine components, and high temperature furnaces. The major objectives in this work are as follows:

- For the first time, investigating the feasibility of using the reactive resistance spot welding as an innovative and user-friendly method for dissimilar joining of C/C composites to metals.
- Finding the optimized parameters, as well as required surface modification to join the 2D and 3D C/C composite to Ti6Al4V and copper through reactive resistance spot welding.
- Obtaining the joints without interlayer or with high melting point interlayer, which can be used at high temperatures applications.
- Investigating the effects of the Ti interlayer in the forms of Ti thin sheet or Ti powder on the microstructure and strength of the 2D C/C composite-copper joints.
- Investigating the mechanism of the joining, microstructure, mechanical strength and interfacial compositions at the interface of the joints through various characterization techniques such as SEM, EDS, XRD, GIXRD and compressive shear test.

1.3 Organization of the thesis

The current work is subdivided into seven chapters.

Chapter 2 provides background information regarding the reactive joining and the parameters, which affect the quality of the joints. Moreover, in this chapter, different techniques and their parameters for similar and dissimilar joining of C/C composites are discussed.

Chapter 3 discusses the materials, experimental methods and equipment used in the current study.

In Chapter 4, the feasibility of the direct dissimilar joining of the flat surface 2D C/C composite to Ti6Al4V is discussed. The aim of this chapter is to investigate the effects of the welding current on

the strength and area of the joints. Furthermore, the mechanisms of the joining and the effects of the open porosity of the 2D C/C composite on the quality of the joints are discussed.

In chapter 5, the feasibility of joining the groove patterned 3D C/C composite to Ti6Al4V is studied. In this chapter, in order to facilitate the infiltration of the melted metal into the 3D C/C composite, the rectangular grooves were machined on the surface of 3D C/C composites. Moreover, the effects of the dimension of the rectangular grooves on the strength and fracture mode of the joints are investigated.

Chapter 6 includes dissimilar joining of the flat surface 2D composite to copper by using the different Ti interlayers. Three different interlayers in the forms of Ti thin sheet and powder were used and the effects of different interlayers on the microstructure and strength of the joints are investigated.

Chapter 7 lists the major conclusions and provides recommendations for future research.

Chapter 2
Literature review

This chapter provides background information regarding the reactive joining and the parameters, which affect the quality of the joints. Moreover, different techniques and their parameters for similar and dissimilar joining of C/C composites are discussed.

2.1 Reactive joining

Combustion or reactive joining is a promising technique for joining of similar and dissimilar materials that is not possible to join them by conventional techniques. Reactive joining has been utilized for similar and dissimilar joining of the C/C composites and other ceramics by using a variety of reactive mixtures such as NiAl, pure Ti, Ti–Al–C, Ti-C,Ti-Al, Ni-Ti-C, Ti–Al–C–Ni, Ti–Si–C, etc. [2, 8, 45-51]. In this technique, the reactive interlayer is ignited by an external source to release a significant heat and make a joint between two surfaces. In this section, different reactive joining methods for dissimilar and similar joining of refractory materials are introduced and important parameters, which affect the quality of the joints are discussed.

2.1.1 Motivation for dissimilar joining

Design engineers are increasingly interested to join dissimilar materials, as they are looking creative new structures. Joining of dissimilar materials has a high potential for applications including light-weight automotive structures, energy production industries, next generation medical products and military applications [45, 46]. Possibility of using reactive joining procedures for joining of a wide range of materials like joining of C/C composite to C/C composite, C/C composites to TiAl, NiAl to Ni-based superalloy, NiAl to Fe, NiCrAlY to Ni-based super-alloy, SiC to Ni-based super-alloys, SiC to aluminum alloy, etc. has been widely studied [45, 46, 52]. The results of these studies showed that reactive joining is a promising technique for similar and dissimilar joining of a wide range of refractory materials.

2.1.2 Challenges and solutions for dissimilar joining

There are some challenges to join dissimilar materials as a result of large differences in their structural and physical properties like difference in melting point, thermal conductivity and coefficient of thermal

expansion (CTE). A large difference in properties can cause high residual stress at the interface of the joints which results in decohesion/delamination at or near the interface of the joints and consequently deterioration of mechanical properties of the joints [45, 46, 52]. Using a transitional interlayer between dissimilar materials and using a local heat source to melt the interfaces are promising approaches to solve these problems. Moreover, the composition and microstructure of the interlayers should be compatible with the substrates. Therefore, using reactive materials can be an appropriate approach to solve the problems. The final products of the reactive interlayer can be used as filler, as well as provide local heat to join the pieces. Moreover, the selected reactive composition must make a strong bonding with two different substrates [45].

2.1.3 Introduction to combustion synthesis and reactive joining

There are two different general modes for combustion synthesis. The first major category is Self-Propagated High-Temperature Synthesis (SHS) and another mode is Volume Combustion Synthesis (VCS). In the so-called SHS mode, the reaction should be locally initiated by an external source like laser, electrically heated metal wire or electrical arc. Then self-sustained combustion wave propagates along the reactive media and final products are formed from reactive reactants. In VCS mode, the reactive materials are uniformly preheated to reach to its ignition point. Then, the reaction is initiated at the same time throughout the entire volume of the reactants. The VCS mode is a proper procedure for reaction systems with low reactivity that they need preheating prior to their ignition temperatures [2]. Fig. 2.1 shows the schematic diagram of combustion synthesis in two SHS and VCS modes.

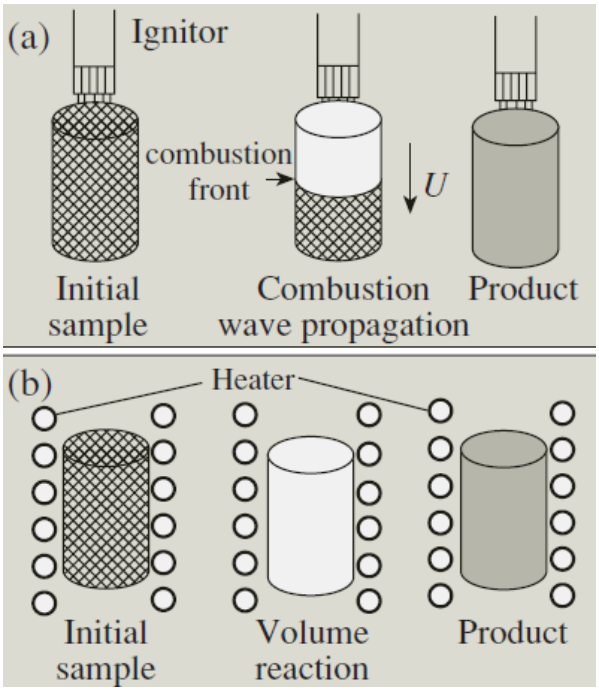

Figure 2.1. Schematic diagram of (a) Self-Propagating High-Temperature Synthesis (SHS) mode, (b) Volume Combustion Synthesis (VCS) mode [45].

Using each mode of combustion synthesis has some advantages and disadvantages. In the SHS, the external source of energy is required just for igniting of the reaction and after ignition, no external energy is required to make joint. However, the propagation of wave of reaction is finite, and thus the distribution of the temperature along the joining layer is not homogeneous. This can cause different microstructures in different area of the joint and consequently affect the mechanical properties of the joint adversely [2].

VCS mode of combustion synthesis can be used for the reactive mixtures with low exothermicity, which cannot achieve a sustainable propagation of reaction wave during SHS mode. In this process, whole joining stack is heated to ignition point (T_{ig}). The ignition point for most gasless mixture is equal to the lowest melting point of the reactant components. As an example, in the reaction system of Ni-Al-Nb-B or Ni-Al-Ti BN, aluminum has the lower melting point of the reactant components and the ignition temperature is the melting point of the aluminum (660 °C) [45, 53, 54]. In some cases, the lower melting point of the components is too high, and thus it is difficult to reach that temperature. Moreover, sometimes, low heating rate in combustion synthesis causes some pre-ignition solid-state reaction that can have an important influence on the reactivity and microstructure of the final products. Pre-ignition

solid-state diffusion can decrease the heat released after ignition and consequently decrease the combustion temperature. A decrease in combustion temperature leads to drop in the melting phase content in the final products and decreases densification of the joining interlayer. Increasing the heating rate is an appropriate approach to hinder pre-ignition solid-state reaction [45, 53, 54].

2.1.4 Reactive joining techniques

2.1.4.1 Induction heating reactive joining

This technique is classified in VCS category. In this procedure, the reactive interlayer is placed between the joint components. Then, the assembly is placed in an induction-heating furnace and heated in an inert or vacuum atmosphere. Finally, an external pressure is applied on the stack for condensation of the reaction products. Fig. 2.2 shows the schematic diagram of joining system and the sample assembly [52].

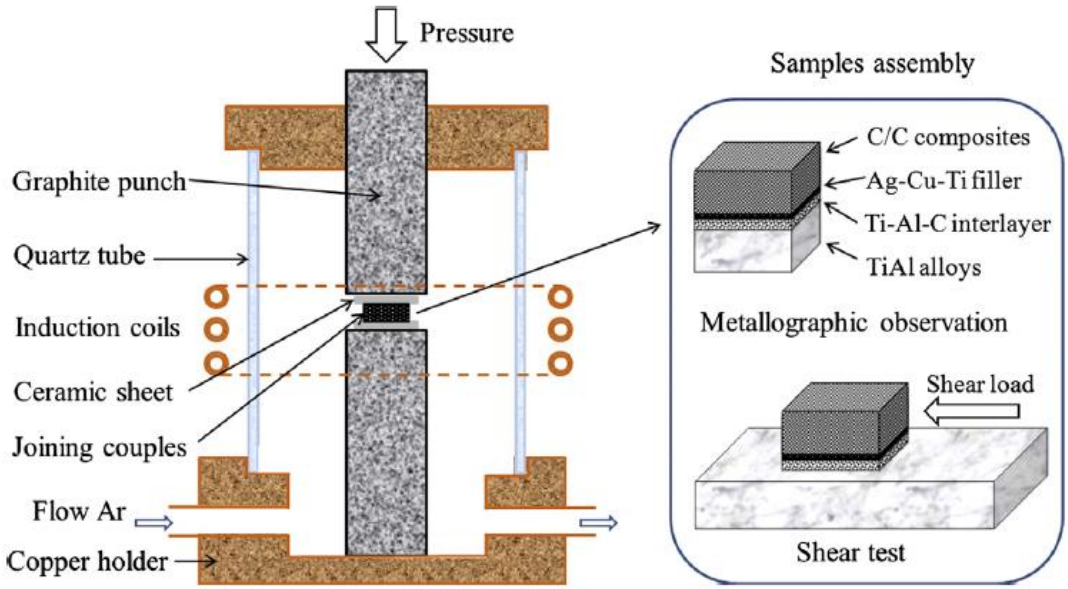

Figure 2.2. The schematic of apparatus for the joining procedure and the sample assembly [52].

2.1.4.2 Reactive Resistance Welding (RRW)

Fig. 2.3 and Fig. 2.4 show the schematic and the assembled apparatus of the RRW. The reactive resistance welding uses the features of conventional resistance welding technique. In this procedure,

reactive interlayer is placed between two substrates that should be joined. Then, the stack is placed between two electrodes. The electrodes have two functions during the joining process. First, the electrodes are connected to a DC source and they are used to apply electrical current for ignition of the reactive interlayer. Second, they are used to apply pressure for the condensation of the final products. A DC current is utilized to uniformly heat the reactants to their ignition point. It should be considered that the resistance of the compacted reactive interlayer is higher than other parts as a result of its high porosity content (compacted powder). Therefore, the increase in the temperature in the reactive interlayer is higher than other part of the stack (Fig. 2.5) [31, 55].

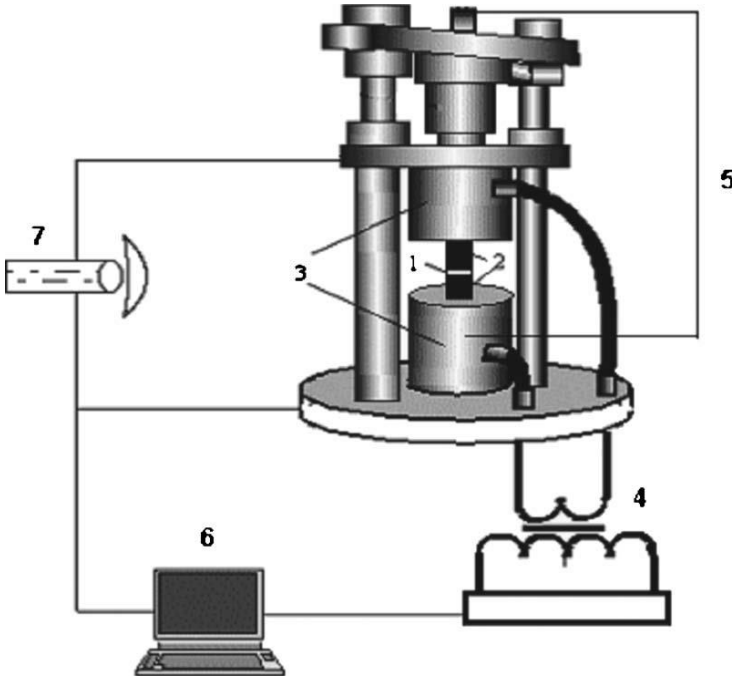

Figure 2.3. Different components of the RRW set up: 1. reactive layer, 2. substrates, 3. electrodes, 4. high current power supply [55].

Figure 2.4. Assembled apparatus for Reaction Resistance Welding (RRW) of refractory materials [55].

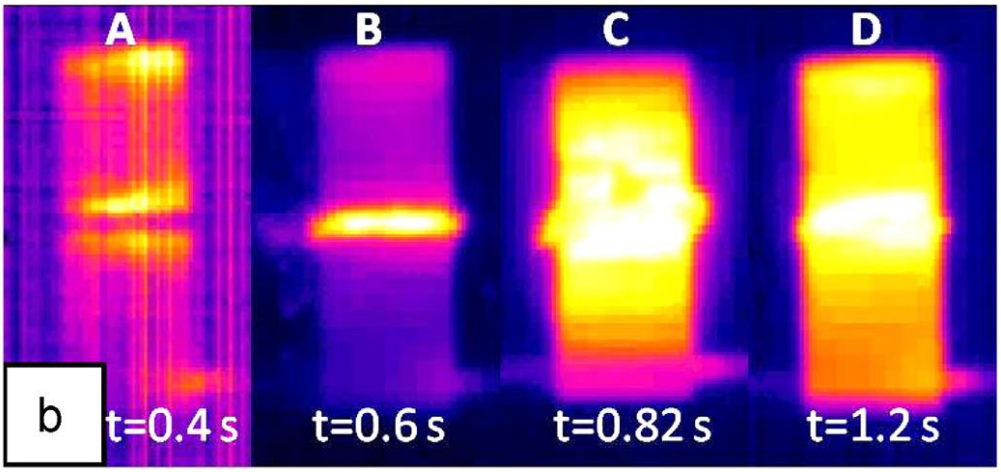

Figure 2.5. Typical temperature–time profile for similar joining of C/C composite with compacted powder interlayer [31].

2.1.4.3 SHS-reactive joining

In this technique, reactive interlayer is placed between two pieces that should be joined and an external pressure is applied to condense the products of the joining. In order to ignite the interlayer, an external

heating source like laser, electrically heated metal wire or electrical arc can be used. Laser is more appropriate ignition technique because laser beam can be focused in the gap between two substrates [9]. Fig. 2.6 shows the schematic of the components of SHS-reactive joining process, using laser beam for ignition.

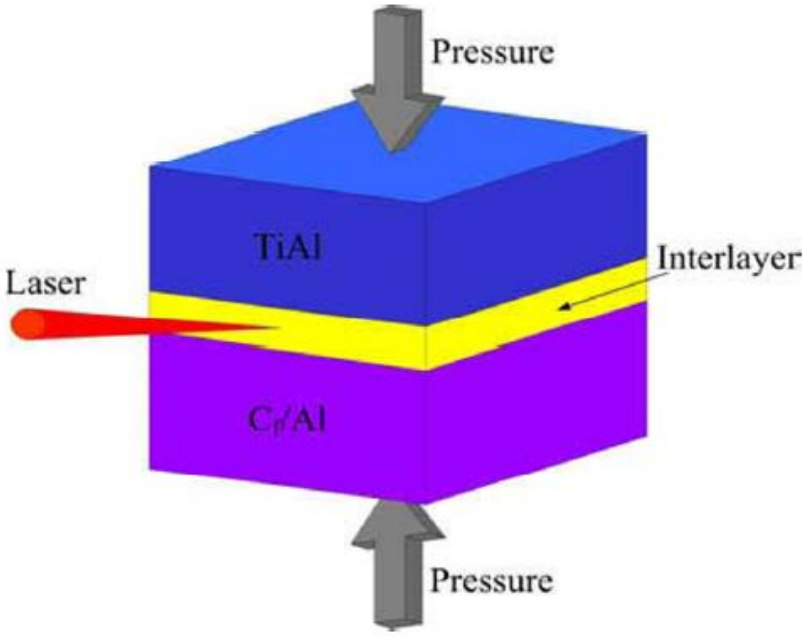

Figure 2.6. Using laser for ignition in SHS-reactive joining [56].

2.1.5 Different types of interlayers

Interlayers can be used in two different forms of compacted powders and reactive multilayers for reactive joining.

2.1.5.1 Reactive compacted powder

In reactive compacted powder interlayers, after mixing the powders, the mixture is compacted by a press to make a pellet. Preparation the reactive interlayer by this technique is very cost effective and has the flexibility to change the composition of the mixture and it is possible to mix more than two different powders. Presence of porosity in the pellet is a disadvantage of using compacted powders. This problem can be solved by applying pressure during joining to condense the products of reactions [45].

2.1.5.2 Reactive multilayers

In this technique, different layers of the reactive mixture are deposited by physical vapor depositions (PVD) techniques. Fig. 2.7 shows the reactive multilayers of Al/CuO reaction system fabricated by magnetron sputtering [57]. This process is expensive and the thickness of the fabricated interlayer should be in micron size range to produce required heat for joining applications. With considering that the deposition rate in sputtering technique is in order of 1-50 nm /min, it takes time to reach the thickness in micron size range. As advantages of the multilayer structures, these structures are condense and there is no porosity in multilayer structures. Moreover, by controlling the thickness of layers it is possible to control the released heat during reaction.

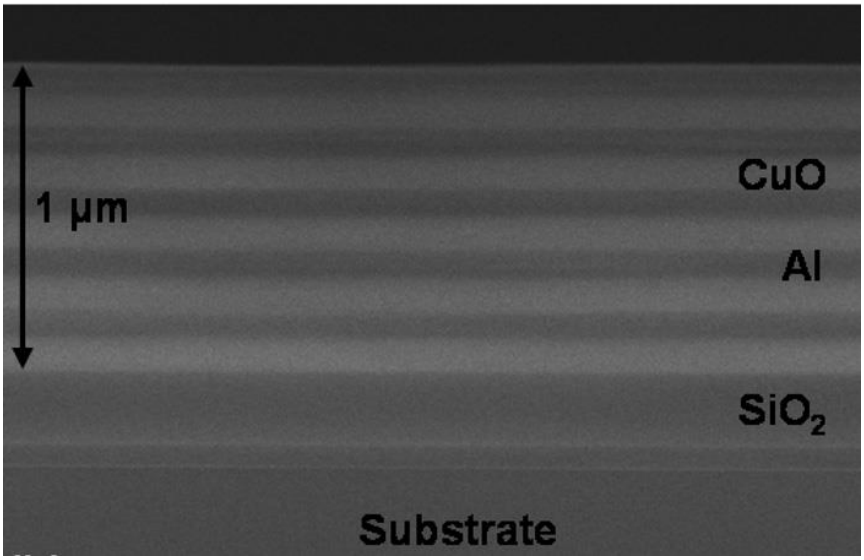

Figure 2.7. SEM cross-section images of multilayers fabricated by magnetron sputtering. Thickness of each layer of CuO and Al is100 nm [57].

2.1.6 Fundamental parameters in reactive joining

2.1.6.1 Composition of reactive mixture

Composition of reactive materials is the most important parameter in the reactive joining. The selected composition for the interlayer should produce an optimum amount of heat for joining. Moreover, the reactive materials should be able to make good chemical bonding with the substrates. Besides, a portion of final products should be melted during reactive joining to fill the pores of final products [52, 56].

2.1.6.1.1 Low exothermicity of reactive materials

Low exothermicity of reactive materials leads to quenching the reaction because of heat loss by substrates. Therefore, the reactions cannot be completed and some unreacted reactants will be remained after joining process. Fig. 2.8. shows quenching of the reactive materials during joining as a result of low exothermicity of the reactants and heat losses by substrates, reactive foil and atmosphere. Therefore, the joint was failed. Furthermore, as a result of low exothermiccity, enough melted materials is not produce during the joining to achieve a condense and void free joint [52, 56].

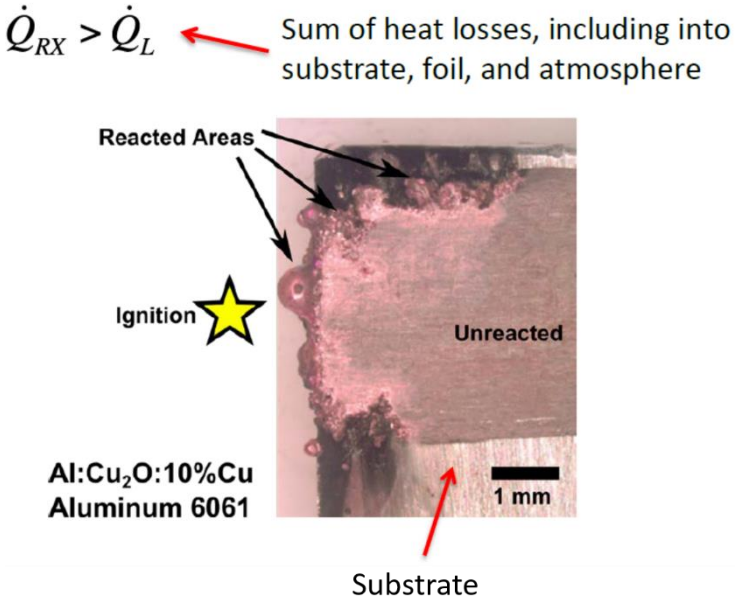

Figure 2.8. Quenching of the reactive interlayer as a result of low exothermicity [58].

2.1.6.1.2 High exothermicity of reactive materials

High exothermicity of reactive materials causes too mass ejection from interlayer during joining. High exothermicity can also cause vaporization of the low boiling reactants and products. Formation of gas phase during welding causes mass ejection and consequently formation of voids in the joints [52, 58]. Fig. 2.9 shows mass ejection during the joining process as a result of high exothermicity and explosive nature of reaction. The cross section image of the joint reveals the formation of a high amount of porosities and voids at the interface of the joint and there is not enough interlayer phase between the joint substrates. These voids cause deterioration of mechanical properties of the joint [58].

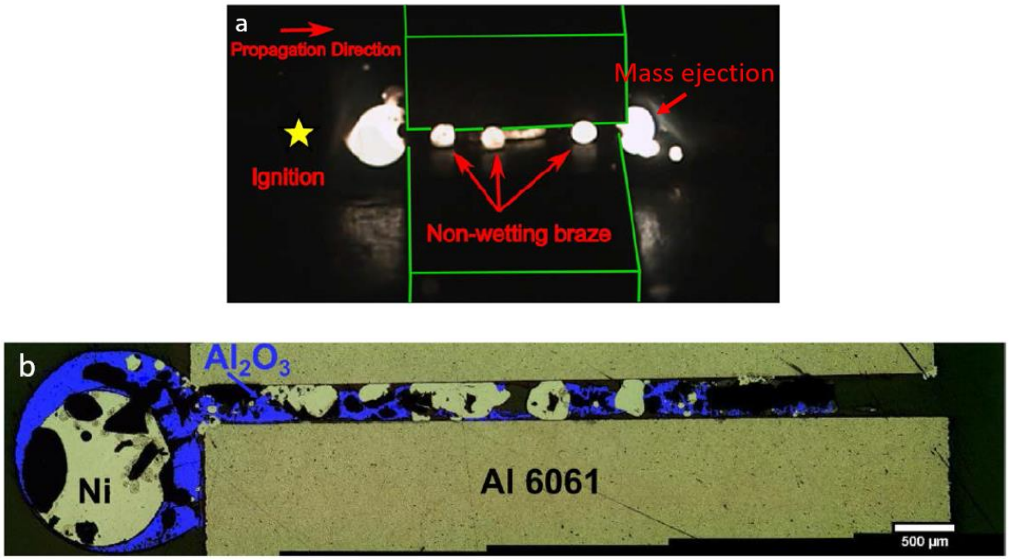

Figure 2.9. (a) mass ejection during joining process, (b) formation of the porosities and voids as a result of the mass ejection [58].

Fig. 2.10 shows two samples with high and proper exothermicity. As can be seen in Fig. 2.10(a), when the exothermicity of the reaction is too high, mass ejection occurred, but by changing the composition, the amount of mass ejection decreased dramatically (Fig. 2.10 (b)).

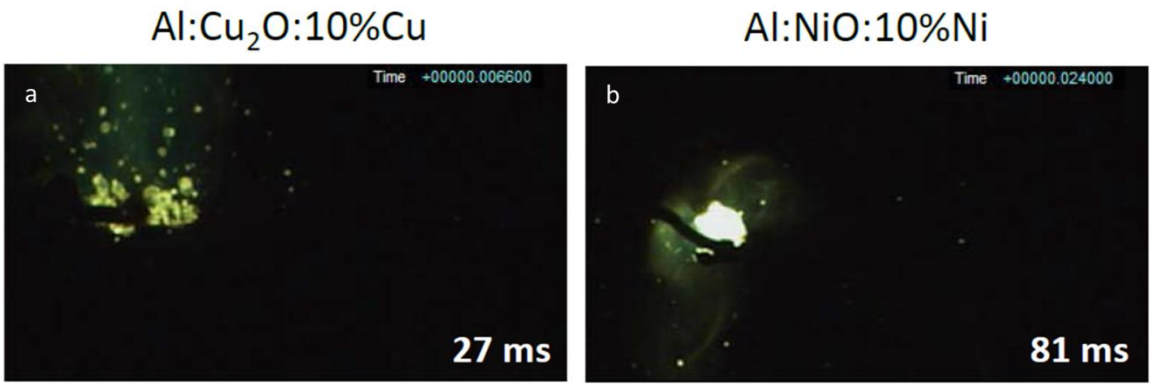

Figure 2.10. Mass ejection for (a) Al:Cu2O:10%Cu and (b) Al:NiO:10%Ni [58].

2.1.6.1.3 Controlling the exothermicity of the reactive materials

Adiabatic temperature is a key parameter to control the exothermicity of the reactants. Adiabatic temperature is defined as the temperature of the reaction in adiabatic condition. In other words, there is no heat loss as a result of conductivity and convection, and the whole released heat of reaction is used for increasing of the temperature of the products. There are two limits for adiabatic temperature of the reactive mixtures for joining applications. Upper limit is defined as a higher allowed amount of the adiabatic temperature, which is the lowest boiling point of the reactants and final products. Lower limit refers the minimum temperature that is allowed to make sure that wave propagation is sustainable. The lower limit is usually considered between 1800 to 2000 °K. In the cases in which the adiabatic temperature is lower than this amount, the reaction is quenched during joining and reactions cannot be completed. The most common way to control and modify the adiabatic temperature and also exothermicity of the reaction is adding diluent materials to high exothermic materials or adding very exothermic materials to the mixtures with low exothermicity [52, 56, 58].

2.1.6.1.4 Adding diluent to control the exothermicity

Fig. 2.11 shows the effects of adding Ni as diluent to Al-NiO-Ni reaction system and adding Cu diluent to Al-CuO-Cu and Al-Cu2O-Cu on their mass ejection and velocity of wave propagation. Fig. 2.11 illustrates that by adding the diluent, exothermicity and velocity of reaction (wave propagation) decreased. Diluent content should be enough to bring temperature of reaction below boiling points of products and reactants. Thus, it is possible to decrease the adiabatic temperature of the reaction, decrease mass ejection in the joining process, and consequently achieve a pore free interlayer. It should

be noticed that there is an optimum amount for diluent content. Adding high diluent content can cause some problems and leads to quenching of reaction. Fig. 2.12 shows upper limits and lower limits of adiabatic temperature for three Al-NiO-Ni, Al-CuO-Cu and Al-Cu2O-Cu reaction systems. In these reaction systems, aluminum has the lower boiling point of the reactants and final products. Then the adiabatic temperature of the reaction should be lower than the boiling point of aluminum, which is 2519 °C [52, 56, 58].

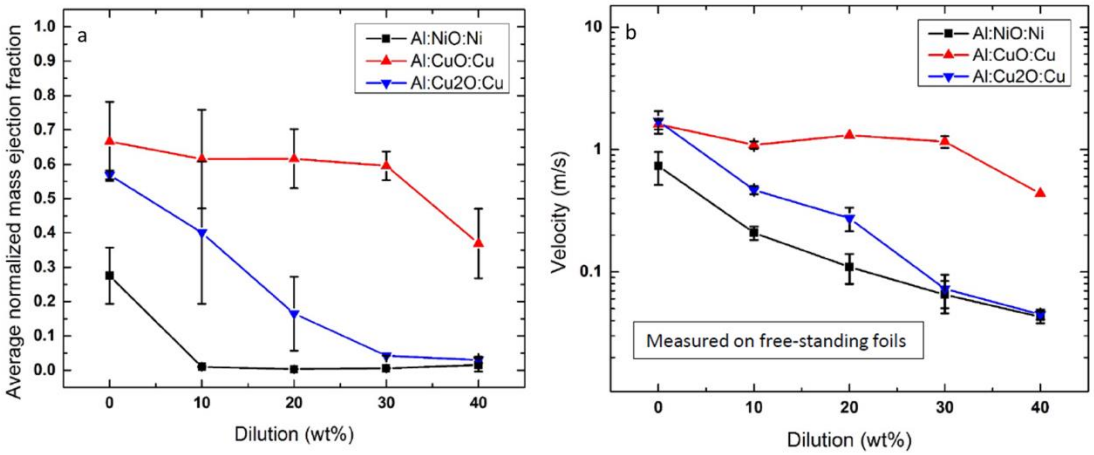

Figure 2.11. Change in (a) mass ejection and (b) velocity of the reaction by changing the diluent content [58].

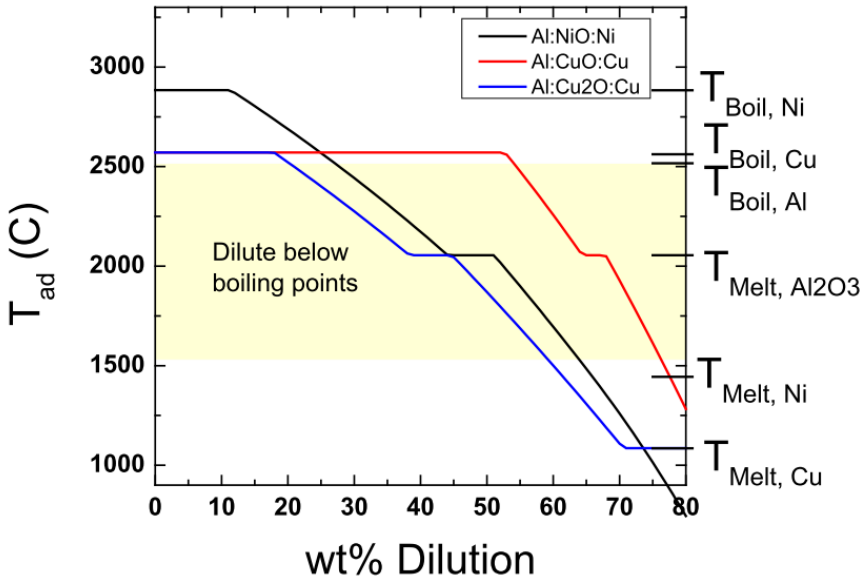

Figure 2.12. Upper and lower limits for adiabatic temperature of reaction [58].

Sometimes adding diluents can provide additional filler materials, which can help the condensation of the interlayers. Fig.2.13 indicates the change in the filler metal content by adding Ni to reactants as a diluent for Ni-Al-NiO reaction system. In this reaction system, Ni and Al_2O_3 are final products and Ni has lower melting point, which is melted at the temperature of the reaction and can be considered as filler metals. Therefore, by adding the Ni diluent in the starting materials, more filler materials can be formed in the final products, which results in more condensation joint interlayer [58].

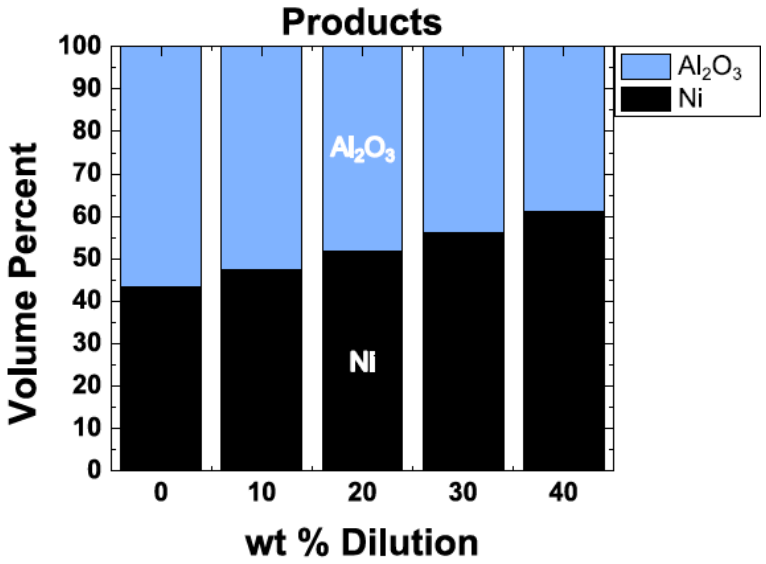

Figure 2.13. Change in filler content by adding Ni diluent to the Al-NiO-Ni reaction system, 3NiO+2Al+xNi= Al2O3+(x+3)Ni [58].

2.1.6.1.5 Adding highly exothermic materials to the mixtures with low exothermicity

In the cases of interlayers with low exothernicity, it is essential to add some high exothermic materials to the mixture. Adding additives with high exothermicity to the mixture is for three important objectives. First, increasing the adiabatic temperature to make sure that the reaction will be sustained after ignition. Second, increasing the adiabatic temperature leads to melting the final products and the melted phases can fill the pores and improve the mechanical properties of the joints. Third, adding the exothermic additive causes more reactivity at the interface between the interlayer and substrates [52].

The change in the adiabatic temperature of the reaction by adding Ti and C to the Ti-Al-C is shown in the Fig. 2.14. In Ti-Al-C reaction system, there are two final products including TiC and TiAl3 (equation 2.1). In this reaction system, the main exothermic reaction is formation of TiC phase. Thus, by increasing the m (molar ratio of TiC in the products) the adiabatic temperature of the reaction is increased [52].

$$(m + 1)Ti + 3Al + mC = mTiC + TiAl3 \quad (2.1)$$

In this investigation, the lower limit of adiabatic temperature was considered 2000 °K to make sure that the reaction will not be quenched during joining. The upper limit of the reaction was considered the boiling temperature of Aluminum.

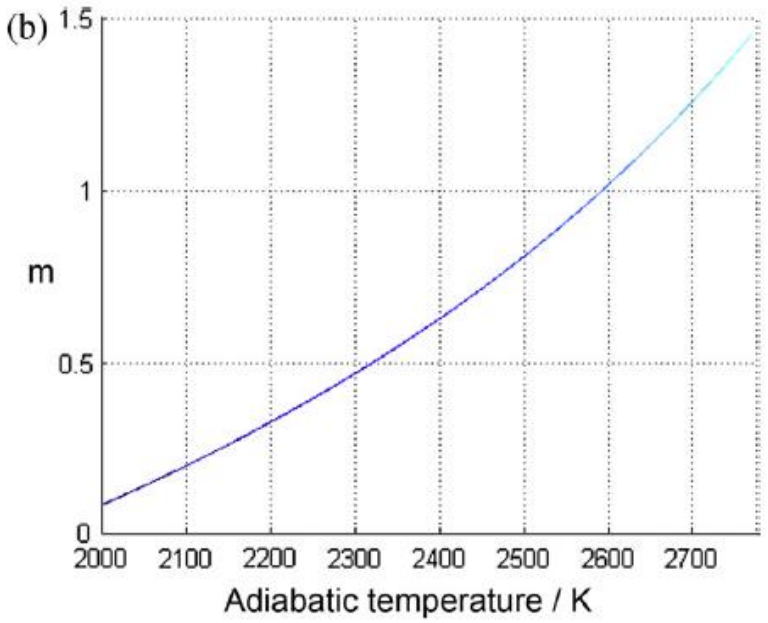

Figure 2.14. The effect of increasing TiC content on overall adiabatic temperature (m: is the molar ratio of TiC, (m + 1)Ti + 3Al + mC=mTiC + TiAl3) [52].

Fig. 2.15 shows the effects of TiC content on the microstructure of the joints between TiAl and C/C composite. The ratio of TiC to TiAl3 in the Fig. 2.15 (a) is 0.4. The microstructure of Fig. 2.15 (a) reveals that some pores are existed in the final products because the released energy of the reaction was not sufficient for densification of the reaction products and resulted in formation of pores in the reaction products. By increasing the ratio of TiC to TiAl3 from 0.4 to 1.1, a pore free microstructure was

achieved because this amount of TiC content provided a interlayer with higher exothermicity. The sufficient produced heat caused proper reaction at the interface and in the interlayer and led to achieving a dense reaction products and a defect-free joint (Fig. 2.15(b)). The microstructure of the joints can signal the mechanical properties and the quality of the joints. Then, pore-free microstructure seems to have better mechanical properties. Fig. 2.16 shows the effect of TiC content on the shear strength of the joints. By increasing the TiC content and densification of the final interlayer products (Fig. 2.15), the shear strength increased dramatically and the maximum strength of the joints was obtained for m=1.1 ((m + 1)Ti + 3Al + mC=mTiC + TiAl3) [52].

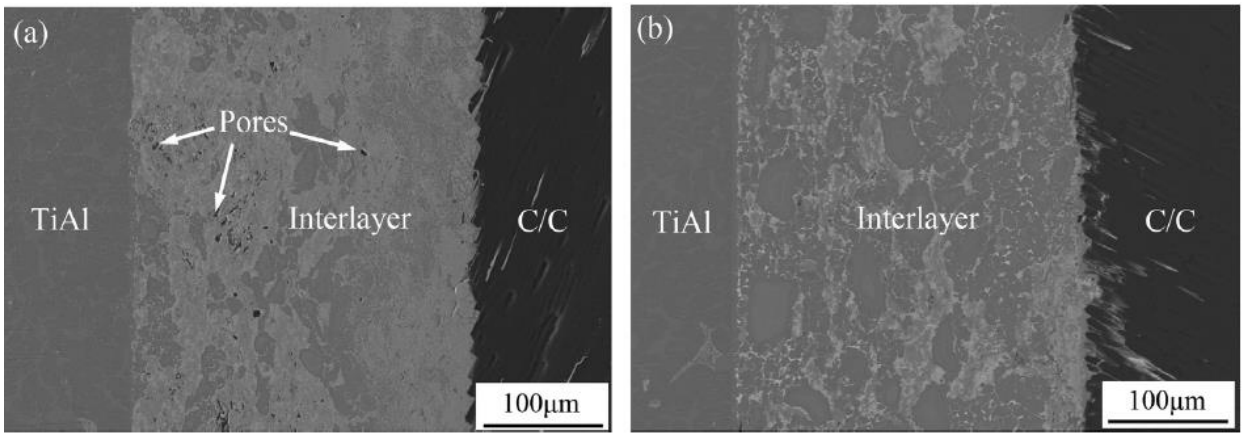

Figure 2.15. Effect of composition of the interlayer on the microstructure of TiAl–C/C composite joints (a) m = 0.4, (b) m = 1.1, (m + 1)Ti + 3Al + mC=mTiC + TiAl3 [52].

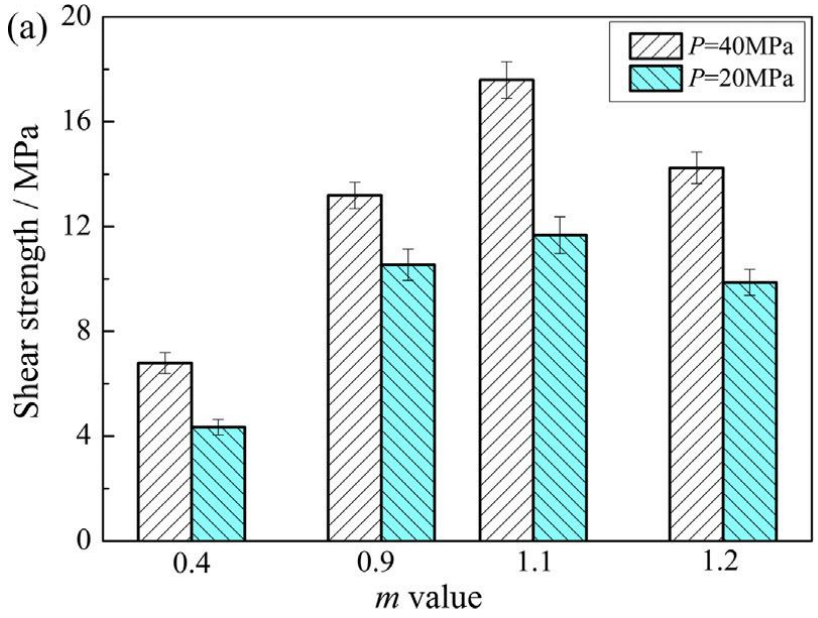

Figure 2.16. Effect of the composition of interlayer (m=the ratio of TiC to TiAl3) and external pressure on the shear strength of the joints [52].

2.1.6.1.6 Adding additives to produce low melting products

Sometimes exothermicity of the reaction is not enough to melt the final products and manipulation of the composition of the reactants is an approach to produce low melting point products. Cao et al, investigated the effects of the Ti-Al content on the microstructure and mechanical properties of of Cf/Al composite-TiAl joints. In this study, adding Ti-Al to reactive mixture caused formation of some low melting point products (equation 2.2) [56].

Ni+(m+1)Al+mTi=NiAl+mTiAl (2.2)

Fig. 2.17 shows the change in the adiabatic temperature by changing the Ti-Al content. As illustrated in Fig. 2.17, by adding the Ti-Al content, the adiabatic temperature was decreased. The upper limit of using Ti_Al is m=1.66, because adding Ti-Al more than this amount can increase the risk of quenching the reaction during joining [56]. The microstructures related to compositions with four different contents of Ti-Al (m=0, 0.05, 0.1, 0. 2) are shown in Fig. 2.18. When the Ti-Al content was zero, NiAl was the only product phase. By adding Ti-Al, a ϒ phase with the composition of Ni0.35Al0.30Ti0.35 was formed. The produced ϒ phase has lower melting point in comparison to NiAl phase. Then

formation of Ɣ phase caused increasing the existing time of the molten products. Increase in the existing time of the molten products helped filling the pores and leads to densification of the joint interlayer. For the sample with zero content of the NiAl, there are some pores in the microstructure. By adding 0.05 Ti-Al, the amount of pores decreased. Pore-free structure was achieved for sample with 0.1 content of Ti-Al because the melted Ɣ phase content was enough to fill the pores. Adding more content of Ti-Al decreased the quality of the joining. As mentioned, by adding the Ti-Al content, the adiabatic and exothermicity of the reaction is decreased. For sample with m=0.2 Ti-Al content there are some cracks at the interface of the TiAl substrates and interlayer. The produced heat during reaction was not enough to cause sufficient reaction at the interface between TiAl substrate and interlayer, which caused rapid drop in the thickness of Ɣ phase -Ni0.35Al0.30Ti0.35 at interface. Then cracks produced at the interface propagated to the interlayer (Fig. 2.19(d)). Fig. 2.20 shows the shear strength of the joints for different compositions. There is an optimum amount for Ti-Al content in the Ni-Ti-Al reaction system for achieving the proper joining. For sample with zero Ti-Al content, shear strength is low as a result of high pore content. However, by adding the Ti-Al to the reactive mixture and formation of Ɣ phase, the pore content decreased dramatically. Excessive increase in Ti-Al content, decreased the shear strength as a result of crack formation at the interface between the substrates and interlayer because the heat of reaction was insufficient to make an appropriate bonding [56].

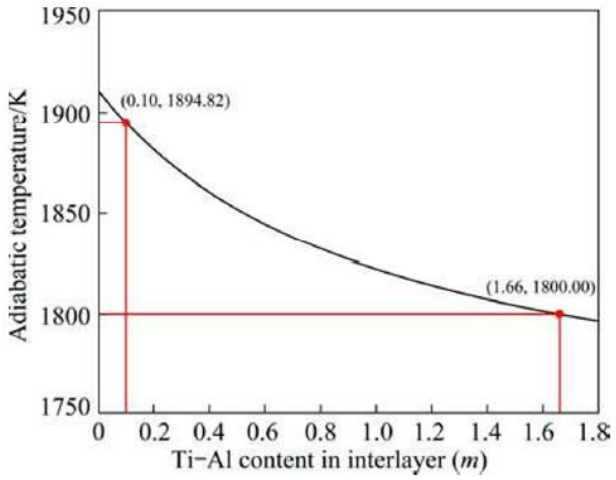

Figure 2.17. Effect of Ti−Al content on the adiabatic temperature of Ni−Al−Ti reaction system, Ni+(m+1)Al+mTi=NiAl+mTiAl [56].

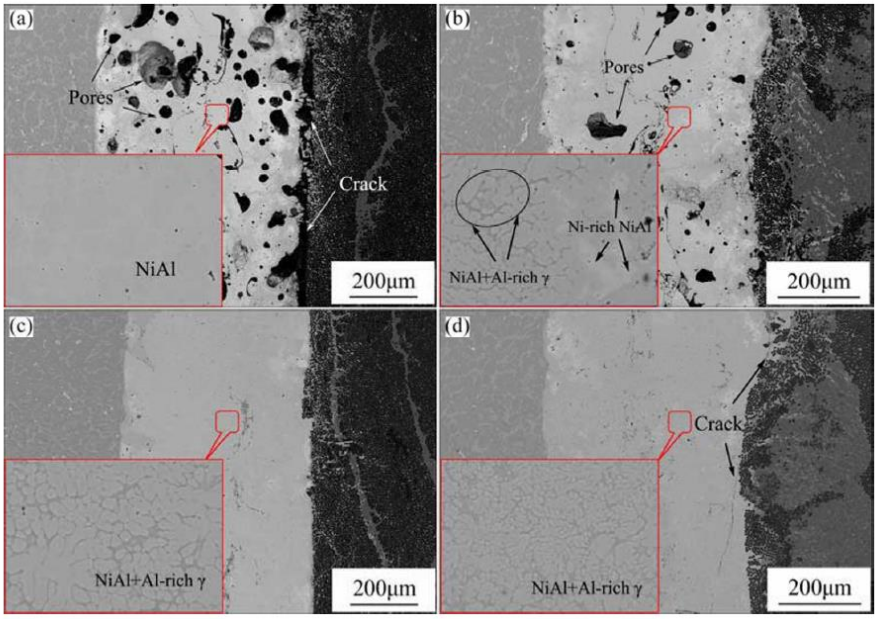

Figure 2.18. Microstructure of the joints with different content of Ti−Al: (a) m=0, (b) m=0.05, (c) m=0.1, (d) m=0.2, (Ni+(m+1)Al+mTi=NiAl+mTiAl) [56].

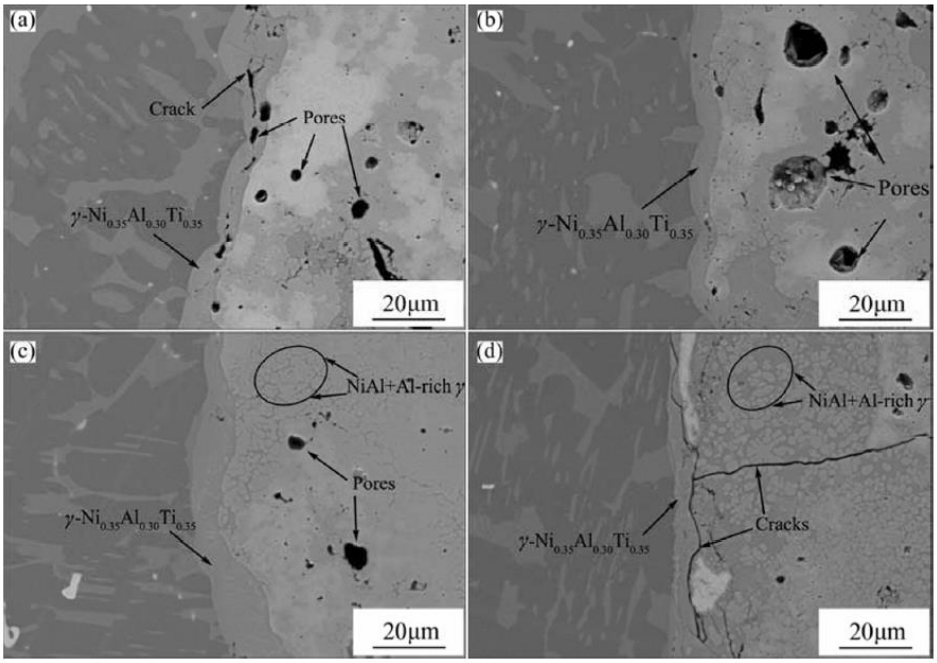

Figure 2.19. Microstructure of TiAl/interlayer interface with different contents of Ti−Al (a) m=0, (b) m=0.05, (c) m=0.1, (d) m=0.2, (Ni+(m+1)Al+mTi=NiAl+mTiAl) [56].

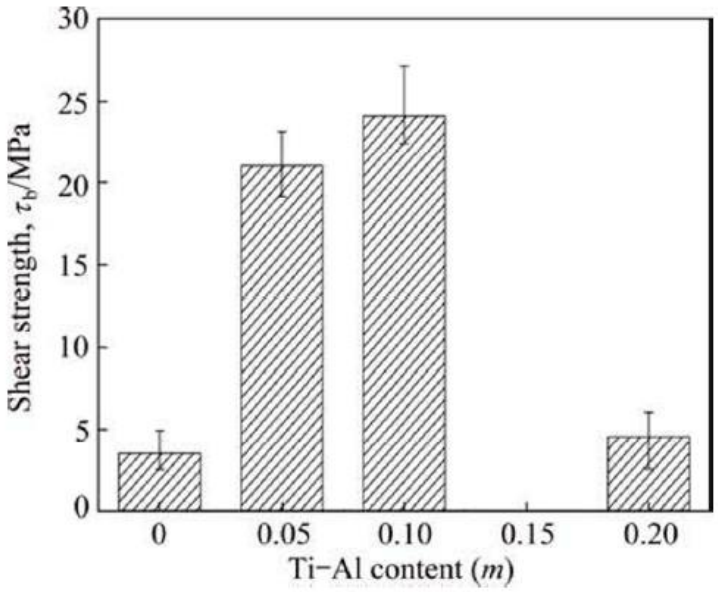

Figure 2.20. Shear strength of the joints with different contents of Ti−Al [56].

2.1.6.2 Applied pressure

The applied pressure is an important factor of joining because enough pressure can provide appropriate contact between substrates and the reactive materials. Furthermore, increasing the pressure can facilitate the condensation of the final products of joining. Fig. 2.21 shows the effects of the pressure on the microstructure of joints. In Fig. 2.21 (a) the applied pressure during joining was 20MPa. This amount was not enough to condense the final products of the reaction. Therefore, there are some pores in the final products. Fig. 2.21 (b) indicates that by increasing the external pressure to 40 MPa, a dense interlayer can be achieved because the applied pressure is sufficient to condense the final products. Increase in the shear strength of the joined samples by increasing the pressure from 20 MPa to 40 MPa can be seen in Fig. 2.16 [52].

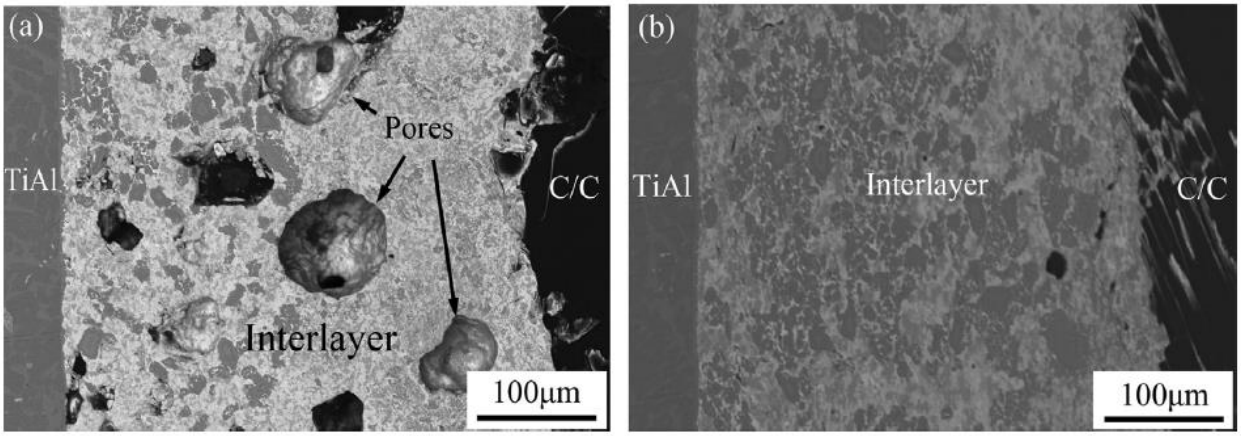

Figure 2.21. Effect of the applied pressure on the microstructure of joining TiAl to C/C composite (a) 20 MPa, (b) 40MPa [52].

2.1.6.3 Thickness of reactive interlayer

Thickness of the interlayer can also affect the quality of the joint and an optimum amount should be considered. Cao et al. [52] investigated the joining of TiAl to C/C composite by using Ti-Al-C as reactive interlayer and Ag-Cu-Ti as filler. The components of joining stack are shown in Fig. 2.22. Their investigation on the effect of changing the thickness of reactive materials on the quality of the joining showed that there is an optimum amount for the thickness of the interlayer. Fig. 2.23 shows the effect of the thickness of the reactive interlayer on the shear strength of the joints. In the case that the interlayer is not thick enough (250 μm) the shear strength is not good because an interlayer with small thickness cannot generate enough heat for a sufficient interfacial reaction. By increasing the interlayer thickness, the total exothermic heat increased and the molten filler metal can fill the voids of the reaction products, and a defect-free joint was obtained. Moreover, as a result of increase in the reactivity of mixture, sufficient interfacial reaction led to a better bonding at the interface between interlayer and substrate. Further increase in the thickness of the interlayer caused decrease in the shear strength since the molten filler (Ag-Cu-Ti) metal was insufficient to fill all the pores in the interlayer and the reaction products contains some pores, which result in deterioration of mechanical properties. In general, the joint strength depended upon the interfacial joining and the overall properties of the reaction products [52].

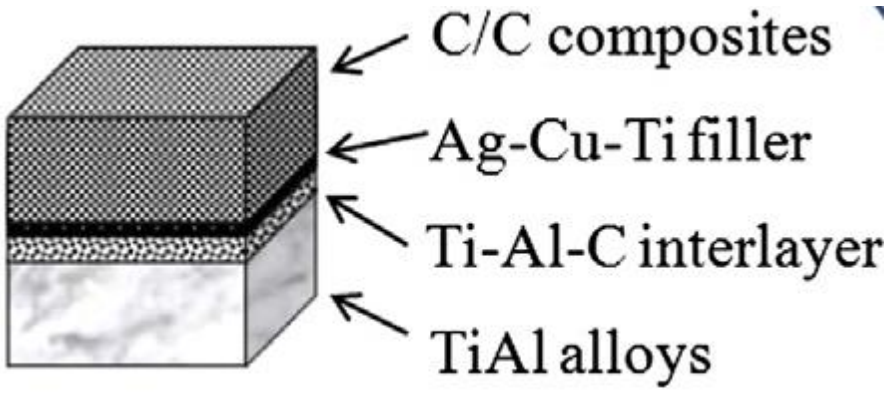

Figure 2.22. Components of the joint assembly [52].

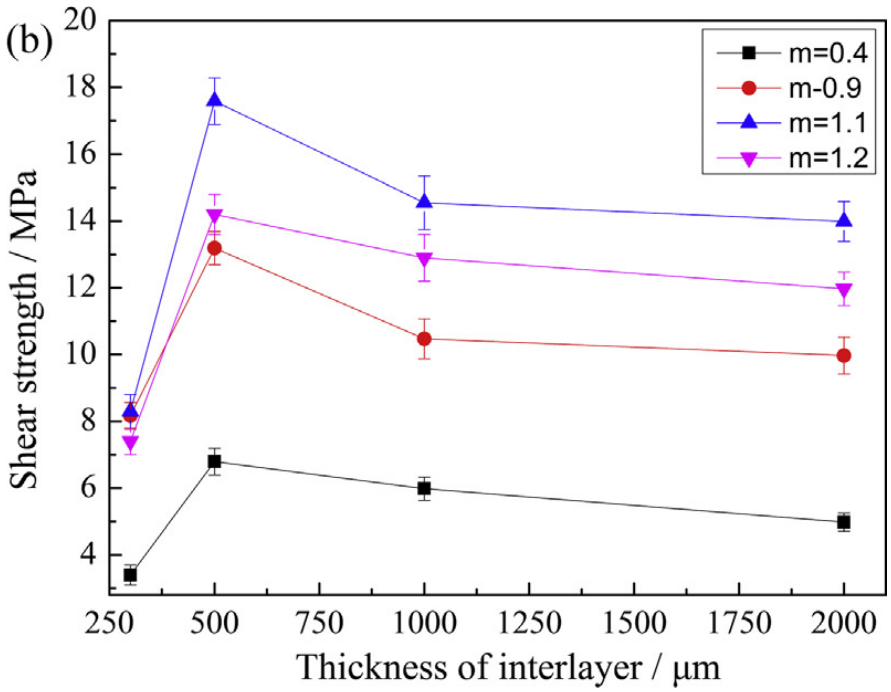

Figure 2.23. Effect of the thickness on the shear strength of the joint (m= the ratio of the TiC to TiAl3, (m+1)Ti+3Al+mC=mTiC+TiAl3) [52].

2.1.6.4 Using filler and braze foil

Using filler has some important advantages. First, it can improve wetting of the interlayer on the joint substrates. Second, filler can use for improving the bonding between the substrates and interlayer by contribution in reaction with substrates. For example, in similar joining of C/C composite, Ti foil was

used for formation of a thin TiC layer at the interface of the joints as a result of reaction between Ti and carbon of C/C composite. Formation of this phase improved the bonding of interlayer with C/C composite substrates. Third, filler can be used to fill the porosity of the reaction products and improve mechanical properties of the joint [2, 52].

2.2 Conventional techniques for similar and dissimilar joining of the C/C composites

C/C composites have attracted great interest as an attractive material for high temperature applications on account of its fascinating characteristics such as high thermal stability, low coefficient of thermal expansion (CTE), low density, good ablation and thermal shock resistances, and high strength-to-weight ratio at elevated temperatures [3, 59-62]. These characteristics make the C/C composites as important high-temperature structural materials for a variety of high temperature applications including heat shields, hot press dies, nozzles, turbine engine components, brakes, and high temperature furnaces [2, 7-12].

C/C composites are refractory materials and have high melting point temperature. Therefore, joining of the C/C composite by conventional fusion welding techniques seems to be impossible and very challenging [63] because C/C composites are not melted at the welding temperature due to the high melting point of carbon. In recent years, a lot of research has done to find the promising approaches to overcome the difficulty of joining of the C/C composites. Nowadays, joining of the C/C composite is carried out by a variety of novel procedures such as brazing and adhesive bonding [2, 9, 11, 14, 22-26].

2.2.1 Brazing

Brazing is one of the most conventional and popular techniques for similar and dissimilar joining of C/C composites, there are three major challenges to obtain the high quality joints by brazing. Firstly, the high difference between the CTE of the joining components leads to severe residual stresses at the interface of the joints. Secondly, the braze materials normally have a high wetting angle on the C/C composite which results in poor bonding between C/C composite and braze material. Thirdly, the service temperature of many braze joints are very low because the conventional braze materials contain silver and copper which have low melting points [11, 24, 28, 30, 64].

2.2.1.1 Improving the wettability of braze

Normally the conventional braze materials do not have good wetting on the C/C composites. The wettability of the conventional braze materials can be improved dramatically in two ways. One way is adding some active elements such as Ti, Si, Cr and Zr to the braze materials to make active braze materials such as CuAgTi, CuNiTi, CuSiAlTi, TiZrNiCu, TiCuZrNi NiCrPCu [2, 10, 17, 19, 21, 31-36, 38, 39, 65-68]. These active elements react with the carbon of the C/C composite and form a carbide compounds. This carbide layer makes a chemical bond on the C/C composite and improves the mechanical strength of the joints [2, 10, 17, 19, 21, 31-36, 38, 39, 65-68]. Another approach is making a coat of active elements such as Cr, Mo, Ti, W or Si on the surface of the C/C composite to improve the wettability of the conventional braze materials on the C/C composite [22, 38, 69-73]. These coating layers also form a carbide layer at the interface of the joint, which consequently improve the wetting of braze materials on the C/C composite and enhance the strength of the joints.

2.2.1.2 Reducing in the interfacial residual stress

2.2.1.2.1 Multilayer interlayer

One promising approach to decrease the residual stress at the interface of the joints between C/C composite and metals is to use a composite or multilayer between joining components. Qin et al. [24] joined the C/C composite to Ti6Al4V by using the TiZrNiCu as active filler metal and Mo and Cu interlayers. The assembly of the C/C composite/TiZrNiCu/Mo/ TiZrNiCu /Cu/ TiZrNiCu/TC4 joint set up is shown in Fig. 2.24.

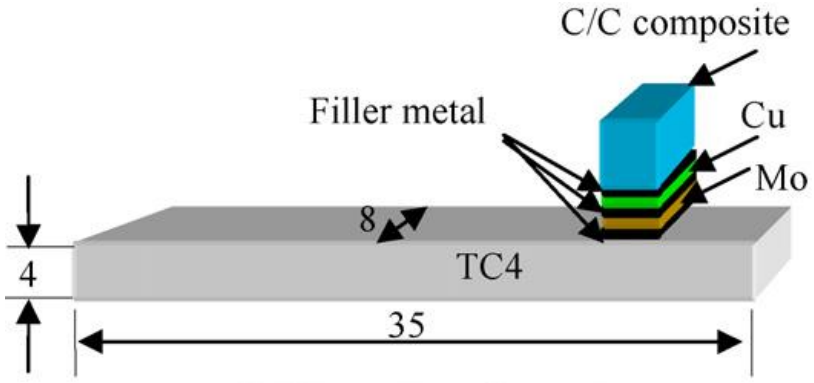

Figure 2.24. The schematic of the joint assembly [24].

The TiZrNiCu active filler alloy contains Ti and Zr. These two elements react with the carbon of the C/C composite to form carbides at the interface of the joints. Formation of the carbide layer at the interface of the joint increases the wettability of the liquid brazing alloy on the C/C composite. Furthermore, the Cu and Mo composite interlayers were used to release the interfacial residual stress and consequently increase the strength of the joints. The interface of the C/C composite/TiZrNiCu/TC4 joints without using Cu and Mo interlayers can be seen in Fig. 2.25. Even though chemical bonding was formed at the interface of the joints as a result of the formation of the carbide layer, but some cracks observed at the interface of the joint. Thus, the strength of the joints was only 5 MPa. The origin of these cracks is a high interfacial residual stress caused by difference between the CTE of the C/C composite, TiZrNiCu braze layer and TC4.

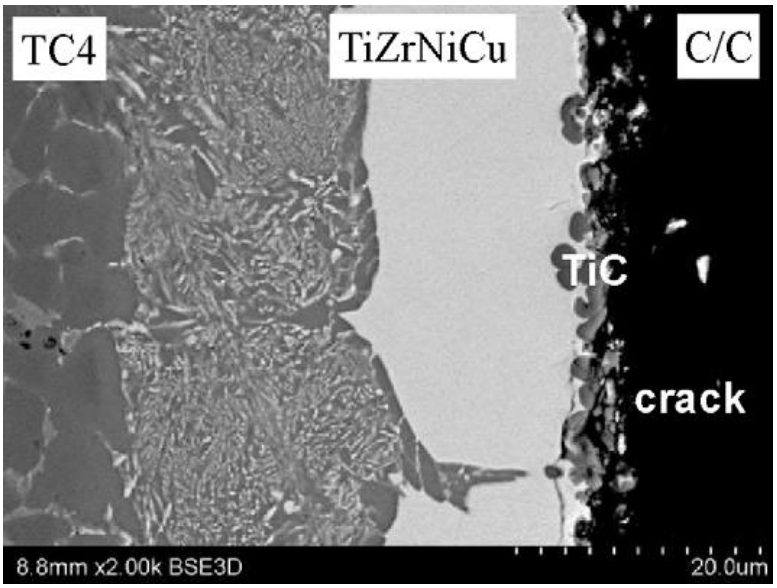

Figure 2.25. Microstructure of the C/C composite/TiZrNiCu/TC4 joint without using Cu and Mo interlayers [24].

On the other hand, in the case of using Cu and Mo as interlayer, the interface of the joint was free of the interfacial cracks (Fig. 2.26). Therefore, the strength of the joints significantly increased and reached to 21 MPa. The increase in the strength of the joints can be explained by the role of the copper and Mo in decreasing the interfacial residual stress. Cu has very low yield strength about 50 MPa. The residual stress induced during cooling is higher than the yield strength of the Cu. Therefore, part of the residual stress can be released by plastic deformation of the Cu. Regarding the Mo layer, Mo has a very

low coefficient of thermal expansion about 4.8×10^{-6} $^{\circ}C^{-1}$ which is close to the CTE of C/C composite. As a result, part of the stress was transferred to the Mo layer which led to decreasing in the residual stress at the C/C composite-filler interface. According to the mentioned reasons, the residual stress at the interface of the joints decreased significantly, which resulted in higher strength of the joints.

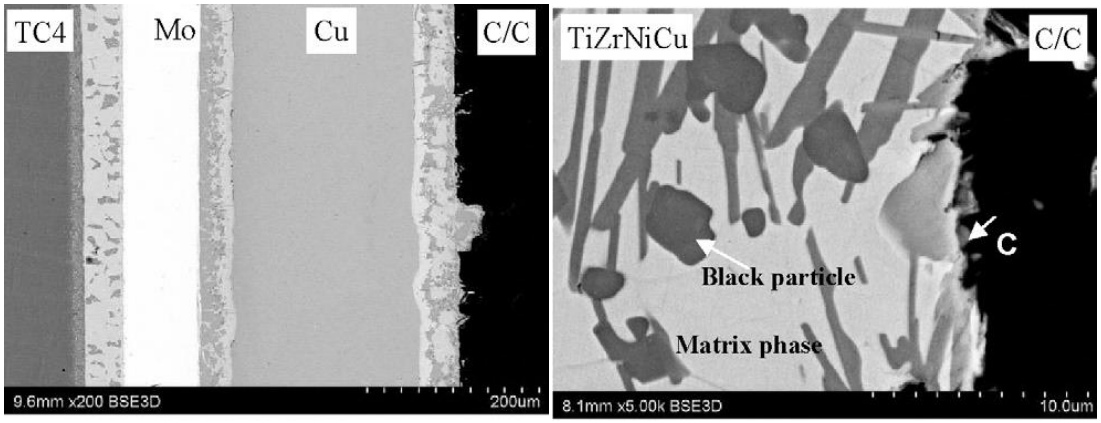

Figure 2.26. (a) Panorama microstructure of the C/C composite-Ti6Al4V joint with Cu and Mo interlayers and (b) the interface between filer metal and C/C composite [24].

2.2.1.2.2 Composite braze interlayer

As mentioned the difference between the CTE of metals or brazing alloys and C/C composite can cause the high residual stress at the interface of the joint. One approach to decrease the difference between the CTE of the brazing alloys and C/C composite is modifying of the CTE of the braze alloys by adding the low CTE reinforcement phases such as Al2O3, Si, SiC, CNTs and TiB_w [7, 19, 21, 30, 41, 66]. Moreover, adding additives to the brazing materials (matrix) leads to forming composite interlayers that have higher mechanical properties than the matrix. For instance, Song et al. investigated the effects of the adding multiwall carbon nanotubes (MWCNTs) to the TiCuZrNi brazing alloy for joining of the C/C composite to Ti6Al4V [41]. In this research, the MWCNTs were used as a reinforcing phase to strengthen the TiCuZrNi brazing alloy interlayer. The obtained shear strength of the joints with braze interlayer containing 1 wt.% MWCNTs was 38.38 ± 2 MPa which was significantly (73%) higher than that the strength of the joints without MWCNTs. The increase in the strength of the joints can be described by the formation of the TiC phase in the composite interlayer. The Ti element of the braze alloy was reacted with the MWCNTs and resulted in the in situ formation of the TiC during the brazing. The TiC phase acted as a reinforcement phase, which significantly increased the strength of the joints. Moreover, the TiC phase caused the reinforcement effects including crack deflection, particle fracture

and interface debonding which all contributed to the strength of the joints (Fig. 2.27). In addition, the CTE of TiC (7.4 ×10 $^{-6}$ K^{-1}) is between the C/C composites (0-2 ×10^{-6} K^{-1}) and brazing alloy (9.8 × 10^{-6} K^{-1}). Thus, the formed TiC phase decreases the residual stress between the C/C composite and braze alloy. Their results also indicated that there was an optimum amount for the MWCNTs content. In Fig. 2.28 (a) can be seen that no defect is observed at the interface of the joint with the 1 wt.% MWCNTs, whereas some pores were formed by increasing the MWCNT contents to 3 wt.% (Fig. 2.28(b)). The effect of the MWCNTs content on the strength of the joints is shown in Fig. 2.29. As can be seen by increasing the MWCNT content to 3 wt.%, the strength of the joints decreased dramatically. Increasing the MWCNT content to 3 wt.% caused consumption of the Ti element of the braze alloys. Therefore, there was insufficient Ti element to react with the C/C composite and make a robust interfacial bond. Moreover, the high content of the MWCNTs caused formation of the pores, agglomeration of the MWCNTs and decrease in the wettability of brazing alloy on the C/C composite, which consequently led to deterioration of the quality of the joints (Fig. 2.28 (b,c)).

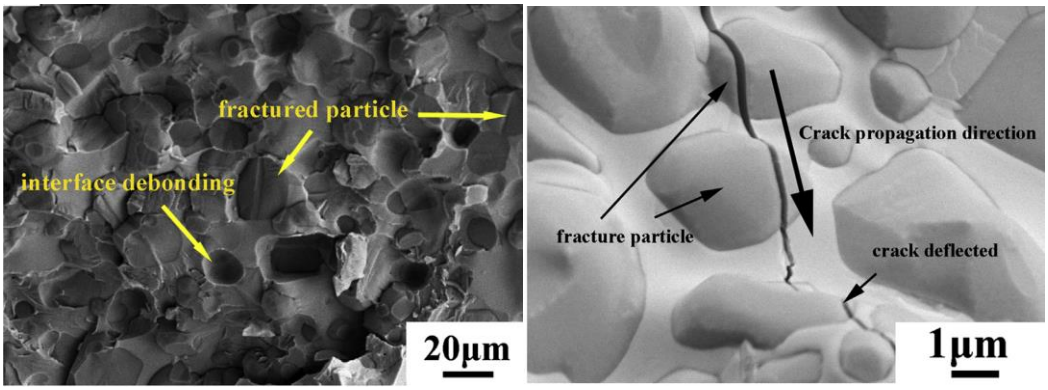

Figure 2.27. SEM images of the fracture surfaces of brazing of C/C composite toTi6Al4V by using the TiCuZrNi reinforced with 0.1 wt.% MWCNTs (a) interface debonding and particle fracture and (b) the crack propagation and deviation [41].

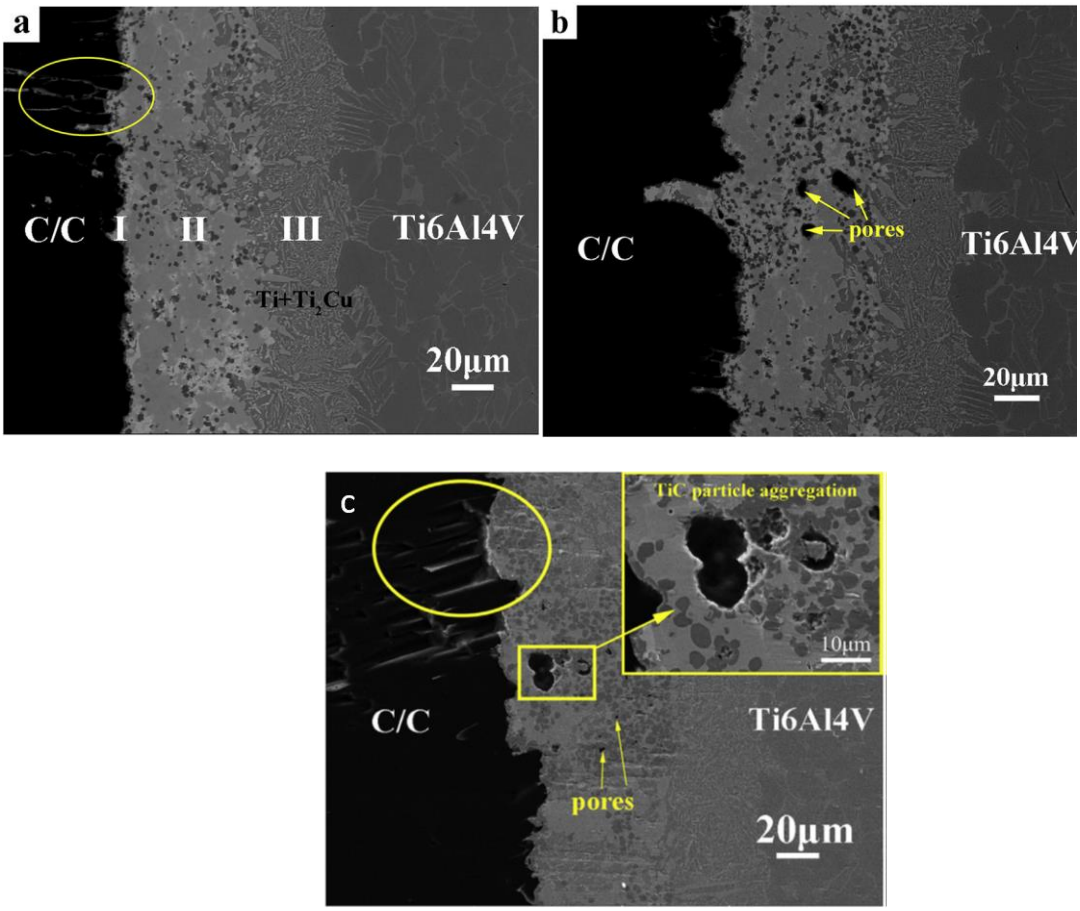

Figure 2.28. SEM images of brazing of the C/C composite toTi6Al4V with composite interlayer containing (a) 0.1 wt.% MWCNTs, (b) and (c) 3 wt.% MWCNTs [41].

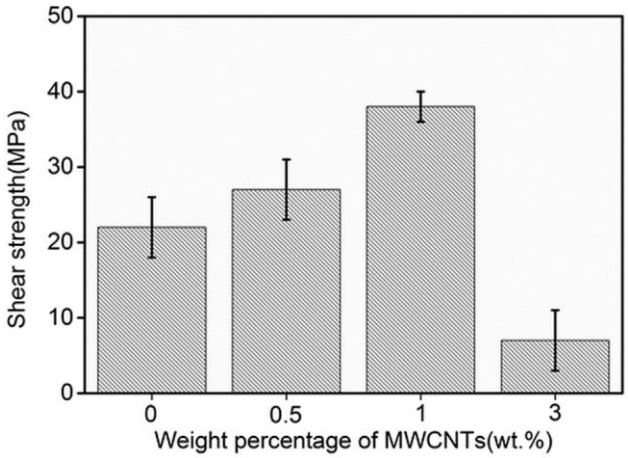

Figure 2.29. Strength of the C/C composite-Ti6Al4V brazed joint for different contents of MWCNTs [41].

2.2.1.2.3 Patterned interface structures

As mentioned a significant residual stress is formed at the interface of the joining between C/C composite and metals as a result of the difference between the CTE of the joint components. The high residual stress causes formation of cracks and defects at the interface of the joints. The typical examples of formation of interfacial cracks for the joints with flat interface are provided in Fig. 2.30. These interfacial cracks are formed as a result of high residual stress at the interface of the joints caused by difference between the CTE of the joints components which leads to deterioration of the joints.

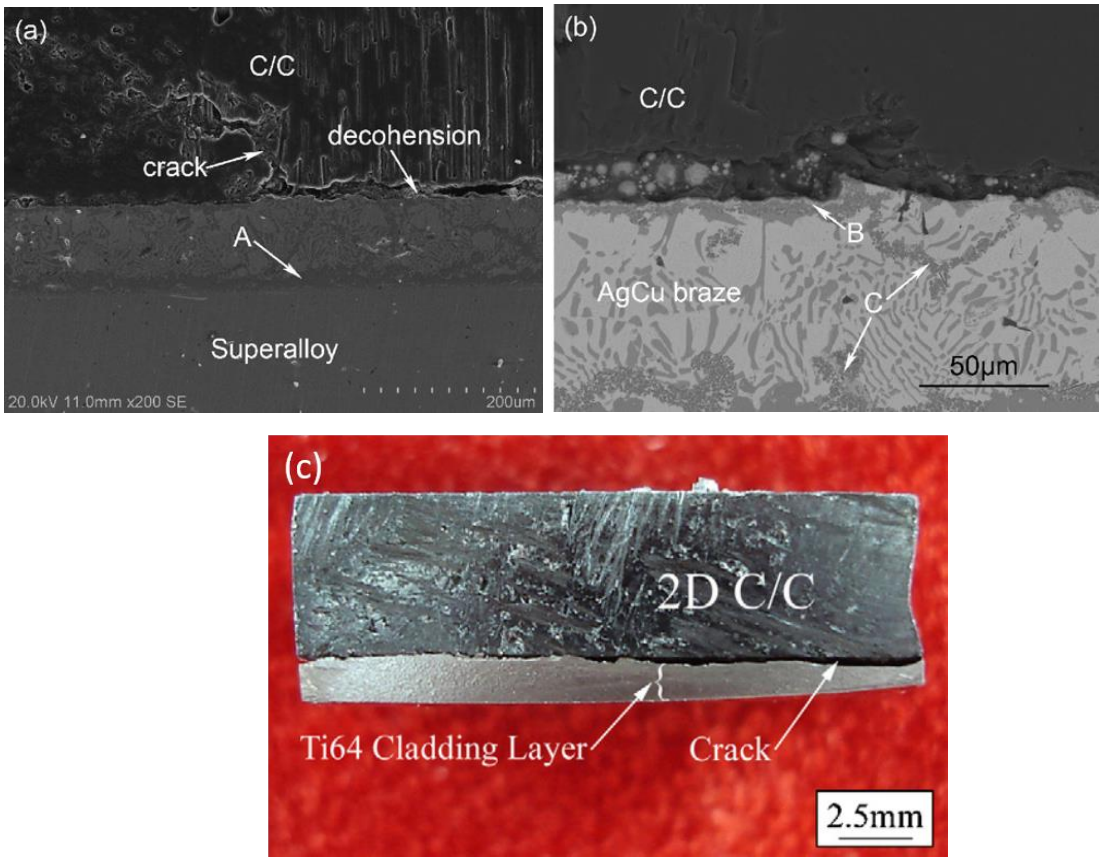

Figure 2.30. The formation of cracks at the interface of the joints with flat interface, (a) and (b) joints between C/C composite and superalloy with Ag-28Cu eutectic alloy foil and (c) the joints between Ti6Al4V and C/C composite with Ti6Al4V clad interlayer [27, 30].

One innovative approach to reduce the residual strength at the interface of the joints is using the patterned interface structure. Many researchers have studied the effects of different surface patterned structures such as surface puncturing and wave pattern interface for dissimilar joining of ceramics to the metals [11, 27-30, 42-44, 74]. They have shown that using the interfacial patterned interface is a promising approach to regulate and decrease the residual stress as well as inducing the compressive normal stress at the interface of the joints. Such a stress field is in favor of suppressing the interfacial cracks and increasing the mechanical strength of the joints. Moreover, using interfacial patterned structures increase the joining area. In addition, infiltration of the interlayer into the patterned interface causes the pinning at the interface of the joints. The mentioned factors are all beneficial to the strength of the joints [11, 27-30, 42-44, 74]. The patterned surfaces can be fabricated by laser for micron scales, or mechanical drilling for millimeter scales [27, 30]. Fig. 2.31 shows some different interfacial patterns

on the surface of the C/C composite for dissimilar joining of the C/C composite to metals. Some joints obtained by using the patterned structures are provided in Fig. 2.32. As can be seen, unlike the joints with flat interface no interfacial defects such as cracks are observed in the case of using the patterned interface.

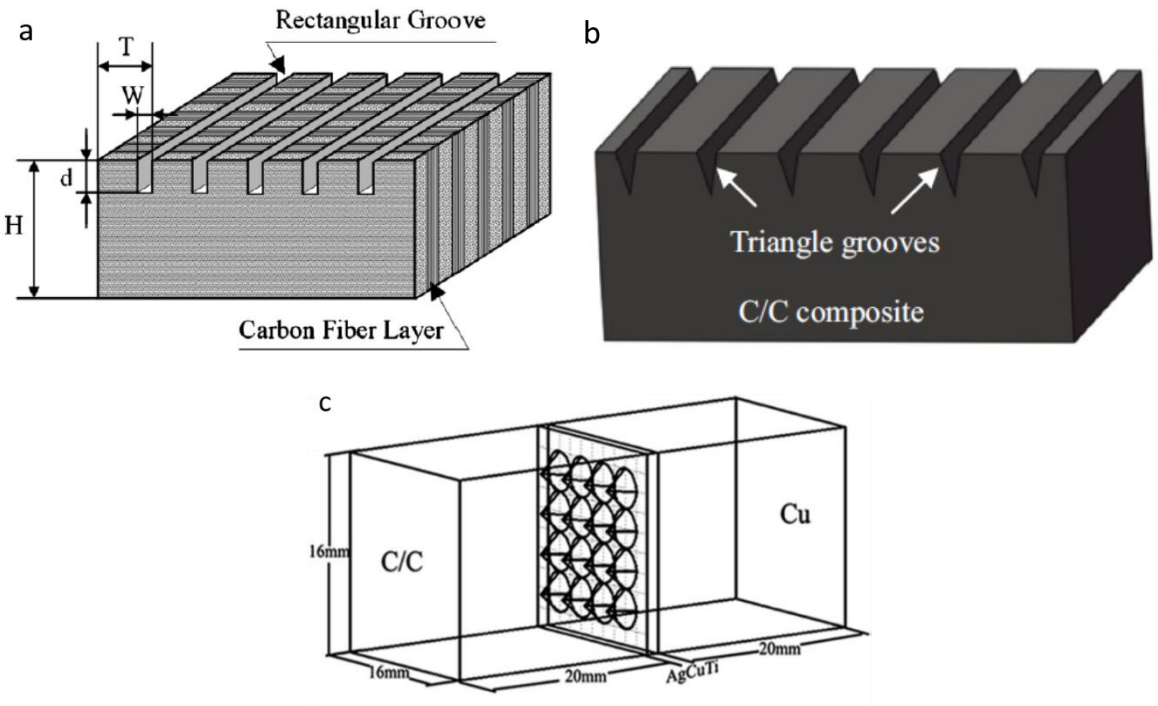

Figure 2.31. Schematics of the different surface patterning on the C/C composite, (a) rectangular groove pattern, (b) zigzag triangle groove pattern and (c) conical hole pattern [27-29].

The effects of the surface patterning on the shear strength of the joints and comparison between flat and patterned interface are provided in the Table 2.1. As can be seen, the strength of the joints with flat interface is significantly lower than the strength of the joints with patterned structure as a result of the difference in the interfacial residual stress. Based on the literature review, surface patterning leads to decrease in the interfacial residual stresses as well as induces compressive normal stresses at the interface of the joint, which prevents the formation of the interfacial cracks [11, 27-30, 42-44]. Furthermore, the infiltrated structure embedded in the C/C composite, pins the interface of the joints and also expand the joint area which results in higher mechanical strength of the joints.

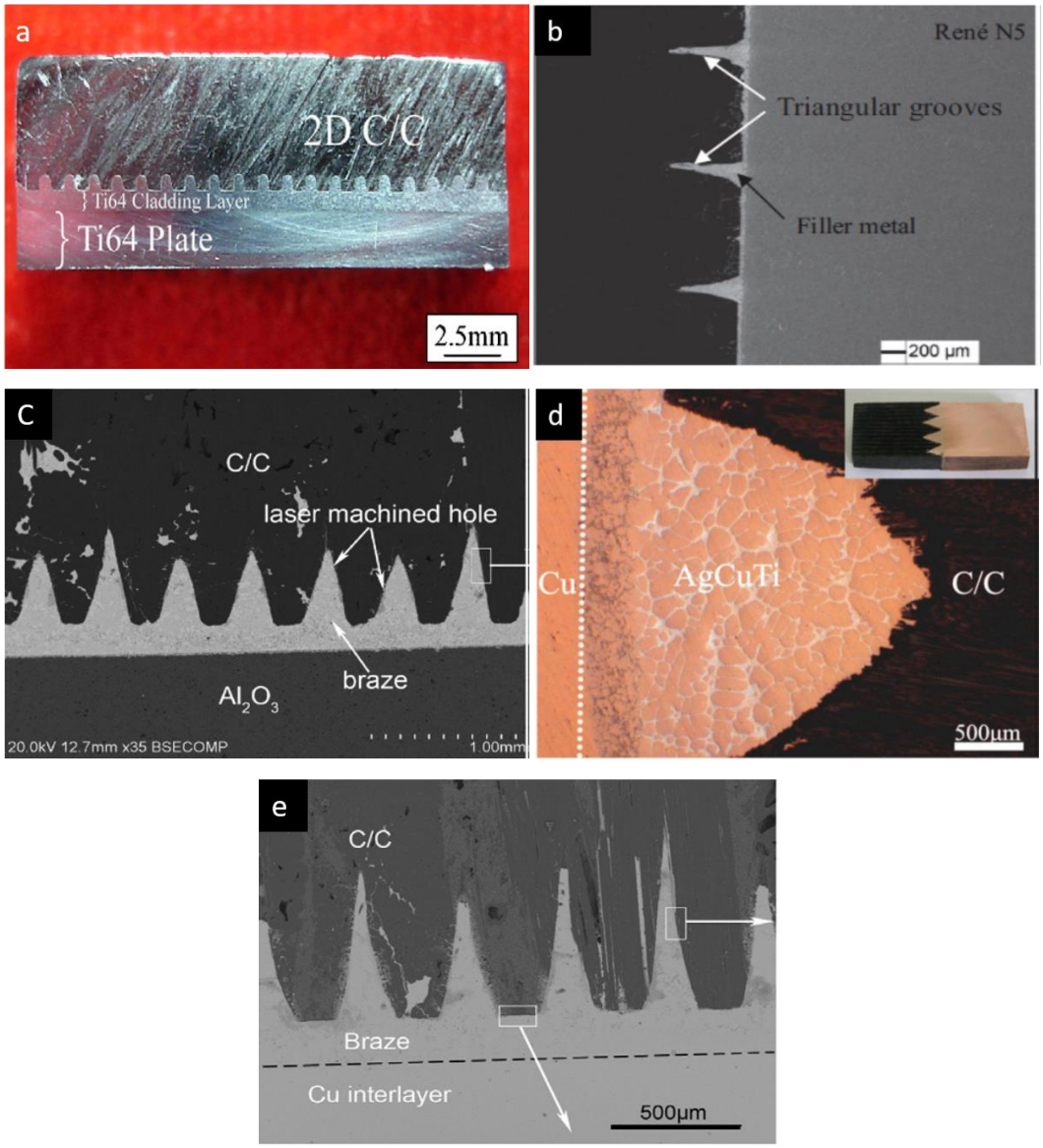

Figure 2.32. Joints with different surface patterning on the C/C composite, (a) rectangular groove pattern, (b) zigzag triangle groove pattern and (c), (d) and (e) conical hole pattern [27-30, 75].

Table 2.1. The shear strength of the joints with flat and patterned interfaces.

Joining surfaces	Interlayer	Pattern structure	Mechanical test	Strength of flat joints (MPa)	Strength of patterned joints (MPa)
C/C-Ti6Al4V [27]	Ti6Al4V clad	Rectangular grooves	Compressive shear	Interfacial debonding	41.63
C/C-Ni base superalloy [30]	Ti coating, Ag-28Cu and Al2O3	Conical holes	Four point bending	33	73
C/C-Cu [28]	Ag-68.8Cu-4.5Ti	Conical holes	Four point bending	14	52
C/C-TiAl [11]	Ag–26.7Cu–4.6Ti	Holes	Compressive shear	12.9	26.4
C/C-Cu [76]	Ti-Si	Conical holes	Compressive shear	-	53.7–73.4
W-Cu[43]	Cu	Holes	tensile	41.34	120.43
C/C-Rene N5[29]	Ag-Cu-Ti	Triangle grooves	Compressive shear	18.7	31
C/C-Cu [75]	Cu-Si-Ti	Conical holes	Compressive shear	44	79
Al2O3-stainless steel [44]	35Cu- 2Ti	Arc grooves	Compressive shear	24	66

Literature review on dissimilar joining of the patterned structure C/C composite to metals indicates that there are two different fracture mode after mechanical strength tests. In mode 1, the fracture occurs along the interface between the C/C composite and metal. Therefore, the metal that was infiltrated into the patterned structures completely pulls out from the C/C composite. Regarding the mode 2, the cracks propagate through the infiltrated structure which leads to fracture within the infiltrated structure [28-30, 44, 76]. These two modes of fracture or combination of them have been reported on dissimilar joining of patterned interface C/C composite or Al2O3 to metals [28-30, 44, 76]. For instance, Shen et al. investigated the joining of the C/C composite to Ni-based superalloy with flat or conical holes on

the C/C composite surface. The SEM images of the fracture surfaces on the superalloy side for flat and patterned interfaces are shown in Fig. 2.33 and Fig. 2.34. In the case of the joints with flat interface the fracture surface was flat and the joints cracked at or near the interface of the joints (Fig. 2.23). These observations are the characteristics of the brittle fracture. Therefore, the joints had low strength and the bending strength was 33 MPa. On the other hand, the fracture behavior was changed completely by fabrication of the conical holes on the surface of the C/C composite. In this case, some braze spikes pulled out form the C/C composite which signals that the cracks have propagated along the interface of the joints. Moreovere, some braze spikes were broken which reveals that the cracks propaged through the infiltrated braze material (Fig. 2.24). Therefore in this case the fracture is a combination of mode 1 and 2. Fig. 2.34(c) shows a pulled out braze spike. As can be seen, some C/C fibers stick to the pulled out braze spike which shows the cracks are deviated into the C/C composite. In the case of broken spike, a dimple dominated microstructure is observed at the fracture surface which indicates a significant plastic defromation and is the caracteristics of the tough fracture (Fig. 2.34(d,e)). Therefore, this mode of fracture is beneficial for increasing the compact resistance of the joints. Fig. 2.34(a) shows the crack propagation pass for the patterned interface joints. As seen in Fig. 2.34(a), the cracks pass was deviated several times. The crack deviation increases the crack propagation path and consequently more energy is consumed for crack propagation. This condition is beneficial to change the fracture mode from brittle to pseudo-plastic, and prohibit the catastrophic fracture [29, 30].

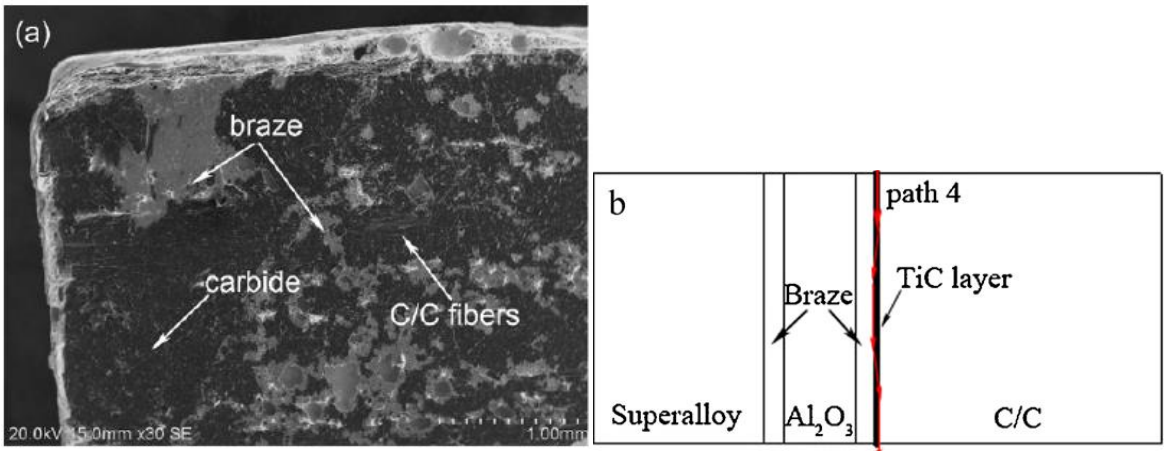

Figure 2.33. (a) fracture modes and (b) schematic of the fracture mode for the joining of superalloy to the flat surface C/C composite [30].

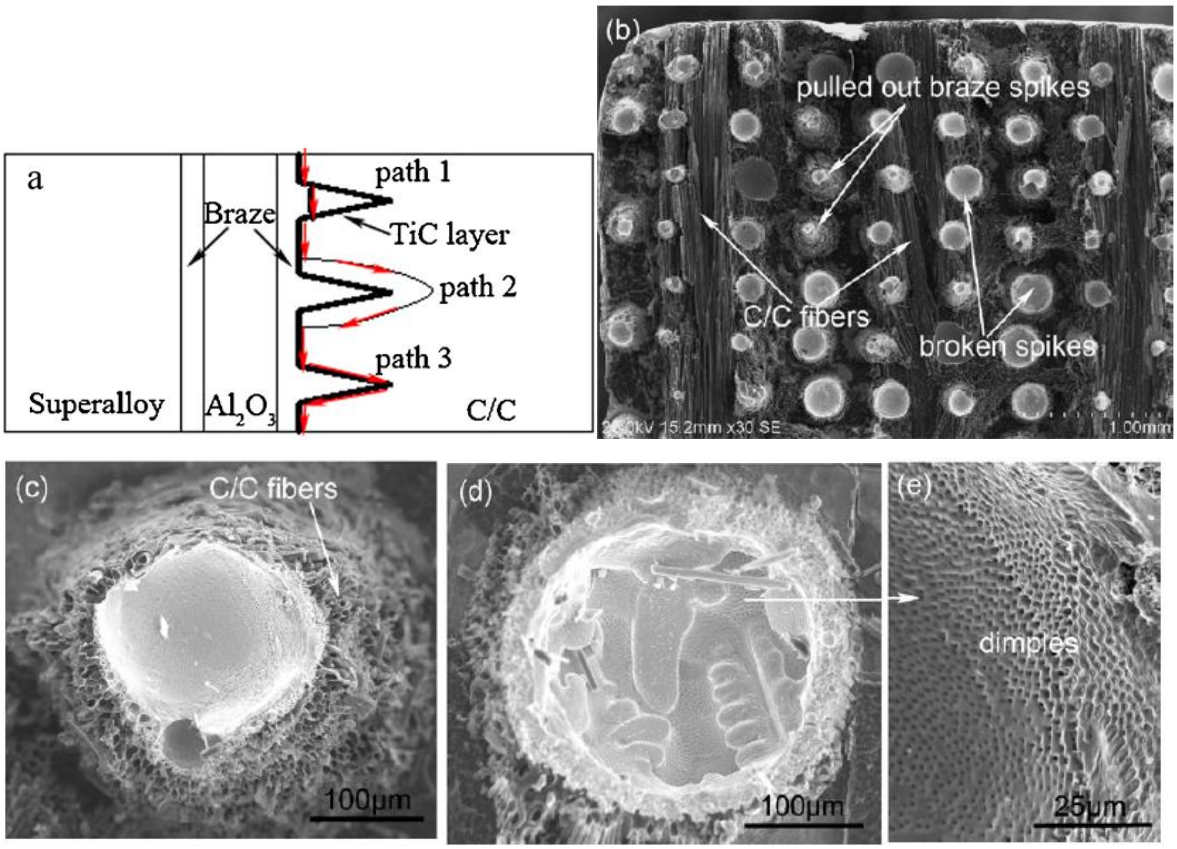

Figure 2.34. (a) Crack propagation path , (b) SEM images of the fracture surface of patterned interface, (c) pulled out braze spike and (d,e) broken spike [30].

2.2.2 Adhesive bonding

Adhesive bonding is another technique for integration of the C/C composites. This technique is normally used for similar joining of C/C composites. In adhesive bonding technique, normally the interlayer adhesive contains two components. The first part is matrix, which is an adhesive, and the second part is filler or reinforcement phase. There are two major categories of adhesives for similar joining of the C/C composites. One category is organic adhesives like phenolic resin and tetraethylorthosilicate adhesives and the second category is inorganic adhesive, such as barium aluminum borosilicate (SABB). Regarding the filler phase, different fillers such as B4C, SiC_w and CNTs can be used to reinforce the adhesive matrix [3, 9, 26, 77, 78]. In order to make a joint by adhesive composite, first the adhesive matrix and reinforcing phase should be homogeneously mixed. After making the joining assembly, the adhesive composite should be cured at the temperature around 200 °C and under pressure. The last step is to calcine the cured joints at high temperature [78].

The organic adhesives are very brittle and they are required to have better toughness to be used in engineering applications [3, 78]. An effective approach to improve the strength and toughness of adhesives is adding whiskers or nanotubes to them. In order to achieve a proper composite adhesive, the reinforcing phase should be dispersed uniformly in the matrix and a sufficient interfacial bonding between matrix and reinforcement phase is required [78]. In this part, two major factors in adhesive bonding including reinforcement phase content and calcination temperature are discussed.

2.2.2.1 Reinforcement phase optimization

Finding the optimum content of the reinforcing phase is important because there is an optimum amount of the reinforcing phase to obtain the highest joint strength. It is very important to note that the reinforcing phase should be dispersed properly in the adhesive matrix to avoid agglomeration. If the reinforcement content is increased higher than optimum amount, the quality of adhesive joint will decreased as a result of lack of infiltration of the adhesive matrix into the agglomerated areas and consequently stress concentration in these areas. In the case of using whiskers or nanotubes as reinforcing phase, there is a considerable van der Waals-forces between reinforcing phases. Therefore, these materials are prone to make contact and be agglomerated. As a result, it is difficult to disperse them in the matrix if exceed the optimum content. The study on the effect of the SiC_w and CNTs content in the polymer base adhesive composite showed that the optimum amounts of the CNTs and SiC_w content are 0.3 and 0.75 wt% respectively. Fig. 2.35 shows the effects of the different SiC_w and CNTs contents in the adhesive on the shear strength of the joints for calcination temperatures of 700 and 1100 °C. As can be seen, for both calcination temperatures, the maximum strength of the joints were obtained for 0.75 of SiC_w and 0.3 wt% of the CNTs. Fig. 2.36 shows the distribution of the CNTs within the matrix for 0.3 and 1 wt% of the CNTs contents. It is obvious, when adhesive contains 0.3 wt% CNTs, the reinforcing phase was homogenously distributed on the adhesive matrix. By contrast, in the case of 1 wt% Content of CNTs, the CNTS were agglomerated and distributed inhomogenously. The adhesive matrix cannot be infiltrated into the agglomerated CNT. Therefore, the bonding between the adhesive matrix and CNTs was weak which caused the stress concentration in the agglomerates. As a result of the stress concentration, the agglomerated CNTs were prone to crack, leading to joining defects and deterioration of the joints [78].

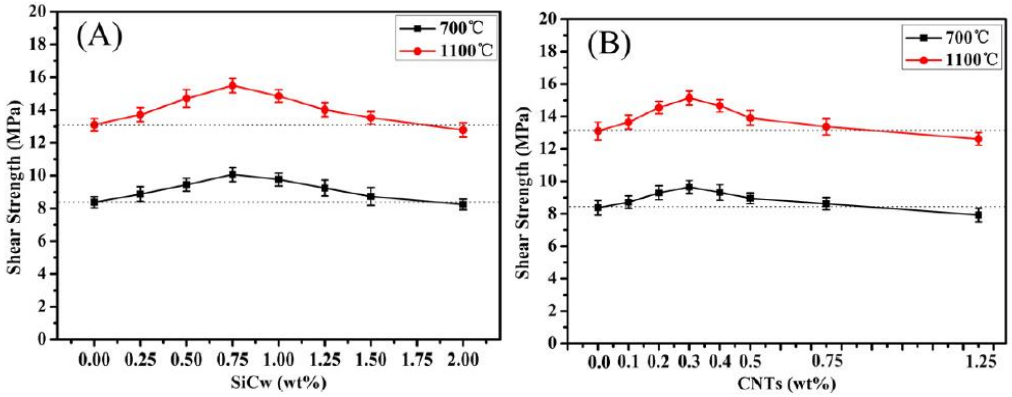

Figure 2.35. Shear strength of the C/C composite similar joints with different contents of (A) SiC_w and (B) CNTs in the adhesive [78].

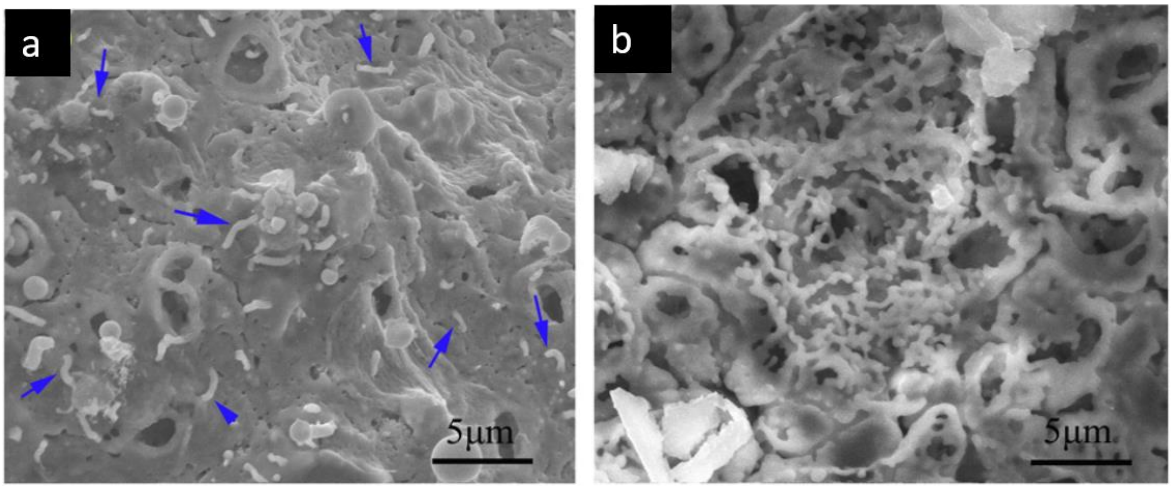

Figure 2.36. SEM images of distribution of the CNTs (a) 0.3 wt% and (b) 1 wt% [78].

2.2.2.2 Calcination temperature

The heat treatment or calcination temperature affects the quality of the joints as a result of the changing the composition and structural evolution of the adhesive by changing the temperature [3, 78]. For instance the composition evolution for silicone resin adhesive modified by Al, SiC, B4C and low-temperature melting glass powders (SSP) is shown in Fig.2.37. As can be seen by increasing the temperature, some phases are formed and some phases are disappeared which consequently affect the strength of the joints. Fig. 2.38 shows the room temperature shear strength (RTSS) of the joints by changing the calcination temperatures from 200 to 1500 °C. As can be seen, there is high fluctuation in

the shear strength of the joints at different calcination temperatures. According to the Fig. 2.38 the RTSS curves contains 4 different distinct zones. First, by increasing the temperature from 200 to 300 °C, the shear strength of the joints increases from 6.8 to 9.3 MPa which was ascribed to the further polymerization of silicon resin. Regarding the second zone, the temperature between 300 to 500 °C, the shear strength was decreased from 9.3 to 7.2 MPa as a result of the decomposition of the silicon resin and consequently formation of the porosities. The shear strength of the joints increased gradually from 7.2 to 16.3 MPa by increasing the temperature from 500 to 1300 °C describing by following reasons: (1) The Al and B4C were oxidized by oxygen containing molecules of resin and led to producing considering volume expansion and consequently compensating the volume contraction caused by resin decomposition. (2) The melted SSP glass and formed B2O3 and borosilicate glass with high viscosity filled pores and cracks at the bonding area and provided strong glass-bonding strength after solidification. (3) By increasing the temperature, a significant amount of heat resistance ceramics such as SiC, Al2O3, AlPO4 and mullite were generated which increased the strength and thermal stability of the joints. (4) the SiO2 reacted with the C/C composite as well as penetration of SiC into the C/C composite formed a composition gradient at the interface of the joints which decreased the residual stress caused by difference between the CTE of the components. Regarding the fourth region, by increasing the temperature from 1300 to 1500 °C, the shear strength decreased to 7.5 as a result of the decomposition of AlPO4, amorphous glass and borosilicate [52].

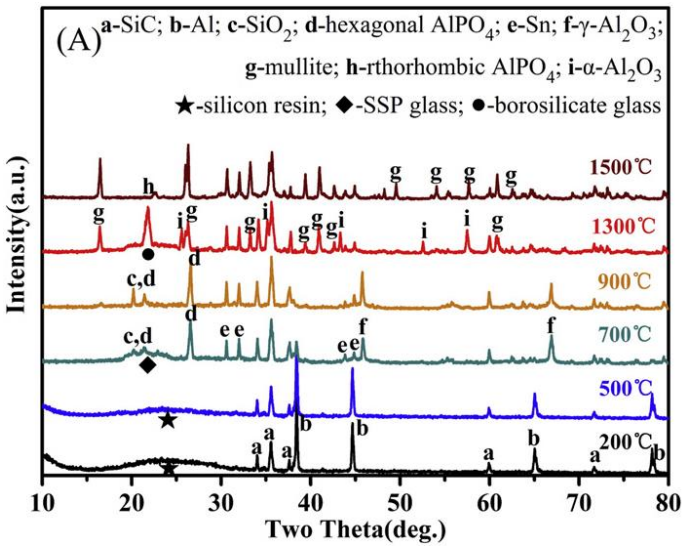

Figure 2.37. XRD analysis of the adhesive composite calcined at different temperatures [3].

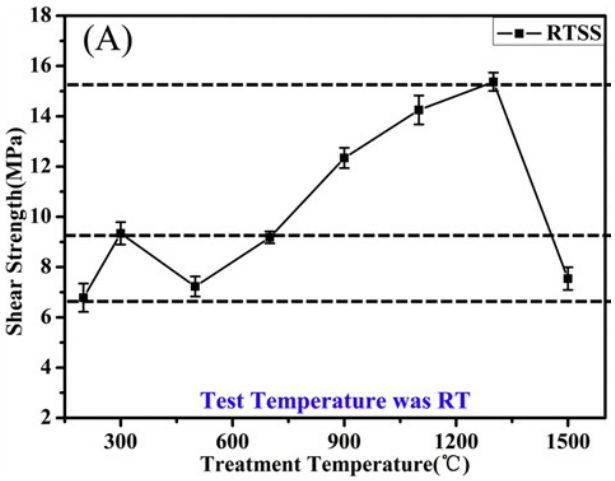

Figure 2.38. RTSS results of the adhesive composite calcined at different temperatures from 100 to 1500 °C [3].

Chapter 3
Experimental methods

3.1 Materials

3.1.1 C/C composites

The two different C/C composites used in this study were a multi-ply 2D woven C/C composite with high porosity content (low strength) and a 3D C/C composite with low porosity content (high strength). The multi-ply 2D woven carbon–carbon composite laminate with the thickness of 2 mm (6 laminas), electrical resistivity of 26.5 μΩ.m and the interlaminar shear strength of 8 MPa were purchased from CeraMaterials. This 2D C/C composite has a density of 1.51 g/cm^3 and open porosity content of 14.8%, which was made with the Polymer Infiltration and Pyrolysis (PIP) process. The 3D C/C composite with a thickness of 5 mm, electrical resistivity of 9 μΩ.m, density of 1.86 g/cm^3 and open porosity content of 4.1% was purchased from HTMAGROUP. This high strength 3D C/C composite was fabricated by the Chemical Vapor Infiltration (CVI) process.

3.1.2 Titanium

A 1 mm Ti6Al4V (Grade 5) was purchased from the Titanium Joe for purpose of the dissimilar joining of the 2D and 3D C/C composites to Ti6Al4V. The composition of the Ti6Al4V is provided in Table 3.1.

Table 3.1. Chemical composition of the Ti6Al4V.

Element	Content (%)
Titanium, Ti	87.6 - 91
Aluminum, Al	5.5 - 6.75
Vanadium, V	3.5 - 4.5
Iron, Fe	≤ 0.40
Oxygen, O	≤ 0.20
Carbon, C	≤ 0.080
Nitrogen, N	≤ 0.050
Hydrogen, H	≤ 0.015

3.1.3 Copper

The copper C110 plate with composition of >99.90% Cu and the thickness of 1.3 mm is used for the purpose of the dissimilar joining of the 2D C/C composite to copper.

3.1.4 Interlayers

Three different interlayers including Ti6Al4V thin sheets with the thickness of 200 and 400 µm were used as interlayer for dissimilar joining of the 2D C/C composite to copper. A Ti powder (purity >99%, particle size< 44µm) was used as an interlayer for joining of the 2D C/C composite to copper and joining of groove patterned 3D C/C composite to Ti6Al4V.

3.2 Metallographic preparation

For metallographic preparation, an abrasive cut-off saw was used to cut the samples in desired dimension. Then samples were cold mounted by epoxy resin (Struers Polyfast^{Tm}) and grounded using silicon carbide papers with the grit of 180, 320, 400, 600, 800 and 1200. Diamond suspension sprays (LECO^{R}) with the particle size of 9, 6, 3, 1 and 0.25 micron were used for accomplishment of polishing.

3.3 Preparation of the surfaces of the substrates

Before joining, the surfaces were ground up to 600 grit by means of silicon carbide paper and were ultrasonically cleaned in acetone for 30 minutes.

3.4 Joining process

Reactive resistance spot welding was conducted using DC spot welding machine (Centerline Ltd., Windsor, ON, Canada) with a median-frequency and it is shown in Fig. 3.1. The welding electrodes were RWMA Class II, with the diameter of 8, 12 and 16 mm for different joining procedures. The joining components were held in place between two copper electrodes which were used for applying DC current and force during the joining process. Weld force, for all experiments, was set at 2 kN and a single 200 ms pulse was used for the weld cycle. The hold time was 5 s and the coolig water flow rate was 4 L/min. The welding current detremined based on the different experiments and joining components and will provided later.

Figure 3.1. MFDC RSW machine.

3.5 Shear strength

The most commonly used characterization technique to evaluate the load-bearing capability of the similar and dissimilar joining of the C/C composite is compressive shear testing. This method has been widely used in previous studies as a result of its simplicity in specimen fabrication and testing. In shear test, the most important measured factor of the quality of the joint is the load to fracture. To evaluate

the mechanical properties of the joints, shear strength tests of the joined samples were performed with the universal testing machine with capacity of 5kN at a rate of 0.5 mm/min, and five replicates of shear tests were done for each condition of joining. The shearing fixture and the schematic representation of shear set-up are shown respectively in Fig. 3.2 and Fig. 3.3.

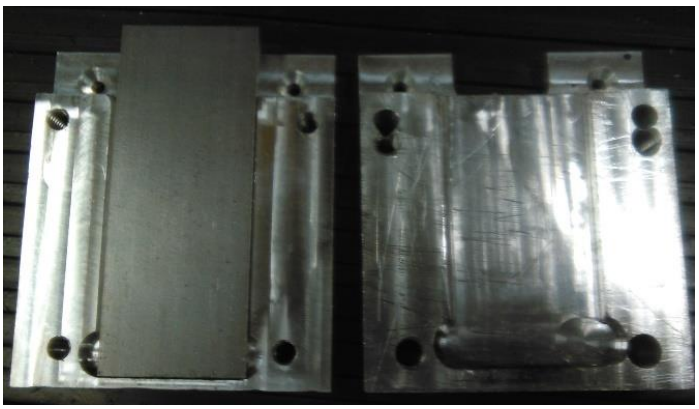

Figure 3.2. Fixture for shear test.

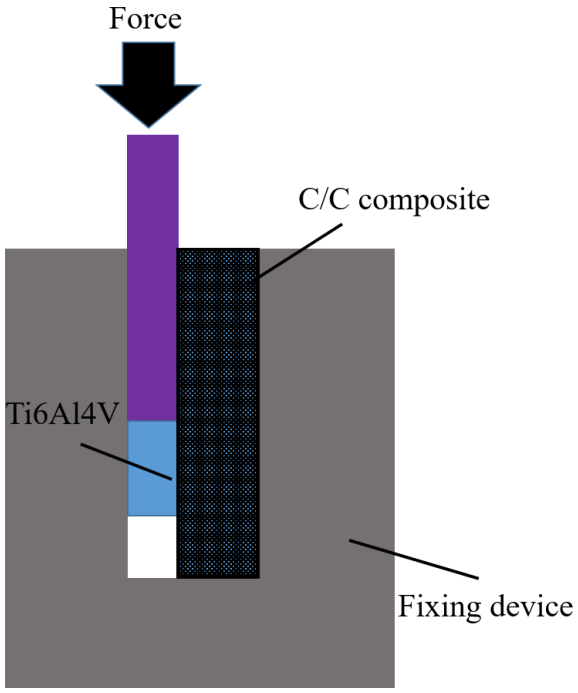

Figure 3.3. Schematic of the shear test setup.

3.6 Grazing Incidence X-ray Diffraction (GIXRD) and X-Ray Diffraction (XRD)

GIXRD was used to investigate the composition of thin layer at the interface between C/C composite and Ti. Moreover, XRD was used to determine the chemical composition at the interface between the Ti interlayer and copper. The GIXRD and XRD patterns were captured by a CuKa1 radiation (k = 0.15406 nm) (Bruker D8 diffractometer). The accelerating voltage and current were 50 kV of 40 mA, respectively. The diffraction data collected with the rate of 1 º min-1. Fig. 3.4 shows the machine for GIXRD and XRD analysis. The XRD patterns were analyzed by X'pert HighScore software.

Figure 3.4. GIXRD and XRD machine.

3.7 Microscopy

The microstructure examination of the weld samples was conducted by optical microscopy (OM) and scanning electron microscopy (SEM). Optical microscopy was conducted by Olympus BX51M with image analysis software QCapture Pro Ver. 5.1. Moreover, The SEM micrographs were obtained using a Zeiss Merlin scanning electron microscope equipped with field emission gun. An energy dispersive spectroscopy (EDS) microanalysis system was coupled to the electron microscope to identify elemental compositions at the interface of the joint.

Chapter 4

Fabrication of 2D Carbon/Carbon composite-Ti6Al4V hybrid structures by using direct dissimilar joining through reactive resistance spot welding

In Chapter 4, the feasibility of the direct dissimilar joining of the flat surface 2D C/C composite to Ti6Al4V is discussed. The aim of this chapter is to investigate the effects of the welding parameters on the strength and area of the joints. Furthermore, the mechanisms of the joining and the effects of the open porosity of the 2D C/C composite on the quality of the joints are discussed.

4.1 Introduction

C/C composites are well known as a promising material for high temperature applications due to a number of factors including their low density, low coefficient of thermal expansion (CTE), high thermal stability, good ablation and thermal shock resistances, and high strength-to-weight ratio at elevated temperatures [3, 59-62]. As the result of a combination of these properties, C/C composites are expected to be widely used in automotive and high temperature operation fields such as turbine engine components, heat shields, brakes, nozzles, hot press dies, and high temperature furnaces [2, 7-12]. One of the most essential requirements for extending the applications of C/C composites at high temperatures is to couple them with other materials such as TiAl, copper, and Ti6Al4V [8, 14, 17-23]. In many advanced applications, C/C composites must be joined to Ti6Al4V that is extensively used in a variety of thermal advanced structures due to its low density, specific strength, and excellent high temperature properties [17, 19-21, 24]. However, it is not easy to obtain high quality joints between the C/C composites and other materials such as metals or ceramic because of the unique crystal structure, and as well as special physical, chemical, and mechanical properties of carbon and C/C composites.

In the first place, joining of C/C composites by conventional fusion welding techniques seems to be impossible due to the high melting point of C/C composites, which cannot be melted at the welding temperature. However, the literature on reactive brazing of C/C composites reveals that in the cases in which the braze alloys contained Ti as the reactive element, the reaction between Ti and carbon results in a robust bonding between braze materials and the C/C composite [2, 10, 31-39]. The same approach can be employed for direct dissimilar joining of the 2D C/C composite to Ti6Al4V by using the spot

welding technique due to the solid-liquid state reaction between melted titanium and solid carbon, along with the infiltration of melted metal into the 2D C/C composite's porosity.

The 2D C/C composite used in this study is very inexpensive with excellent thermal and moderate mechanical properties, the joining of which to Ti6Al4V will consequently result in a hybrid structure with interesting mechanical and thermal properties. In this research, for the first time an innovative method for direct dissimilar joining of 2D C/C composite to Ti6Al4V is introduced. The major goal of the present study is to investigate the possibility of direct dissimilar joining of the 2D C/C composite to Ti6Al4V by the reactive resistance spot welding technique. Moreover, the mechanism of the joining and the optimum parameters of the joining are investigated.

4.2 Experimental procedure

The C/C composites used in this study were a multi-ply 2D woven C/C composite with high porosity content (low strength). The multi-ply 2D woven carbon–carbon composite laminate with the thickness of 2 mm (6 laminas), electrical resistivity of 26.5 μΩ.m and the interlaminar shear strength of 8 MPa were purchased from CeraMaterials. This 2D C/C composite has a density of 1.51 g/cm^3 and open porosity content of 14.8%, which was made with the Polymer Infiltration and Pyrolysis (PIP) process. The 1 mm thick Ti6Al4V sheets were cut into 25 mm × 30 mm pieces. The 2D C/C composite panels were then cut into 25 mm × 30 mm × 2 mm slices for microstructural analysis, and 50 mm × 30 mm × 2 mm for the shear strength testing. Before joining, the surfaces were ground up to 600 grit by means of silicon carbide paper and were ultrasonically cleaned in acetone for 30 minutes. The 2D C/C composites with flat surface were directly joined to Ti6Al4V. A DC spot welding machine was used for the purpose of joining. Flat welding electrodes were RWMA Class II, with the diameter of 16 mm. The 2D C/C composite and Ti6Al4V were held in place between two flat copper electrodes which were used for applying DC current and force during the joining process. A schematic diagram of the joining assembly is shown in Fig. 4.1. Weld force, for all experiments, was set at 2 kN and a single 200 ms pulse was used for the weld cycle. The hold time was 5 s and the coolig water flow rate was 4 L/min. The welding current was varied from 4 kA to 8 kA to investigate the effects of the current on the strength of the joints.

The cross-sections of the joints and fracture surfaces were investigated by optical microscope and scanning electron microscope (SEM) equipped with Energy-dispersive X-ray spectroscopy detector

(EDS). In addition, Grazing Incidence X-ray Diffraction (GIXRD) was utilized to identify the composition at the interface of the joint. Shear strength tests of the joined samples were then performed with the universal testing machine at a rate of 0.5 mm/min, and five replicates of shear tests were done for each condition of joining. The shear strength of the joints was calculated as the ratio of the maximum force to the area of joint surface. The area of the joint was considered as the area that C/C composite adhered to the Ti6Al4V side and was measured by ImageJ software.

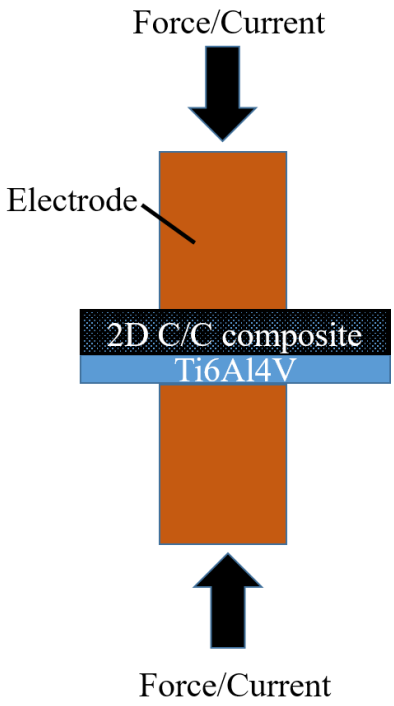

Figure 4.1. Schematic of the joining setup.

4.3 Results and discussion

4.3.1 Characterization of the microstructure of the joints

Fig. 4.2 depicts the surface microstructure of the 2D C/C composite. As can be seen, a high content of cracks and porosities are observed on the surface of the 2D C/C composite. The high cracks and porosity content can facilitate the infiltration of the melted Ti into the C/C composite. Fig. 4.3(a) shows the typical optical microscope image of the cross section of the joint between 2D C/C composite and

Ti6Al4V. As shown in Fig. 4.3(a), a fusion zone was formed at the Ti6Al4V side as a result of melting and solidification of Ti6Al4V during the joining process. Fig. 4.3 (b-e) depicts the SEM microstructure of the Ti6Al4V-2D C/C composite joints for the currents from 4 to 8 kA. It was observed that for all the currents, the interfaces between the Ti6Al4V-2D C/C composite joints were microstructurally sound and the interfaces of the joints were free of any commonly-found interfacial defects such as micro voids, pores, and cracks. It can be seen from Fig. 4.4 that some melted Ti6Al4V infiltrated into the inherent fabrication process pores and cracks of the 2D C/C composite. The high open porosity content of 2D C/C composite (14.8%) facilitated the infiltration of the melted Ti6Al4V into the 2D C/C composite by a capillary action. This infiltrated structure is typical and beneficial as it increases the contact area between the 2D C/C composite and Ti6Al4V. Such a structure can form a mechanical occlusion between the joining components, which tightly pins up the interface of the joint and consequently contributes to the joining strength [10, 11, 28, 40, 41].

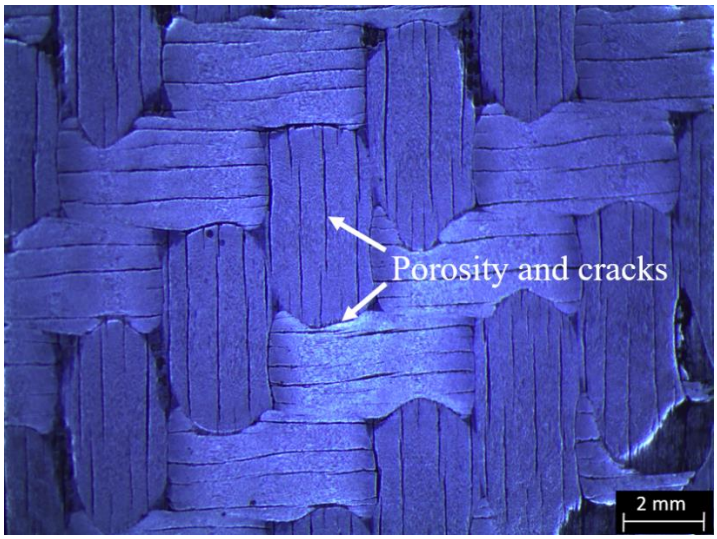

Figure 4.2. The surface of the 2D C/C composite.

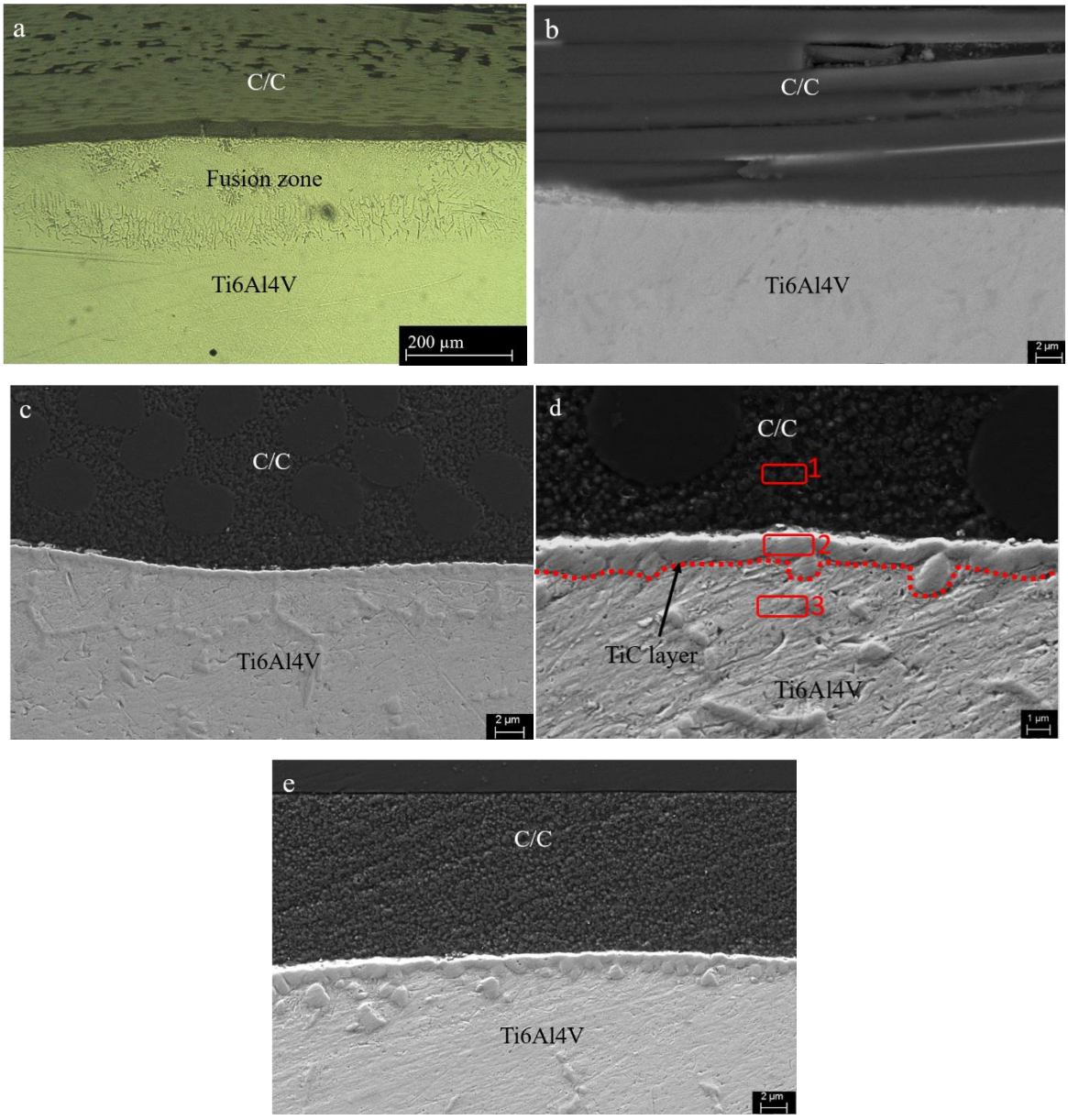

Figure 4.3. (a) Typical low magnification image of the joint interface, (b) the interface between the 2D C/C composite and Ti6Al4V for a current of 4 kA, (c) 5 kA, (d) 6 kA and (e) 8 kA.

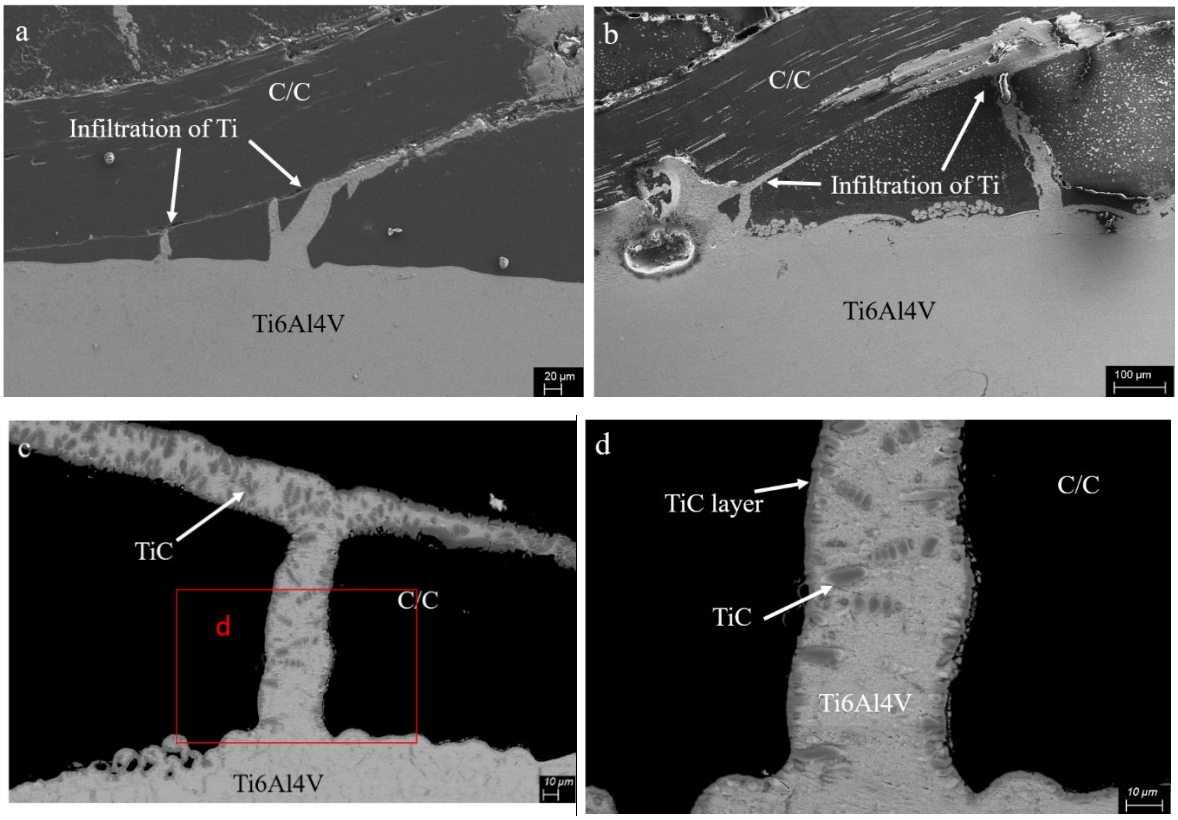

Figure 4.4. Typical images of the penetration and infiltration of the melted Ti6Al4V through the pores and cracks formed in the 2D C/C fabrication process, (a) 5 kA, (b) 6 kA, (c) SEM-backscattered of 6 kA and (d) selected area in (c).

A highly magnified image of the interface of the 2D C/C-Ti6Al4V joint shows the formation of a thin layer with the thickness of 1 to 2 μm (Fig. 4.3(d) and 4.4(c,d)). SEM-backscattered images of Fig. 4.4(c,d) clearly shows the formation of the continuous dark gray phase at the interface and also dark gray particles which are embedded in the light gray Ti matrix. The formation of the interfacial phase can be attributed to the reaction between the C/C composite and Ti6Al4V [20, 34, 35, 79]. In the case of similar joining of the C/C composite by using compacted titanium powder or titanium foil, the formation of a thin TiC layer as a result of the reaction between Ti and carbon of C/C composite has been reported [2, 31, 32, 55]. The EDS analysis of Fig 4.3(d) are presented in the Table 4.1. As EDS analysis indicated (Table 4.1), the reaction layer and particles are rich in the elements of C and Ti which is an evidence of the formation of the TiC as a result of high chemical affinity between Ti and C. According to the thermodynamics point of view, the Gibb's free energy of formation of TiC is highly negative, indicating the formation of TiC at the interface between Ti and the C/C composite is

thermodynamically favorable [36, 67, 80]. The GIXRD results of the interface of Ti6A4V-2D C/C composite joint are shown in Fig. 4.5. As already expected, three phases including Ti, Carbon, and TiC were detected in the GIXRD spectrum. The detection of the TiC phase at the interface of the joint is in good accordance with the EDS analysis results.

Table 4.1. EDS analysis for Fig. 4.3(d).

Point	1				2				3			
Element	C	Ti	Al	V	C	Ti	Al	V	C	Ti	Al	V
Weight %	93.80	5.78	0.08	0.35	25.37	70.89	2.33	1.42	3.46	85.15	6.54	4.85
Atomic %	98.36	1.52	0.04	0.09	57.00	39.93	2.33	0.75	11.98	73.97	10.08	3.96

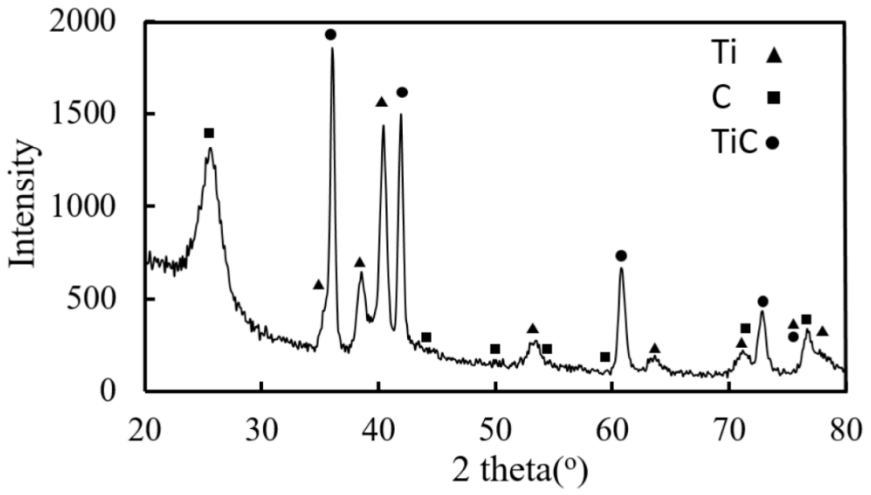

Figure 4.5. GIXRD at the interface of Ti6A4V-2D C/C composite joint.

Based on the microstructure observations, EDS and GIXRD results, it can be inferred that the solid-liquid reaction between Ti6Al4V and the 2D C/C composite, as well as the infiltration of the melted metal in the pores of the 2D C/C composites were the dominant mechanisms of the joining and contributed to both metallurgical and mechanical bonding. The Joule heating caused by resistance welding can melt the Ti6Al4V, but the 2D C/C composite cannot be melted due to its high melting point. Therefore, the formation of a TiC at the interface of the joint can be described by a conceivable solid-liquid reaction between the melted Ti and the carbon of the 2D C/C composite. In fact, the formation of a TiC phase at the interface of the C/C composites joints, in the cases where the interlayers

contained titanium, has been widely reported in previous investigations [2, 10, 31-38, 81, 82]. Moreover, a carbide layer forming at the interface can decrease the interfacial tension, and consequently improve the wettability of the molten Ti on the C/C composite [33-37]. Such effects, as well as the importance of Ti on the wettability, have been reported in many Ti-containing brazing systems [33-38].

4.3.2 Mechanical properties of the joints

Fig. 4.6(a) shows the shear strength of the 2D C/C composite-Ti6Al4V joints for different welding currents ranging from 4 to 8 kA. As shown, the shear strength of the joints was almost the same in the current range from 4 to 6 kA at about 7 MPa which is comparable to the maximum interlaminar shear strength of the 2D C/C composite (8 MPa). It should be noted that for all the joining conditions, fracture occurred in the 2D C/C composite and not at the interface of the joints (Fig. 4.7). Therefore, it can be deduced that the shear strength of the joints is not determined by the strength of the interfaces of joints, but by the 2D C/C composite. Therefore, the effective shear strength of the joints cannot exceed the maximum interlaminar shear strength of the 2D C/C composite. This is the reason for the almost constant shear strength of the joints in the current range from 4 to 6 kA. Failure of the joints within the C/C composite has also been widely reported in previous publications [2, 26, 28, 31, 34, 36, 68, 70, 83]. A typical fracture surface of joints is shown in Fig. 4.7. As can be seen, the joint failed within the 2D C/C composite and the line scanning image of Ti element shows the presence of the Ti at the fracture surface which is the result of infiltration of melted Ti6Al4V into the 2D C/C composite porosities. As seen in Fig. 4.6(a), by increasing the current from 4 to 6 kA, the fracture shear force increased as a result of increase in the joint area. By increasing the current, the Joule heating is increased, therefore more melted metal is formed at the interface of the joint and consequently the joint area and the fracture shear force are increased (Fig. 4.6(a) and (b)). From Fig. 4.6(a), it can be seen that the fracture shear force and strength decreased dramatically by increasing the current from 6 to 8 kA. The Joule heat produced at current of 8 kA was excessive and caused sticking of the 2D C/C composite surfaces to the copper electrodes. During the detachment of the 2D C/C composites from the electrodes, the 2D C/C surfaces were damaged which caused the deterioration of their mechanical strength (Fig. 4.8(a) and (b)). As can be seen in Fig. 4.8(b) and (c), the surface of 2D C/C was damaged by a current of 8 kA, while such damage did not occur with the current of 6 kA. So, considering the maximum fracture shear force was obtained at current of 6 kA, it can be concluded that this current is the optimum current of joining with the present materials and welding setup.

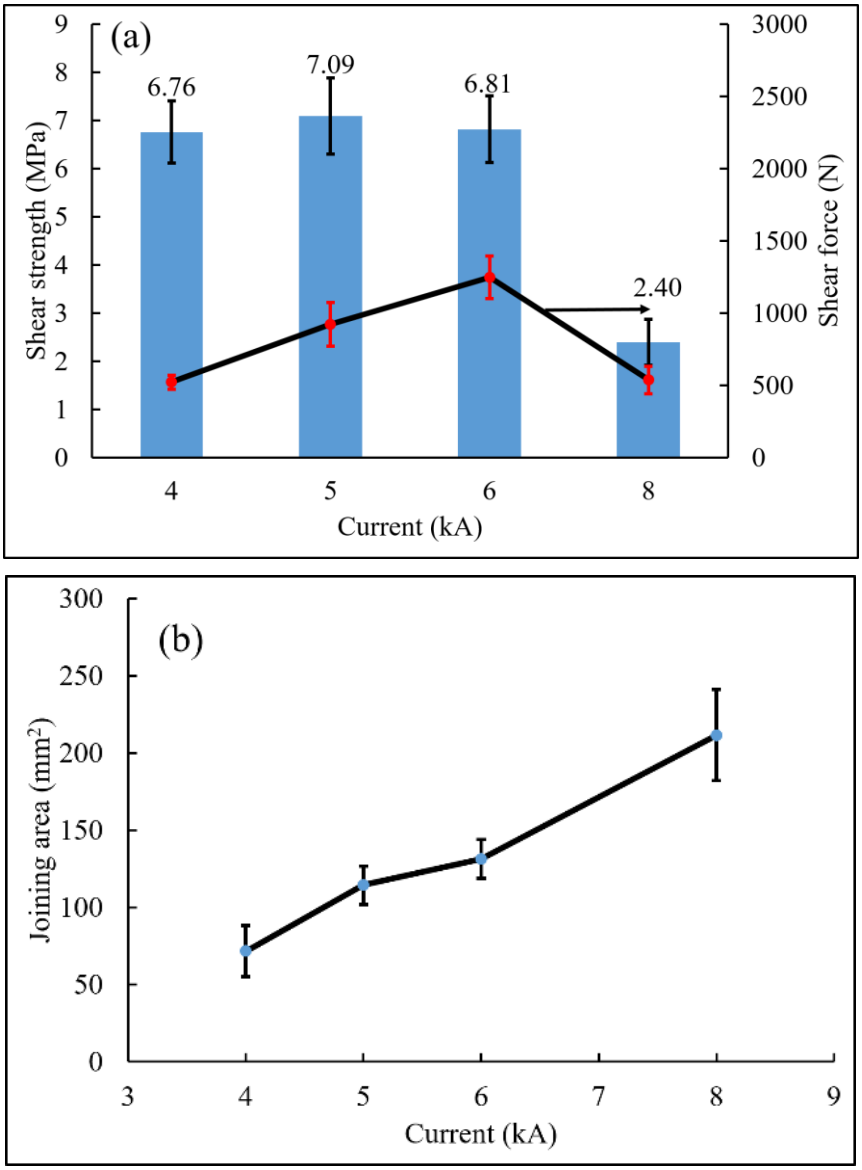

Figure 4.6. (a) Shear strength and shear force and (b) joining area of 2D C/C composite-Ti6Al4V joints at different currents.

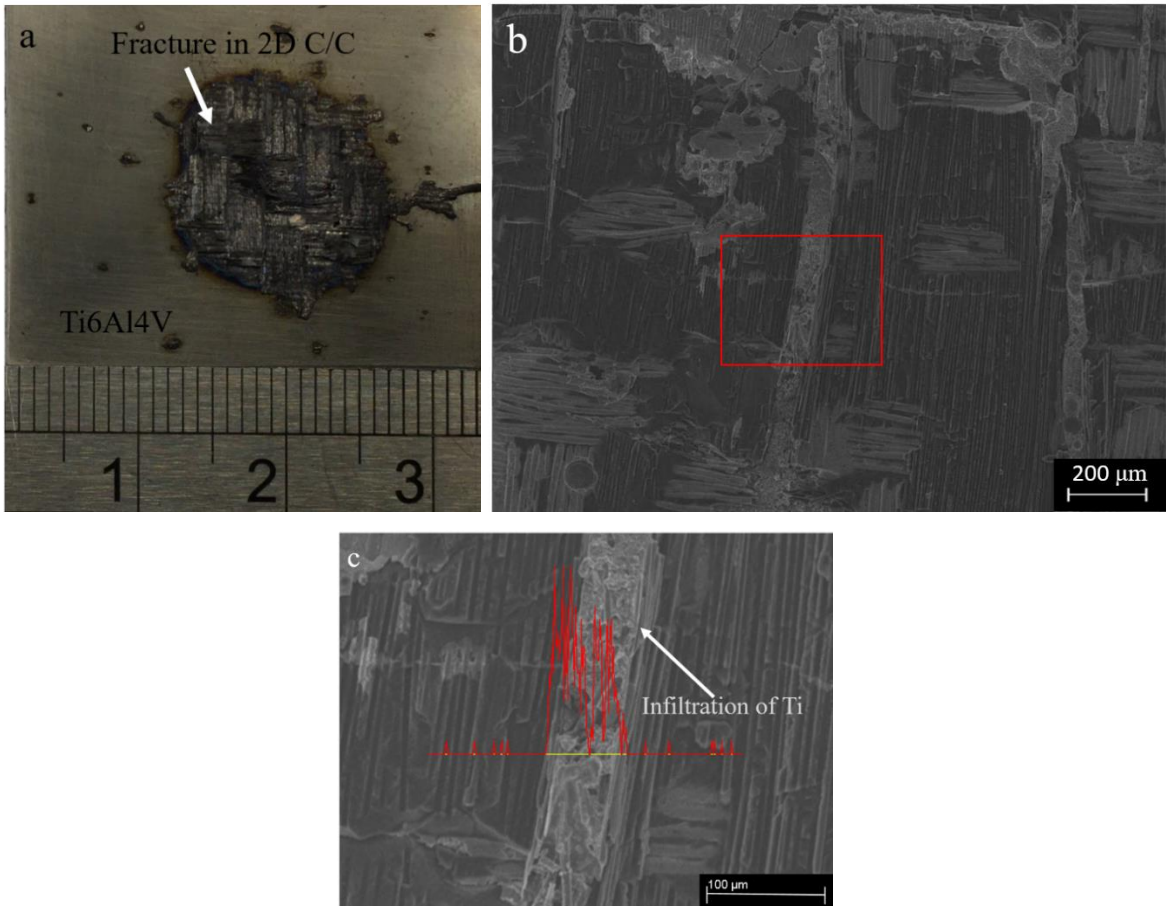

Figure 4.7. (a) Typical fracture surface of the 2D C/C composite-Ti6Al4V joint after the shear test, (b) SEM image of the fractured surface and (c) line scanning analysis of Ti element for the selected area in (b).

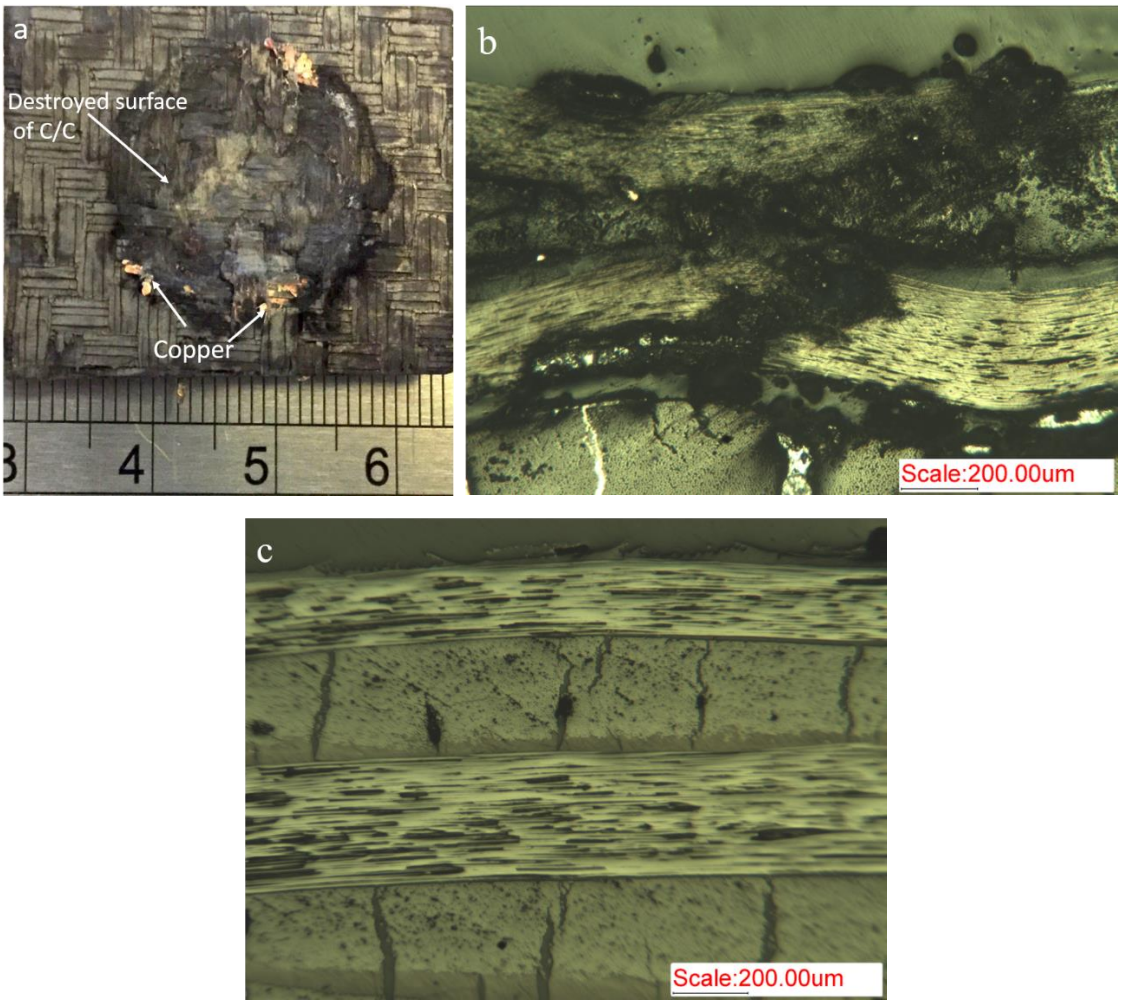

Figure 4.8. (a) Photograph of the damaged surface of the 2D C/C composite in contact with the copper electrodes for the current of 8 kA, (b) cross section of the joints near the surface of 2D C/C composite for the current of 8 kA and (c) 6 kA.

Overall, the shear strength obtained in this research is comparable with the results of the other investigations on the joining of C/C composites [2, 9, 26, 31, 36, 68]. In addition, based on the shear strength obtained, the 2D C/C-Ti6Al4V joints have the potential to be applied in advanced and high temperature applications such as heat shields, nozzles, and turbine engine and high temperature furnace components. The appropriate structures for the mentioned applications must be able to withstand high temperature operating environments while subjected to moderate tensile stresses [31].

4.4 Summary

In this study, the feasibility of the direct dissimilar joining of the 2D C/C composite to Ti6Al4V by the reactive resistance spot welding technique, as an innovative joining technique, was investigated and the following conclusions can be drawn:

1. Microstructure observation indicated that a well-bonded interface formed between the 2D C/C-Ti6Al4V joints. The interfaces were free of the commonly-found structural defects such as microvoids and porosity.

2. The solid-liquid reaction and infiltration of the melted metal in the 2D C/C porosity can be considered as the dominant mechanisms of joining. Ti6Al4V was melted as a result of Joule heat produced during resistance welding. The melted metal reacted with the carbon of the 2D C/C composite to form a thin TiC layer with a thickness of 1 to 2 μm at the interface of the joint. This thin TiC layer improved the mechanical properties of the joint due to the formation of chemical bonding at the interface of the joint. Moreover, the infiltration of melted Ti6Al4V into the 2D C/C composite porosity increased the contact area between the 2D C/C composites and Ti6Al4V. The infiltrated structure acted as micro-nails that tightly pinned the 2D C/C–Ti6Al4V interface.

3. In all shear tests, the failure occurred within the 2D C/C composite and not within the joints, demonstrating that the joining between 2D C/C and Ti6Al4V is mechanically stronger than the 2D C/C composite. The shear strength of the joints was almost the same (about 7 MPa) in the range of current from 4 to 6 kA, making it comparable with the maximum interlaminar shear strength of the 2D C/C composites which is 8 MPa. By increasing the joining current, the heat produced by Joule heating is increased, causing an increase in the surface area of the joints as well as the fracture shear force which eventually made the optimum current of welding 6 KA with the present materials and setup.

Chapter 5

Fabrication of 3D Carbon/Carbon composite-Ti6Al4V hybrid structures using rectangular groove patterned interface through reactive resistance spot welding

In this chapter, the feasibility of joining the groove-patterned 3D C/C composite to Ti6Al4V is studied. unlike the joining by using the 2D C/C composite (high porosity content), in the case of the joints by using the 3D C/C composite, the melted Ti cannot be infiltrated into the low porosity content of 3D C/C composite (4.1%). Therefore, in order to facilitate the infiltration of the melted metal into the 3D C/C composite, the rectangular grooves were machined on the surface of 3D C/C composites. Moreover, the effects of the dimension of the rectangular grooves on the strength and fracture mode of the joints are investigated.

5.1 Introduction

C/C composites are considered as fascinating materials for a wide range of high temperature applications such as heat shields, nozzles, hot press dies, turbine engine components, brakes, and high temperature furnaces [2, 7-13]. The high interest for using C/C composites is due to their small coefficient of thermal expansion (CTE), good ablation and thermal shock resistances, low density, high thermal stability, and high strength-to-weight ratio at elevated temperatures [1-6]. Ti alloys are a very common material for high temperature applications. Therefore, for many applications of the C/C composites, they may need to be joined to Ti6Al4V [17, 19-21, 24].

In this chapter, dissimilar joining of the 3D C/C composite to Ti6Al4V is studied. Dissimilar joining of the 3D C/C composite to Ti6Al4V is very challenging for the following reasons: (1) C/C composites has a very high melting point, which cannot be melted at the welding temperature. (2) A high residual interfacial thermal stress is induced at the interface of the joints as a result of the difference between the CTE of the joining components. Thus, the joints have a strong tendency to crack along the interface of the joints, which consequently leads to deterioration of the joints [11, 27-30]. (3) The 3D C/C composite have high density and low porosity content (4.1%). Therefore, unlike the joining by using the 2D C/C composite (high porosity content), the melted Ti cannot be infiltrated into the porosity of the 3D C/C composite and there is no significant infiltrated structure to contribute to the strength of the joints.

However, the previous literature on brazing of C/C composites have proved that in the cases that the braze alloys contain Titanium, TiC is formed at the interface of the joints as a result of the reaction between the C/C composite and active Ti element. This TiC layer leads to chemical bonding at the interface between the C/C composite and braze materials and robust joins can be obtained [2, 10, 31-39]. Moreover, previous investigations on the joining of dissimilar materials have shown that using surface patterned structures such as surface puncturing and wave pattern interface are promising approaches to regulate the thermal residual stress at the interface of the joint [11, 27-30, 42-44]. The patterned interface decreases the residual shear stress, as well as induces the compressive normal stress at the interface of the joints. This kind of stress field is beneficial to suppressing interfacial cracks. In addition, patterned surface causes enlarging of the joining area and pins the interface of the joints, which are favorable to the mechanical strength of the joints [11, 27-30, 42-44]. The same approach can be employed for direct dissimilar joining of the 3D C/C composite to Ti6Al4V using reactive resistance spot welding technique. The solid-liquid reaction between the melted titanium and solid carbon can form a chemical bond at the interface of the joint. Furthermore, the melted metal can be infiltrated into the groove-patterned surface of the 3D C/C composites, which forms a mechanical occlusion between the joining components and tightly pins up the interface of the joint.

As mentioned, joining of 3D C/C composites to Ti6Al4V by conventional fusion welding techniques seems to be very challenging. In order to overcome these obstacles, an innovative interfacial design and joining technique were used to join the 3D C/C composite to Ti6Al4V. In order to facilitate the infiltration of the melted metal into the 3D C/C composite, rectangular grooves were machined on the surface of the 3D C/C composites. Then the grooves were filled with about 2.5 g Ti powder and the joining assembly was joined by resistance spot welding technique. Moreover, the effects of the dimension of the rectangular grooves on the strength and fracture mode of the joints were also investigated.

5.2 Experimental procedure

The C/C composite used in this study was a 3D C/C composite with low porosity content (high strength). This composite had a thickness of 5 mm, electrical resistivity of 9 μΩ.m, density of 1.86 g/cm^3 and open porosity content of 4.1% and was purchased from HTMAGROUP. This high strength composite was fabricated by the Chemical Vapor Infiltration (CVI) process. The 3D C/C composite panels were then cut into 25 mm × 30 mm slices for microstructural analysis, and 50 mm × 30 mm for the shear strength testing. The 1 mm thick Ti6Al4V sheets were cut into 25 mm × 30 mm pieces for

microstructural analysis and shear strength testing. In order to join the 3D C/C composite with low porosity content to Ti6Al4V, the rectangular grooves were drilled on the surface of the 3D C/C composite to facilitate the infiltration of the melted Ti into the 3D C/C composite. In order to fill the rectangular grooves, about 2.5 g of Ti powder (purity >99%, particle size< 44μm) was used as interlayer. The groove width was changed from 0.7 to 1 mm and the groove depth was changed from 1 to 3 mm to investigate the effects of the dimension of the grooves on the strength of the joints. The schematic of the rectangular groove-patterned 3D C/C composite is presented in Fig. 5.1(a).

Before joining, the surfaces were ground up to 600 grit using silicon carbide paper and were ultrasonically cleaned in acetone for 30 minutes. A DC spot welding machine was used for the purpose of joining. Flat welding electrodes were used, complying to RWMA Class II, with a diameter of 16 mm. The 3D C/C composite and Ti6Al4V were held in place between two flat copper electrodes, which were used for applying a DC current and clamping force during the joining process. The weld force, for all experiments, was set at 2 kN and a single 200 ms current pulse was used for the weld cycle. The hold time was 5 s and the cooling water flow rate was 4 L/min. According to our experiment, the current of 12 kA was set as the optimum current of joining. Hence, the current of the joints for the case of joining 3D C/C composite was fixed at 12 kA, and the effects of the rectangular groove dimention on the strength of the joints were investigated. A schematic diagram of the joining assembly is shown in Fig. 5.1(b).

The cross-sections of the joints and fracture surfaces were investigated by scanning electron microscope (SEM) equipped with Energy-dispersive X-ray spectroscopy detector (EDS). In addition, the Grazing Incidence X-ray Diffraction (GIXRD) was utilized to identify the composition at the interface of the joint. Shear strength tests of the joined samples were then performed with the universal testing machine at a rate of 0.5 mm/min, and five replicates of shear tests were done for each condition of joining. The shear strength of the joints was calculated as the ratio of the maximum force to the area of joint surface. The area of the joint was considered the as area that 3D C/C composite adhered to the Ti6Al4V side and was measured by ImageJ software.

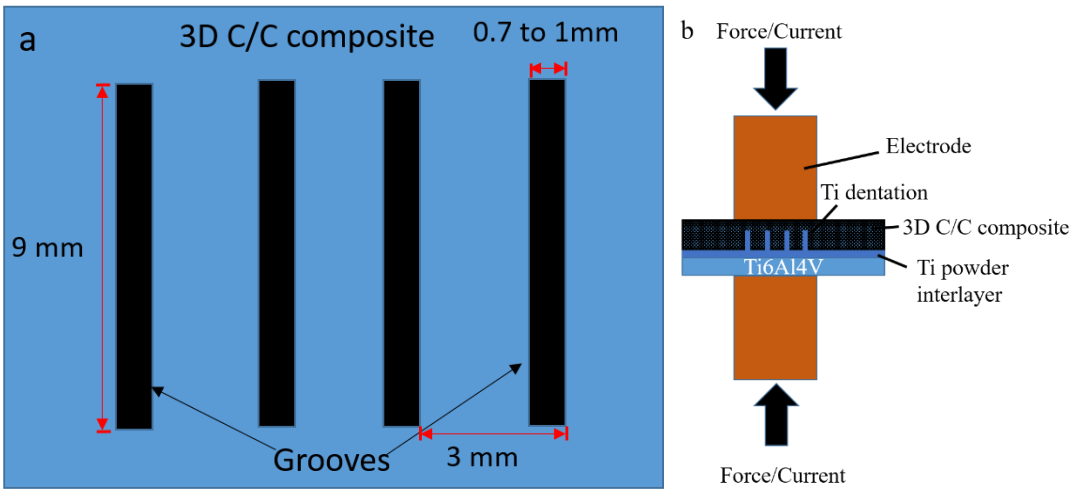

Figure 5.1. Schematic of (a) top view of the fabricated rectangular groove-pattern on the surface of 3D C/C composite and (b) the joining setup for joining the groove-patterned 3D C/C composite to Ti6Al4V.

5.3 Results and discussion

5.3.1 Characterization of the microstructure of the joints

Fig. 5.2 shows the surface microstructure of the 3D C/C composites. As can be seen, no obvious macro cracks and porosities are observed on the surface of the 3D C/C composite. Even though the low content of porosity and cracks is beneficial to mechanical properties of the 3D C/C composite, insufficient cracks and porosity content can prevent the infiltration of the melted Ti into the 3D C/C composite during joining process.

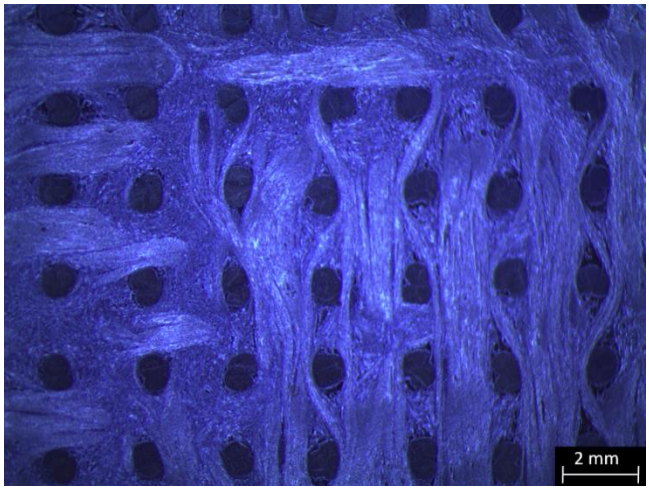

Figure 5.2. The surface of the 3D C/C composite.

Fig.5.3 shows the interface of the joint between the flat 3D C/C composite and Ti6Al4V by using the Ti powder interlayer. Fig. 5.3 clearly shows the formation of a large number of cracks at the interface of the joint and within the 3D C/C composite. Formation of such cracks has been reported for dissimilar joining of the flat surface C/C composites to metals [27, 30]. These cracks are generally formed as a result of high interfacial residual stress caused by the difference between CTE of the joint components [11, 27-30]. Moreover, unlike the case of the joining by using the 2D C/C composite, no infiltration of the melted Ti into the porosity of the 3D C/C composite is observed as a result of its low porosity content (4.1%). Hence, the pinning effect cannot contribute to the integrity of the joint and suppression of the interfacial cracks.

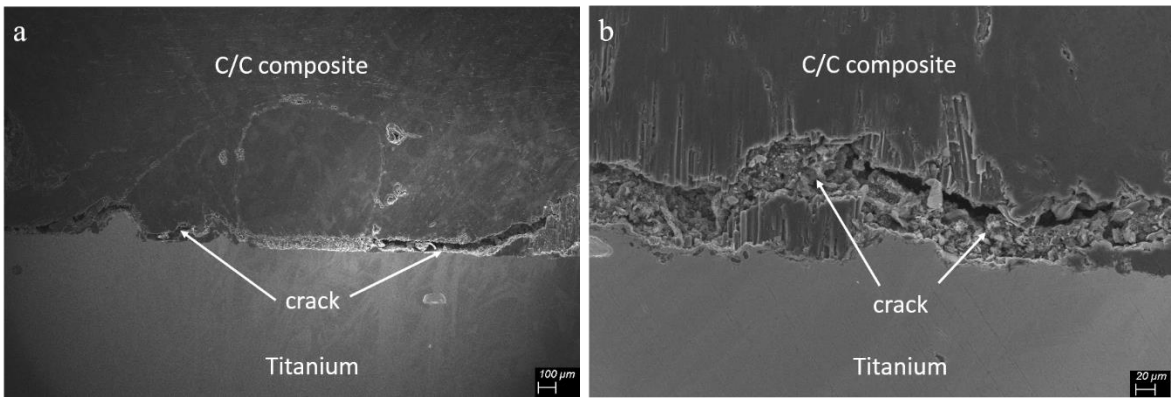

Figure 5.3. The interface of the joint between the flat surface 3D C/C composite and Ti6Al4V.

In order to facilitate the infiltration of melted Ti powder interlayer into the 3D C/C composite, rectangular grooves were machined on the surface of the 3D C/C composite. Fig. 5.4 shows a typical cross section of the 3D C/C composite-Ti6Al4V joint with a rectangular groove-patterned interfacial structure. As shown in Fig. 5.4 and later in Fig. 5.5(a), all the rectangular grooves were completely filled with the melted Ti interlayer. The SEM micrographs of the joint between Ti6Al4V and the rectangular groove-patterned 3D C/C composite are presented in Fig. 5.5. It can be seen in Fig. 5.5(b,c) that the joint interface exhibits sound bonding and is free of structural defects, such as cracks and voids. Moreover, the melted Ti was infiltrated into the cracks of the 3D C/C composite, which resulted in the pinning effect, which is favorable to the mechanical strength of the joint (Fig. 5.5(a,b)). Fig. 5.5(d) shows the formation of some microcracks at the top of the Ti dentation. Such cracks have been reported in previous investigation on the joining of the surface patterned C/C composite and W to metals [27, 42]. Their simulation results showed that a severe residual stress is induced at the top of the dentations. Therefore, this area is the weakest region of the interface, which is prone to cracking [27, 42, 44].

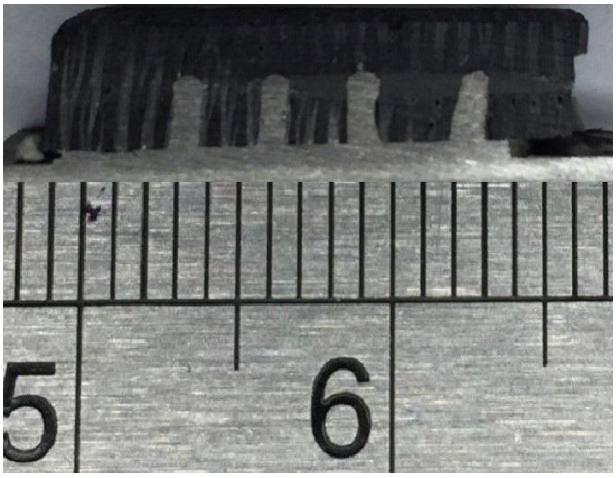

Figure 5.4. The cross section of the joint between the rectangular groove-patterned 3D C/C composite and Ti6Al4V.

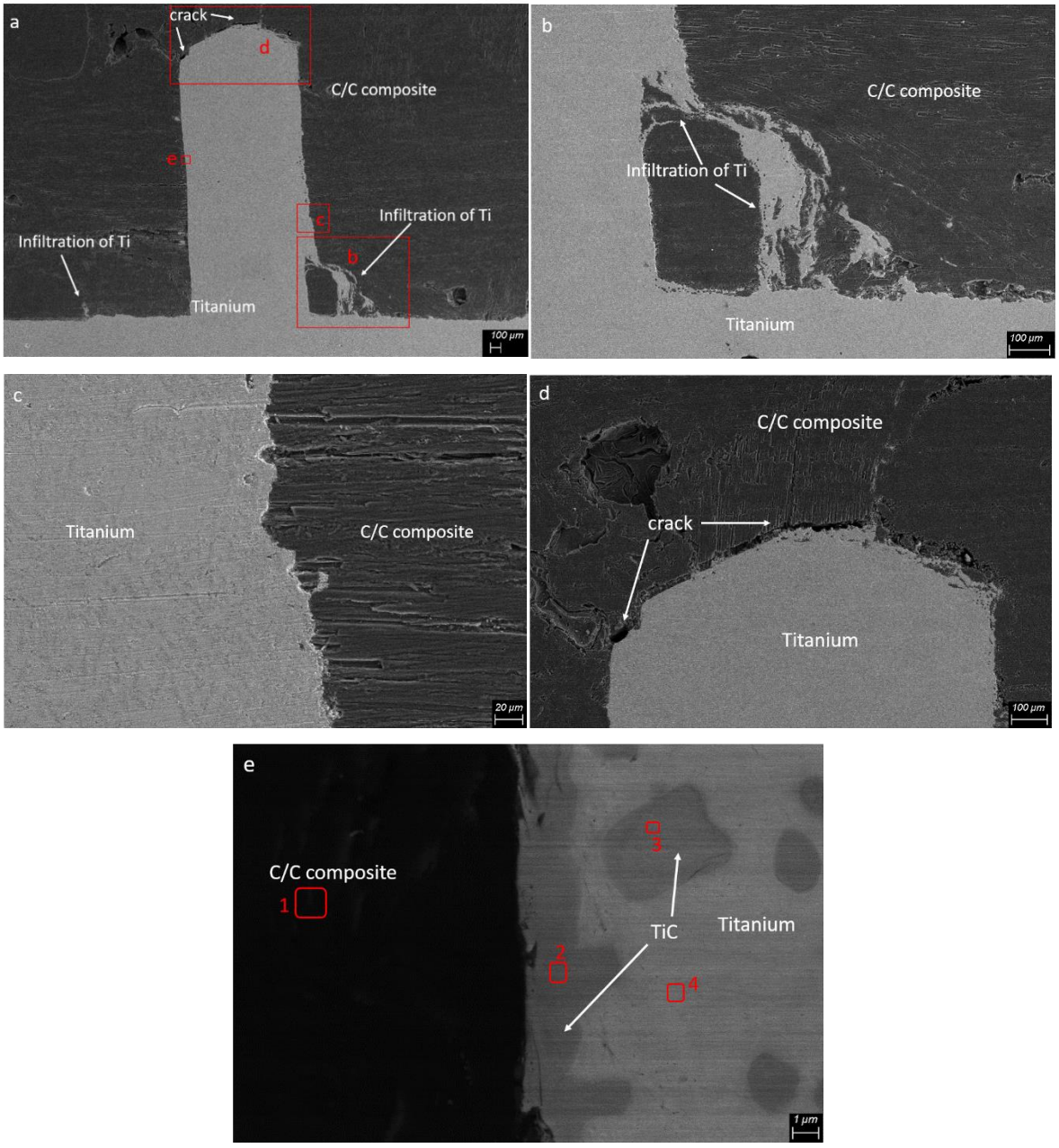

Figure 5.5. SEM image of the cross section of the joint between the 3D C/C composite and Ti6Al4V with the width of 1mm and depth of 3 mm, (a) the panorama of the joint interface and (b) , (c), (d) and (e) are magnified selected area on (a).

Overall, the obtained sound joints by using the rectangular groove-patterned 3D C/C composite can be described by the simulation and experimental results of the previous investigations on joining of the

groove-patterned C/C composite, Al2O3 and W to metals [27, 42, 44]. They proved that the groove-patterned interface decreases the residual shear stress, as well as induces compressive normal stress at the interface of the joints. Therefore, this kind of stress field prohibits the nucleation or growth of the interfacial cracks [27, 42, 44].

A highly magnified image of the interface of the 3D C/C-Ti6Al4V joint shows the formation of a thin layer with the thickness of 1 to 2 μm (Fig. 5.5(e)). SEM-backscattered images of Fig. 5.5 (e), clearly shows the formation of the continuous dark gray phase at the interface and also dark gray particles which are embedded in the light gray Ti matrix. The formation of the interfacial phase can be attributed to the reaction between the C/C composite and Ti6Al4V [20, 34, 35, 79]. In the case of similar joining of the C/C composite by using compacted titanium powder or titanium foil, the formation of a thin TiC layer as a result of the reaction between Ti and carbon of C/C composite has been reported [2, 31, 32, 55]. The EDS results of Fig 5.5(e) are presented in the Table 5.1. As EDS analysis indicated (Table 5.1), the reaction layer and particles are rich in the elements of C and Ti which is evidence of the formation of the TiC as a result of high chemical affinity between Ti and C. According to the thermodynamics point of view, the Gibb's free energy of formation of TiC is highly negative, indicating the formation of TiC at the interface between Ti and the C/C composite is thermodynamically favorable [36, 67, 80].

Table 5.1. EDS analysis for Fig. 5.5(e).

Point	1	2	3	4
Ti (at %)	0.53	57.01	60.58	90.16
C (at %)	99.47	42.99	39.42	9.84

Based on the microstructure observations and EDS results, it can be inferred that the solid-liquid reaction between Ti6Al4V and the 3D C/C composite, as well as the infiltration of the melted metal into the fabricated grooves on the surface of the 3D C/C composites were the dominant mechanisms of joining and contributed to both metallurgical and mechanical bonding. The Joule heating caused by

resistance welding can melt the Ti6Al4V or Ti powder interlayer, but the 3D C/C composite cannot be melted due to its high melting point. Therefore, the formation of TiC at the interface of the joint can be described by a conceivable solid-liquid reaction between the melted Ti and the carbon of the 3D C/C composite. In fact, the formation of a TiC phase at the interface of the C/C composites joints, in the cases where the interlayers contained titanium, has been widely reported in previous investigations [2, 10, 31-38, 81, 82]. Moreover, a carbide layer forming at the interface can decrease the interfacial tension, and consequently improve the wettability of the molten Ti on the C/C composite [33-37]. Such effects, as well as the importance of Ti on the wettability, have been reported in many Ti-containing brazing systems [33-38].

5.3.2 Mechanical properties of the joints

The shear strength of the joints using the 3D C/C composite with the flat and rectangular groove-patterned interface with different dimension is presented in Fig. 5.6. The shear strength of the joints with flat interface is only 2.34 ± 0.67 MPa. The poor strength of the joint is consistent with the observed defects and microcracks at the interface of the joint with flat 3D C/C composite (Fig. 5.3). However, fabrication of the rectangular groove-pattern on the 3D C/C composite surface significantly increased the shear strength of the joints. In the case of joining with the rectangular groove-patterned 3D C/C composite, by increasing the groove depth from 1 to 3 mm and grooves width from 0.7 to 1 mm, the strength of the joint increased from 19.15 ± 4.81 to 46.14 ± 3.92 MPa. The increase in the strength of the joints by increasing the depth and width of the grooves can be described by enlarging the bonding area due to increasing the grooves width and depth. The maximum strength obtained for the groove-patterned interface is significantly higher than the strength of the joints with the flat interface by a factor of about 20. Therefore, it illustrates that the strength of the joints does not rely only on the chemical bonding at the interface and also the interface pattern of the joints plays a key role in the joint strength. According to the literature, the patterned surface structure decreases the residual stresses, as well as induces compressive normal stresses at the interface of the joint, which is beneficial to crack arrest [11, 27-30, 42-44]. Moreover, embedding of the Ti dentations into the rectangular grooves of the 3D C/C pinned the interface of the joint and expanded the joining area, which consequently enhanced the strength of the joints [27-30].

The comparison between the shear strength of the joints using the 2D (chapter 4) and 3D C/C composites indicates that the maximum strength of the joints by using the 3D C/C composite is 46.14

± 3.92 MPa which is about 6.5 times higher than the strength obtained by using the multi-ply 2D woven C/C composite. As mentioned, in the case of joining by using the 2D C/C composite the fracture occurred within the 2D C/C composite and not at the interface of the joints. Therefore, the effective shear strength of the joints cannot exceed the strength of the 2D C/C composite, whereas as a result of higher mechanical properties of 3D C/C composite, higher shear strength can be achieved for the joints using the 3D C/C composite.

The shear strength values of 3D C/C composite-Ti6Al4V in this study are comparable with results of previous investigations [7, 11, 20, 21, 27, 29, 41, 74, 76] which illustrates the groove-pattering method is an appropriate approach to produce high strength joint between the high density 3D C/C composite and Ti6Al4V. Based on the shear strength obtained, the 3D C/C-Ti6Al4V joints have the potential to be applied in the advanced and high temperature applications such as heat shields, nozzles, and turbine engine and high temperature furnace components, which require high mechanical strength at high temperatures. Moreover, unlike the joining of the C/C composites by brazing process, the obtained joints in this study are able to withstand high temperature operating environments because no low melting point braze or filler metal was used.

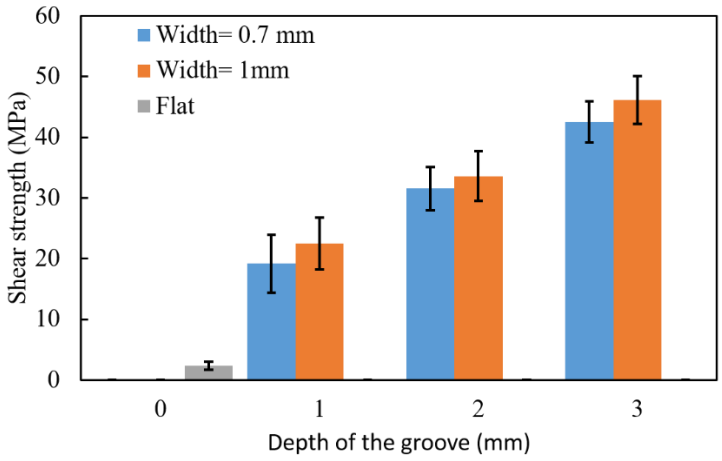

Figure 5.6. Shear strength of the 3D C/C composite-Ti6Al4V joints with flat interface and groove-patterned interface with groove depth between 1 to 3 mm and width between 0.7 to 1 mm.

The macroscopic observation of the fracture surfaces with the naked eye reveals that the fracture mode is dependent on the depth of the grooves. For the joints with the groove depth of 1 mm, the fracture occurred along the interface between the 3D C/C composite and Ti dentations (mode 1), whereas for the joints with the groove depth of 2 and 3 mm, the fracture occurred by crack propagation through the infiltrated Ti dentations (mode 2). The fracture in the modes 1 and 2 or combination of these two modes have been widely reported on joining of dissimilar materials with patterned interfaces [28-30, 44, 76]. Fig. 5.7(a-c) shows the fracture surface for the joints with the groove depth of 1 mm. As can be seen, the Ti dentations were completely pulled out from the 3D C/C composite, which reveals the crack propagation at the interface of the joints. SEM observation of the fracture surface of the joints in Fig. 5.8(a) shows that the Ti dentations remain intact after the shear test and no fracture is observed in the infiltrated Ti dentations. Fracture surfaces on the 3D C/C composite and Ti6Al4V sides for the joints with the groove depth of 3 mm are presented in Fig. 5.7(d-f). As can be seen, the Ti dentations were broken and are remained on the 3D C/C composite side after shear test, which means that the cracks have propagated through the Ti dentations. SEM images of the fracture surface on Ti6Al4V side for the joints with the groove depth of 3 mm are shown in the Fig 5.9. As can be seen, the fracture occurred in the Ti dentations. The cross section micrographs of the fractured dentation with the depth of 3 mm, after shear test, are provided in Fig. 5.10. Fig. 5.10 shows the propagation path of the crack at the interface or within the 3 D C/C composite. It indicates that in the mode 2, cracks propagated in two

ways. Therefore, in addition to the crack propagation through the Ti dentations, cracks also propagated at the interface between the Ti dentations and 3D C/C composite.

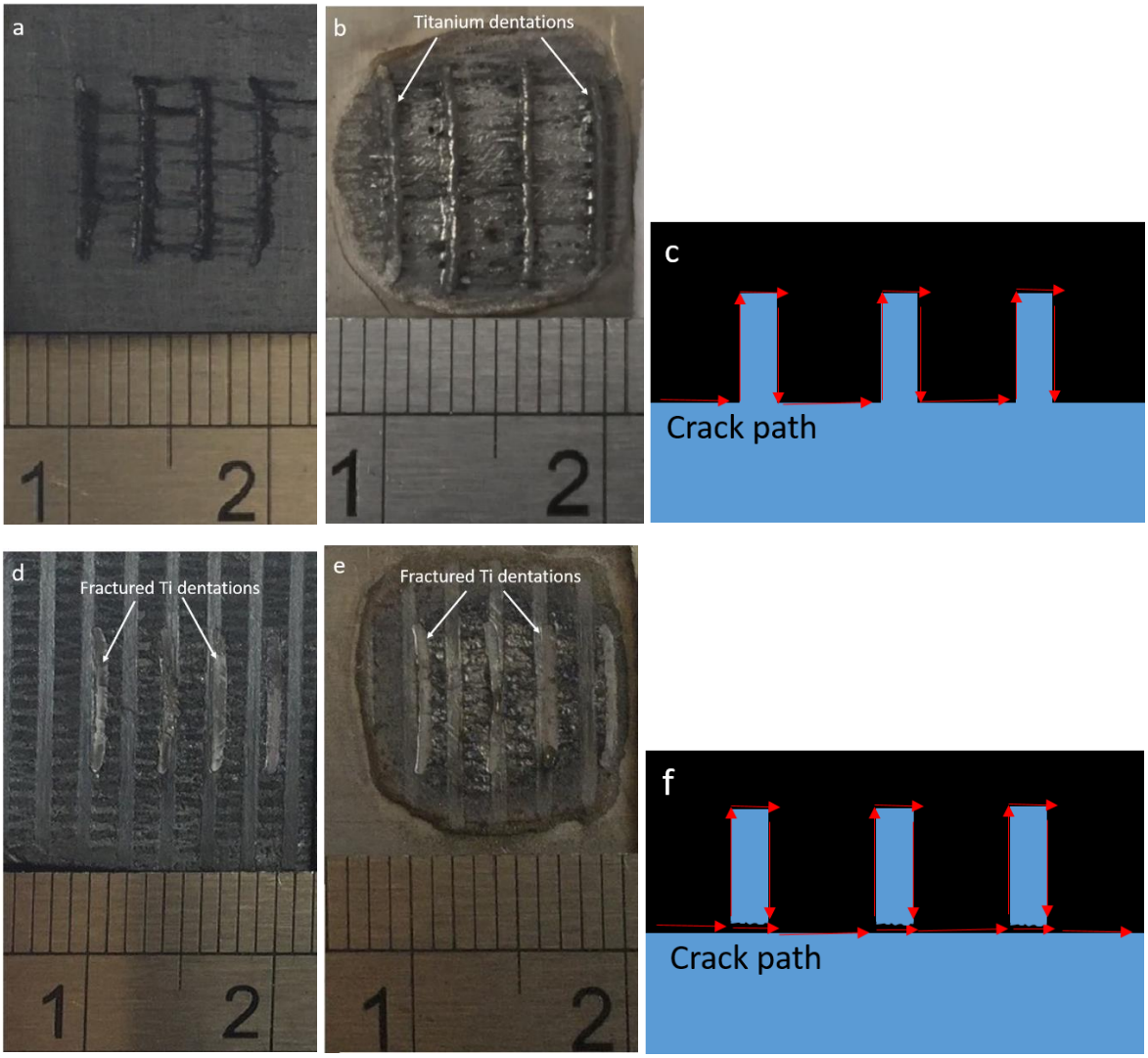

Figure 5.7. Typical fracture surfaces on both Ti6Al4V and 3D C/C composite sides and also crack propagation pass for the joint with (a-c) a groove depth of 1 mm, (d-f) groove depth of 2 and 3 mm.

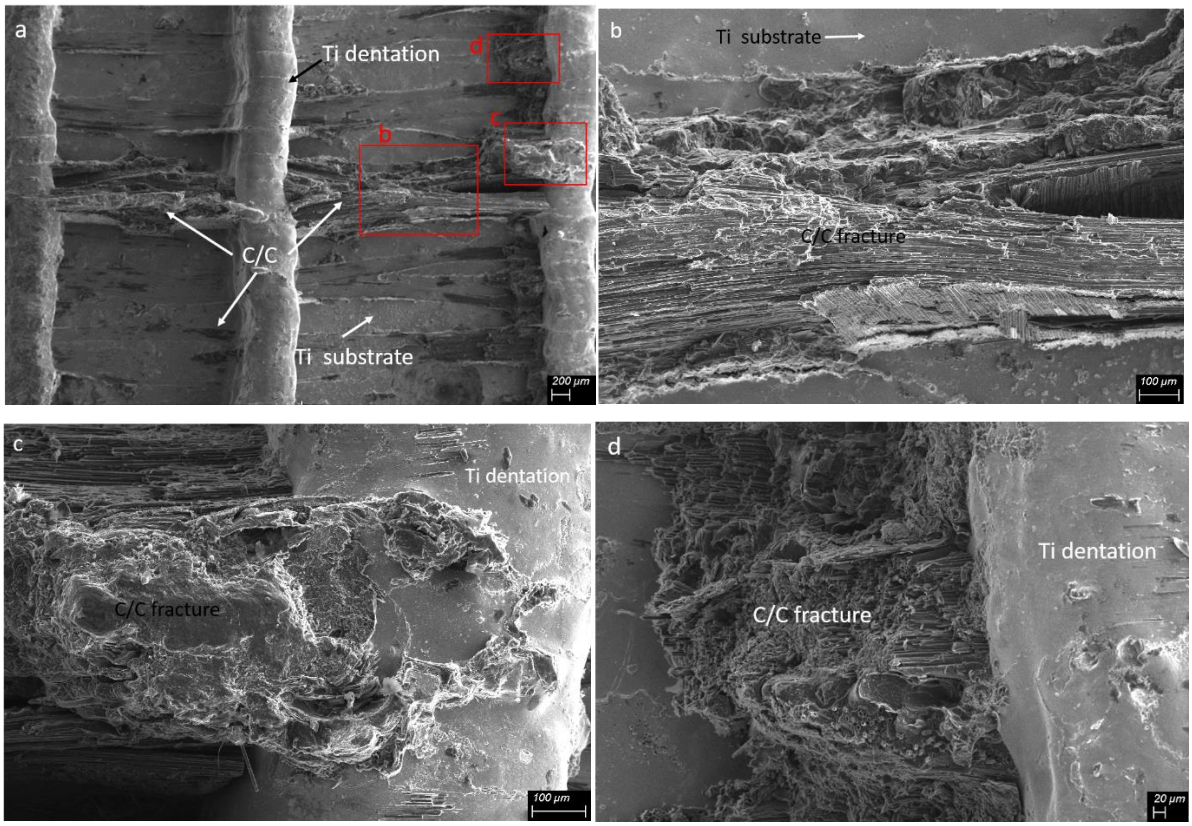

Figure 5.8. Typical fracture surfaces of the 3D C/C composite-Ti6Al4V joints on the Ti6Al4V sides for the joints with the groove depth of 1 mm.

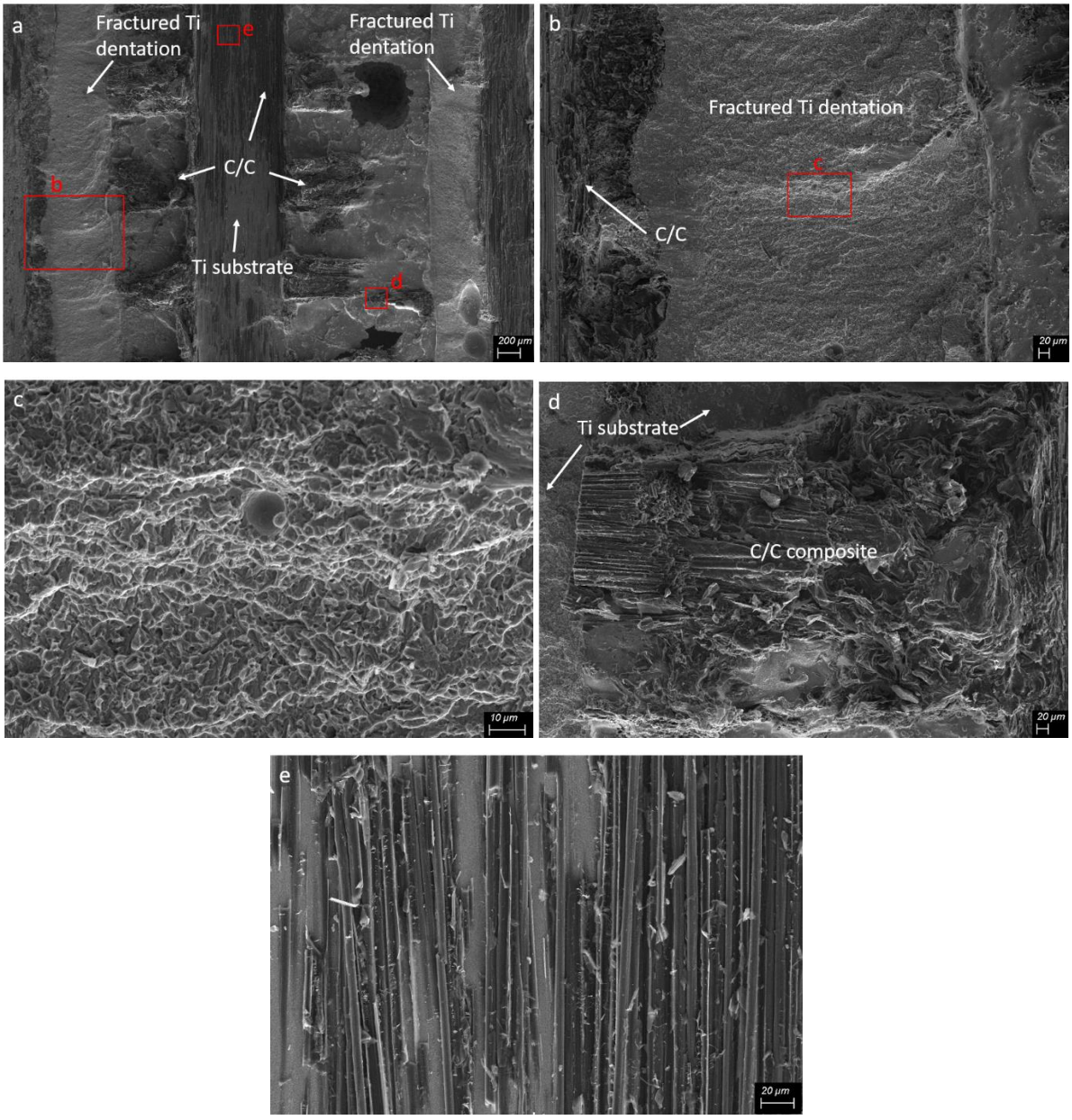

Figure 5.9. Typical fracture surfaces of the 3D C/C composite-Ti6Al4V joints on the Ti6Al4V sides for the joints with the groove depth of 3 mm.

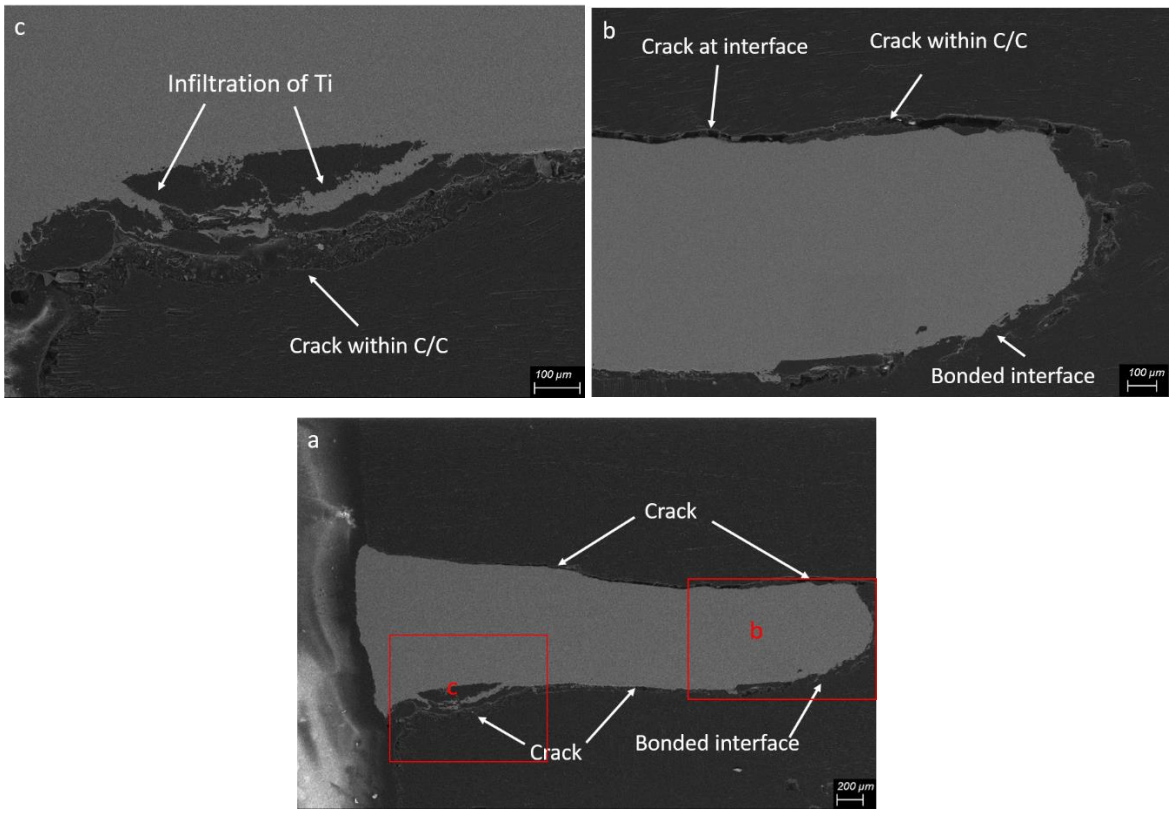

Figure 5.10. Cross section microstructure of the fractured Ti dentation for the 3D C/C composite-Ti6Al4V joint after shear test for the groove depth of 3 mm.

Comparing mode 1 and 2, in both modes, the cracks first initiated at the flat area of the joints and propagated along the interface. In the mode 1, after reaching to the Ti dentations, crack propagation continued at the interface of the Ti dentations and the 3D C/C composite and consequently the Ti dentations pulled out from the 3D C/C composite side. By contrast, in the mode 2, after the cracks reached the Ti dentations, the crack propagation continued in two ways. Regarding the first path, some cracks propagated along the interface between Ti dentations and the 3D C/C composite (Fig. 5.10), while in the second path, some cracks deviated into the Ti dentations and passed through the Ti dentations (Fig. 5.7(d,e) and Fig. 5.9(a-c)). Finally, after reaching the critical load, fracture occurred within Ti dentations while still there was some bonding between the 3D C/C composite and the Ti dentations (Fig. 5.10, Fig. 5.7(d,e) and Fig. 5.9(a-c)).

The higher strength obtained in the mode 2 can be described by analysis of the crack propagation path. In the mode 2, there is a higher joint area and consequently the crack propagating path is longer, as well

as higher energy is dissipated for crack propagation in two ways: first, crack propagation at the interface of the joints, second, crack propagation through the high strength Ti dentations. Therefore, the fracture via mode 2 obviously has higher strength and more energy is dissipated during crack propagation compared to the mode 1 which the crack propagation is restricted to the interface of the joint between the 3D C/C composite and Ti dentations [76].

For both fracture modes, it is observed that the some fractured parts of the 3D C/C composite are attached at the fracture surface on the Ti6Al4V sides (Fig. 5.8 and Fig 5.9). It indicates that in addition to crack propagation along the interface of the joints, cracks were also deflected and propagated form the interface of the joints into the 3D C/C composite. It has been found that crack deflection is favorable to change the fracture mode from brittle to pseudo-plastic and avoiding a catastrophic failure [29, 30].

5.4 Summary

In this study, the feasibility of the dissimilar joining of the 3D C/C composites to Ti6Al4V by the reactive resistance spot welding technique, as an innovative joining technique, were investigated and the following conclusions were drawn:

1. It was found that the infiltrated structure plays a key role in the joining of the 3D C/C composites to Ti6Al4V. The strength of the flat 3D C/C composite-Ti6Al4V joints was weak as a result of the formation of cracks at the interface of the joints. These cracks were formed as a result of the difference between the CTE of the joining components. Fabrication of rectangular grooves on the surface of the 3D C/C composite was required to facilitate the infiltration of the melted Ti into the 3D C/C composite and consequently obtain the desired strength. The groove-patterned interface can cause decreasing the residual stresses at the interface of the groove-patterned joint, enlarging the joining area and strong pinning effect by the infiltrated Ti dentations.
2. The solid-liquid reaction and infiltration of the melted metal into the fabricated grooves on the surface of the 3D C/C composite can be considered as the dominant mechanisms of joining. Ti6Al4V was melted as a result of Joule heat produced during resistance welding. The melted metal reacted with the carbon of the 3D C/C composite to form a thin TiC layer with a thickness of 1 to 2 μm at the interface of the joint. This thin TiC layer improved the mechanical properties of the joint due to the formation of chemical bonding at the interface of the joint. Moreover,

the infiltration of melted Ti into the grooves of the 3D C/C composites increased the joining area and tightly pinned the 3D C/C–Ti6Al4V interface.

3. In the case of joining 3D C/C composite with flat interface, the strength of the joints was only 2.34 ± 0.67 MPa. The poor strength of the joints is due to the formation of cracks at the interface of the joints and lack of the infiltration of the melted Ti into the low porosity content of the 3D C/C composite. By contrast, In the case of joining with the groove-patterned 3D C/C composite, by increasing the grooves depth from 1 to 3 mm and grooves width from 0.7 to 1 mm, the strength of the joint increased from 19.15 ± 4.81 to 46.14 ± 3.92 MPa. Therefore, the maximum strength obtained by using the groove patterned interface is significantly higher than the strength of the joints with a flat interface by a factor of about 20.

Chapter 6
Dissimilar joining of 2D C/C composite to copper by reactive resistance spot welding

This chapter investigates the feasibility of dissimilar joining of the flat surface 2D C/C composite to copper by using different Ti interlayers. Three different interlayers in the forms of Ti thin sheet and powder were used, and the effects of different interlayers on the microstructure and strength of the joints are investigated.

6.1 Introduction

C/C composite is considered a superb material for many advanced applications at elevated temperatures as a result of their low density, high thermal stability, low coefficient of thermal expansion (CTE), high strength-to-weight ratio at elevated temperatures, and good ablation and thermal shock resistances [3, 59-62]. Therefore, this combination of properties makes C/C composites as appropriate candidate for many high temperature applications such as heat shields, nozzles, turbine engine components, hot press dies, brakes, and high temperature furnaces [2, 7-12]. In order to extend the high temperature application of C/C composites, it is essential to join them to a variety of metals such as copper TiAl, and Ti6Al4V.[8, 14, 17-23]. In lightweight heat rejection system applications, C/C composites as plasma facing components, are required to be joined to structural metallic heat sink materials, like Cu [14-16, 25]. However, dissimilar joining of C/C composite to other materials is challenging due to its special chemical, physical, and mechanical properties, as well as the unique crystal structure of carbon. Nowadays, similar and dissimilar joining of C/C composite are carried out by a variety of novel processes such as such as brazing, adhesive bonding, diffusion bonding, and mechanical fastening [2, 9, 11, 17, 24, 84-87]. Regarding brazing and adhesive bonding, the application would be severely restricted by the service temperature because the joints cannot withstand high temperature applications [2, 10, 24]. For example, brazing materials normally have low melting points and cannot withstand high operation temperatures [2, 24]. In the case of joining C/C composites by diffusion bonding, this procedure requires a long procedure time, high pressure, and high temperature up to 1700 °C. However, treatment of C/C composites in such a situation adversely affects their properties [2, 24]. On the other hand, integration of C/C composites by mechanical fastening and bolts causes stress concentration in the area close to the holes of the bolts, which leads to deterioration of mechanical properties of the C/C composites [2, 10].

Dissimilar joining of the 2D C/C composite to copper seems to be very challenging for the following reasons: First, there is a significant difference between the CTE of the C/C composite and Cu, which results in high interfacial residual stress at the interface of the joints. In addition a very high wetting angle of copper on C/C composite (140°) prevents direct dissimilar joining of the C/C composite to copper [38, 71, 88-91]. Moreover, C/C composite is not melted at the welding temperature. Two approaches can be utilized to improve the wettability of the molten copper on the C/C composite. One way is using active braze interlayers which contain active elements such as Ti and Si [28, 66, 67, 92]. The second approach is to make a coating on the surface of C/C composite by using the active elements such as Cr, Mo ,Ti, W and Si [22, 38, 70-73]. These approaches cause formation of the carbide layer on the surface of C/C composite, which significantly improves the wettability of copper on the C/C composite. Moreover, the previous literature on brazing of C/C composites have proven that the presence of Ti as an active element in the braze material can cause robust bonding as a result of the formation of TiC at the interface of the joints [2, 10, 31-39]. Regarding the residual stress at the interface of the joint, it has been reported that infiltration of the melted metal phase into the pores of the C/C composite is beneficial to increase the mechanical strength of the joints via pinning effect [10, 11, 28, 40, 41]. The same approach can be utilized for joining the 2D C/C composite to Cu by using Ti interlayer. Ti can react with the 2D C/C composite to make a robust bonding. In addition, bonding between the Cu and Ti interlayer can be achieved as a result of the formation of intermetallics at the interface between Cu and Ti interlayer. Furthermore, melted Ti can be infiltrated into the porosity of the 2D C/C composite and pin the interface of the joints.

In this study, dissimilar joining of the 2D C/C composite to Cu is investigated. Three different Ti interlayers in the forms of the powder and thin sheet were used and the effects of the interlayers on the microstructure and strength of the joints are investigated.

6.2 Experimental procedure

The C/C composites used in this study were a multi-ply 2D woven C/C composite with high porosity content (low strength). The multi-ply 2D woven carbon–carbon composite laminate with the thickness of 2 mm (6 laminas), electrical resistivity of 26.5 μΩ.m and the interlaminar shear strength of 8 MPa were purchased from CeraMaterials. This 2D C/C composite has a density of 1.51 g/cm^3 and open porosity content of 14.8%, which was made with the Polymer Infiltration and Pyrolysis (PIP) process. The 1.3 mm thick copper sheets were cut into 25 mm × 30 mm pieces. The C/C composite panels were then cut into 25 mm × 30 mm × 2 mm slices for microstructural analysis, and 50 mm × 30 mm × 2 mm

for the shear strength testing. The surfaces of joining components were ground up to 600 grit by means of silicon carbide paper before joining process and were ultrasonically cleaned in acetone for 30 minutes. Joining was conducted by a DC spot welding machine. Welding electrodes were RWMA Class II, with different diameters of 8, 12, and 16 mm to investigate the appropriate electrode for joining. Joining of 2D C/C composite and copper was conducted using Ti powder or sheet as interlayer between 2D C/C composite and copper. The 2D C/C composite, Ti interlayer and copper were held in place between two flat copper electrodes which were used for applying DC current and force during the joining process. Weld force, for all experiments, was set at 2 kN and a single 200 ms pulse was used for the weld cycle. The hold time was 5 s and the cooling water flow rate was 4 L/min. The welding current was varied from 5 kA to 7 kA.

The cross-sections of the joints were investigated by scanning electron microscope (SEM) equipped with Energy-dispersive X-ray spectroscopy detector (EDS). In addition, X-ray Diffraction (XRD) and Grazing Incidence X-ray Diffraction (GIXRD) were utilized to identify the composition at the interface between Ti-Cu and Ti-C/C composite respectively. Shear strength tests of the joined samples were then performed with the universal testing machine at a rate of 0.5 mm/min, and five replicates of shear tests were done for each condition of joining.

6.3 Results and discussion

6.3.1 Electrode diameter consideration

A schematic diagram of the joining setup with appropriate diameter of the electrodes is shown in Fig. 6.1. Diameter of the copper electrodes is a determinant factor to achieve a good joining. Regarding the electrodes in contact with the 2D C/C composite, the electrode diameter should be large enough to avoid sticking of the 2D C/C composite to the electrode. Therefore, the electrode in contact with the 2D C/C composite was a flat electrode with the diameter of 16mm. Moreover, the diameter of the electrode in contact with the Cu sheet should be small enough to make sure that adequate current density passes through the Cu and melts the Cu-Ti interface to achieve a good bonding at this interface. The large diameter size of the electrode in contact with Cu, causes decrease in the current density passes through the interface between the Cu and Ti interlayer and consequently leads to a poor bonding at this interface. The relation between the quality of the bonding at the Cu-Ti interface to the factors including the joining current and the diameter of the electrode in contact with Cu are summarized in the Table 6.1. As can be seen, the diameter of the electrode in contact with the Cu and current can severely affect

the quality of the bonding at the interface between Cu and Ti interlayer. When considering the Table 6.1, for the electrode with a diameter of the 16 mm no bonding between Cu and Ti interlayer can be formed for all currents even at high current of 7 kA. By decreasing the diameter of the electrode, good bonding was achieved for the electrode with diameter of 8 mm at current of 6kA. Therefore, electrodes with the diameter of 8 mm and current of 6kA were selected as appropriate electrode diameter and minimum current of welding for the experiments. Fig. 6.2 shows typical poor bonding at the interfaces between Cu and Ti interlayer. As can be seen in Fig. 6.2(a) for the electrode size of 8mm and currents of 5kA, the bonding between Cu and Ti interlayer was not good because the current of 5kA was not enough to melt the Ti-Cu interface. Regarding the electrode size of 12 mm and current of 6 kA (Fig. 6.2(b)) the electrode diameter was not small enough to provide the adequate current density to melt Cu-Ti interface and obtain the desired joint.

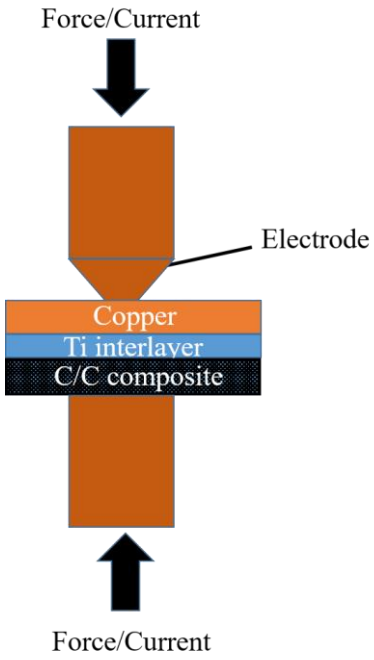

Figure 6.1. Schematic of the joining setup.

Table 6.1. The effects the current and diameter of the electrode in contact with Cu on the quality of the bonding at the interface between Cu and Ti interlayer.

Number	1	2	3	4	5
Diameter of electrode in contact with Cu (mm)	16	12	12	8	8
Current (kA)	5-7	5	6	5	6
Duration of current (ms)	200	200	200	200	200
Quality of the bonding at Cu/Ti interface	No bonding	No bonding	poor	poor	good

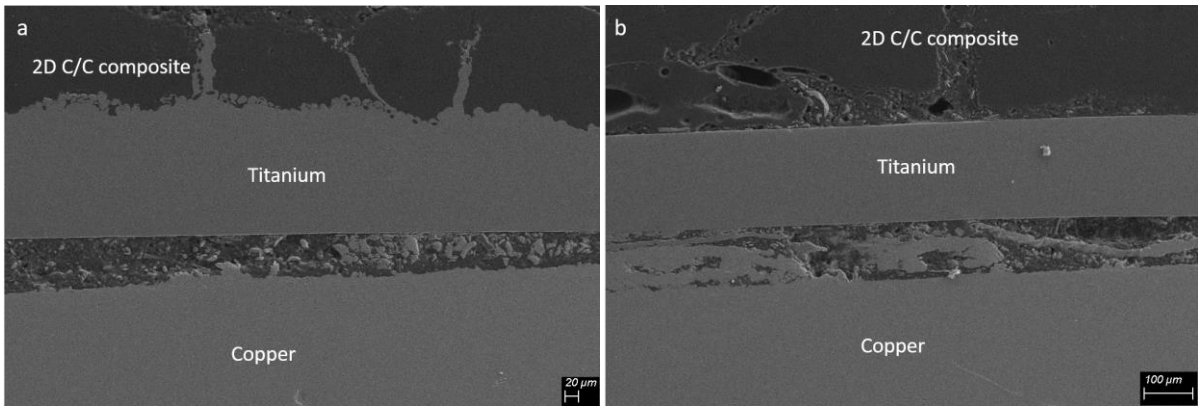

Figure 6.2. The typical microstructure of poor bonding at the interface between the Cu and Ti interlayer for the (a) electrode diameter of 8mm and current of 5 kA, (b) electrode diameter of 12mm and current of 6kA.

6.3.2 Characterization of the microstructure of the joints

The surface microstructure of the 2D C/C composite is provided in Fig. 6.3. As can be observed, a high content of porosity and cracks are seen on the surface of the 2D C/C composite. The high crack and porosity content can facilitate the infiltration of the melted Ti into the 2D C/C composite, which results in the strong pinning effect at the interface of the joint. The SEM microstructure of the 2D C/C composite-copper joints by using Ti sheet and powder interlayer are shown in Fig. 6.4 to Fig. 6.6. Regarding the joints by using Ti sheet interlayer, in some local parts, defect-free microstructures are observed (Fig. 6.4(a) and Fig. 6.5 (a,b)), but in most of the parts, as can be seen in Fig. 6.4(b-d) and Fig. 6.5(c-e), some cracks were formed at or near the interface between Ti interlayer and 2D C/C composite. Observing the cracks at the interface between 2D C/C composite and Ti sheet can be described by distortion and deformation of the Ti sheet interlayer during the joining process. The origin of this distortion and deformation is high cooling and heating rate and applying the pressure during joining procedure. When considering the low thickness of the Ti sheet interlayer (200 and 400 µm),

this condition caused the distortion and deformation of the Ti thin sheet interlayer and induced the residual tensile tension at the interface of the joints. The distortion of the thin sheet increased by decreasing the Ti sheet thickness. Moreover, in the case of joints by using the 200 μm Ti sheet interlayer, in some parts, the Ti interlayer completely removed from the interface of the joints as a result of thinning of the interlayer at high temperature and pressure of the welding process (Fig. 6.4(c,d)). Therefore, copper was in direct contact with the 2D C/C composite which caused more defect at the interface of the joints due to high wetting angle of the copper on the C/C composite and higher difference between the CTE of the copper and C/C composite. By contrast, in the case of joining between the 2D C/C composite and copper by using Ti powder interlayer, an intimate bonding between 2D C/C composite and Ti powder interlayer was observed and the interfaces were free of any commonly-found interfacial defects such as micro voids, pores, and cracks (Fig. 6.6). From Fig. 6.4 to Fig.6.6, It can be seen that the melted Ti interlayer was infiltrated into 2D C/C composite by capillary action through the inherent pores and cracks of 2D C/C composite (14.8%) induced during fabrication process. The infiltrated structure has the appearance a nail, which resulted in increasing the contact area between 2D C/C composite and Ti interlayer. This nail effect is also greatly beneficial to obtain mechanical occlusion between Ti interlayer and C/C composite by pinning the interface of the joint and consequently increasing the joint strength [10, 11, 28, 40, 41]. The observation of the microstructure of the joints by using Ti sheet or powder interlayers revealed that the more infiltrated structure formed in the case of using Ti powder interlayer than the case of using Ti sheet interlayer especially for the Ti sheet interlayer with the thickness of the 200 μm. Moreover, it was observed that some open cracks within the 2D C/C composite were not completely filled by infiltrated Ti, in the case of using Ti sheet interlayers (Fig. 6.5(c)). Therefore, a higher pinning effect is expected for the joints by using the Ti powder interlayer.

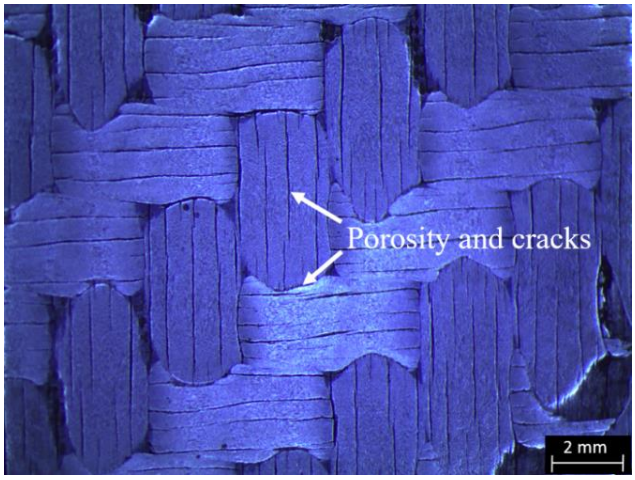

Figure 6.3. The surface of the 2D C/C composite.

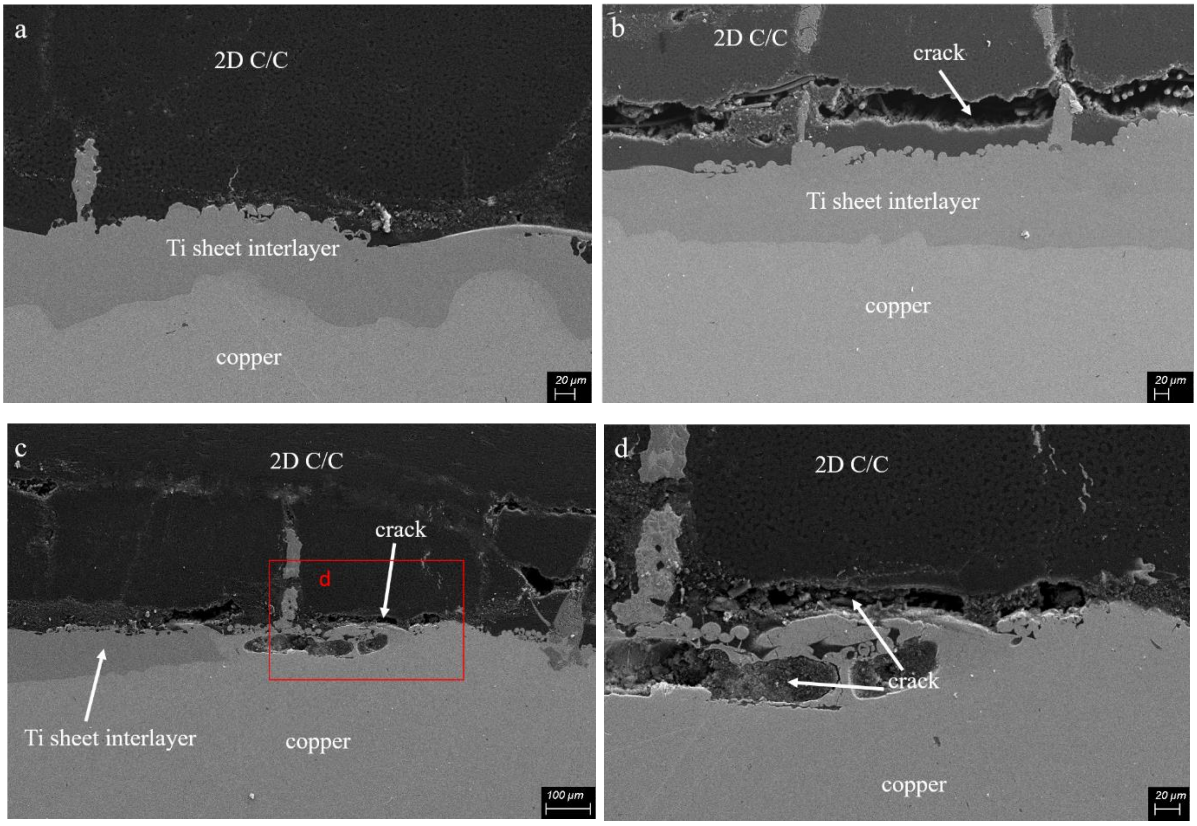

Figure 6.4. The microstructure of the 2D C/C composite-copper joint with 200 μm Ti sheet interlayer at current of 7 kA.

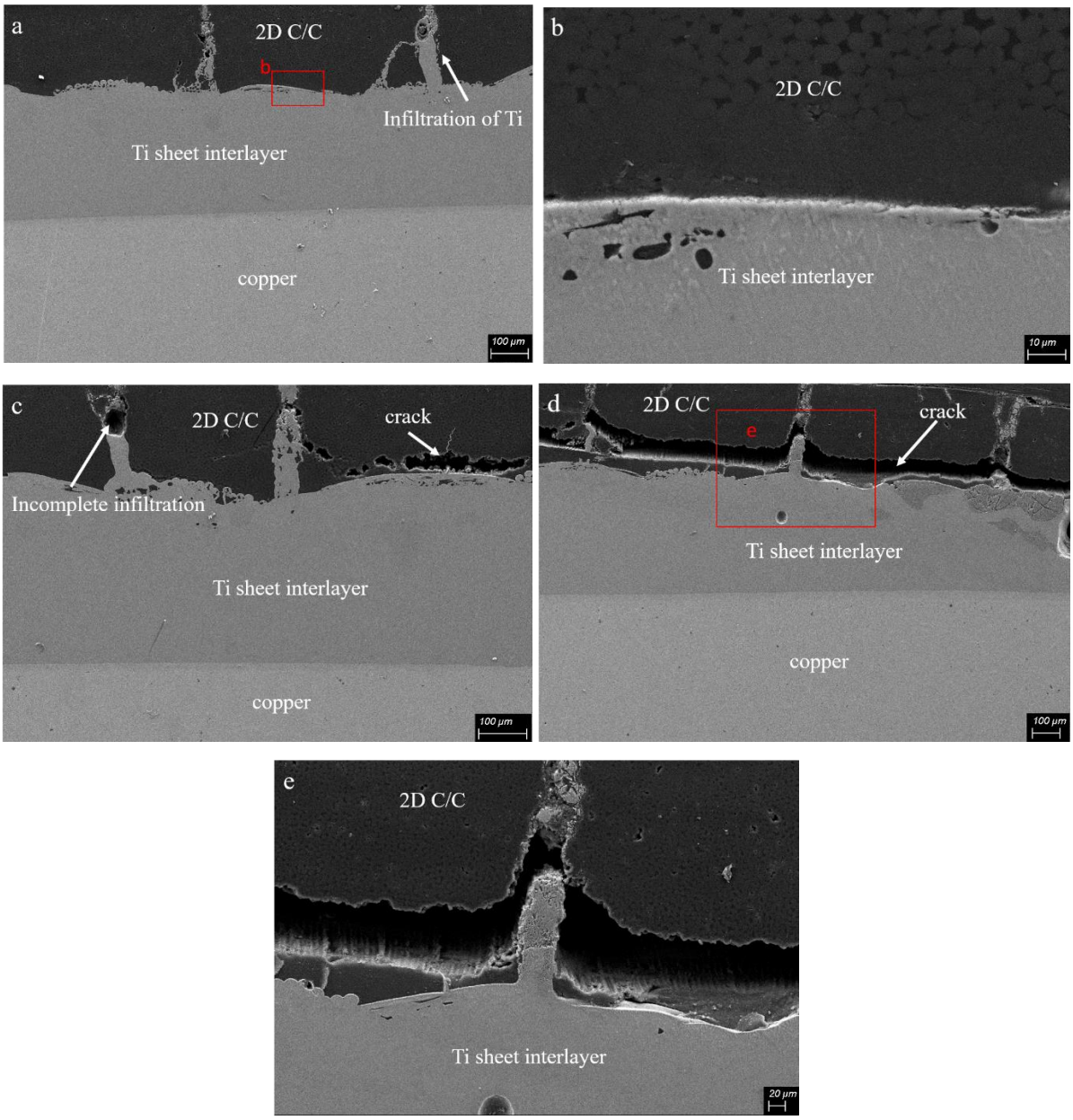

Figure 6.5. The microstructure of the 2D C/C composite-copper joint with 400 μm Ti sheet as interlayer at current of 7 kA.

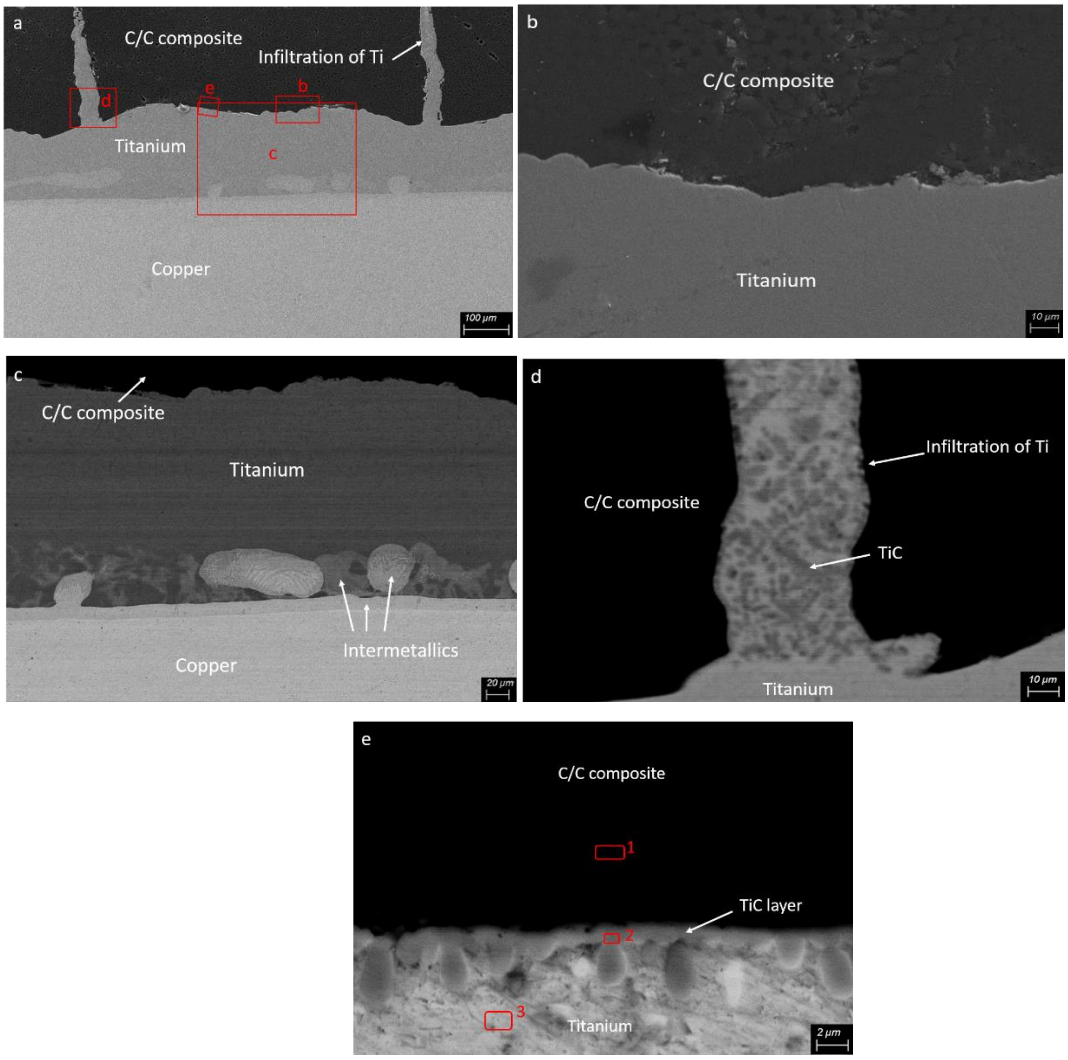

Figure 6.6. SEM image of the cross section of 2D C/C composite-copper joints with Ti Powder interlayer at current of 7 kA (a) the panorama of the joint interface and (b) interface between Ti interlayer and 2D C/C composite, (c), (d) and (e) are the BSE images of the Cu-Ti interface, infiltrated Ti, and Ti-2D C/C composite interface respectively.

The SEM-BSE image of the interface between Ti powder interlayer and 2D C/C composite and the infiltrated Ti into the 2D C/C composite are provided in Fig. 6.6(d,e). As can be seen, a thin dark grey layer with the thickness of 1 to 2 µm was formed at the interface between Ti interlayer and 2D C/C composite. Moreover, dark gray particles are embedded in the light gray Ti matrix in the infiltrated structure (Fig. 6.6 (d)). The formation of this phase can be described by the reaction between the carbon of the 2D C/C composite and Ti interlayer [20, 34, 35, 79]. In previous literature, the formation of the

thin TiC layer as a result of the reaction between the Ti interlayer and C/C composite, in the case of similar joining of C/C composite by using the Ti powder or foil interlayer has been reported [2, 31, 32, 55]. The EDS analysis of Fig 6.6 (e) is presented in Table 6.2. According to the EDS results, the thin layer is rich in Ti and C, which signals the formation of a thin TiC layer. The formation of the TiC at the interface between Ti and C/C composite can be described by high chemical affinity between Ti and C.

The dependence of the reaction enthalpy and Gibbs free energy of formation of TiC on temperature was calculated to investigate the possibility of formation of TiC. The molar Gibbs free energy $G_{x,T}$ of a reactant and product x in equation (6.1) at temperature T can be calculated using Eq. (6.2):

Ti+C=TiC (6.1)

$$G_{x,T} = H_{x,T} - T\,S_{x,T} \quad (6.2)$$

In Eq. (6.2), $H_{x,T}$ and $S_{x,T}$ are the molar enthalpy and the molar entropy at temperature T. $H_{x,T}$ and $S_{x,T}$ can be calculated using Eq. (6.3) and (6.4):

$$H_{x,T} = H_{x,298} + \int_{298}^{T} C_{px,T}\,dT \quad (6.3)$$

$$S_{x,T} = S_{x,298} + \int_{298}^{T} C_{px,T}\,d\ln T \quad (6.4)$$

Where $H_{x,298}$ is molar enthalpy at 298 ºK, $S_{x,298}$ is molar entropy at 298 ºK, $C_{px,T}$ is molar heat capacity at constant pressure at temperature T of a reactant and product x. Finally, the change in the Gibbs free energy and enthalpy of formation of TiC are given by:

$$\Delta H_T = H_{TiC,T} - H_{Ti,T} - H_{C,T} \quad (6.5)$$

$$\Delta G_T = G_{TiC,T} - G_{Ti,T} - G_{C,T} \quad (6.6)$$

According to the thermodynamic data [80], and calculation formula, the enthalpy and Gibbs free energy of formation of TiC were shown in Fig. 6.7. Clearly, this reaction is exothermic and the enthalpy and standard Gibbs free energy of the reaction are negative, indicating the formation of TiC at the interface between Ti6Al4V and the 2D C/C composite is thermodynamically favorable.

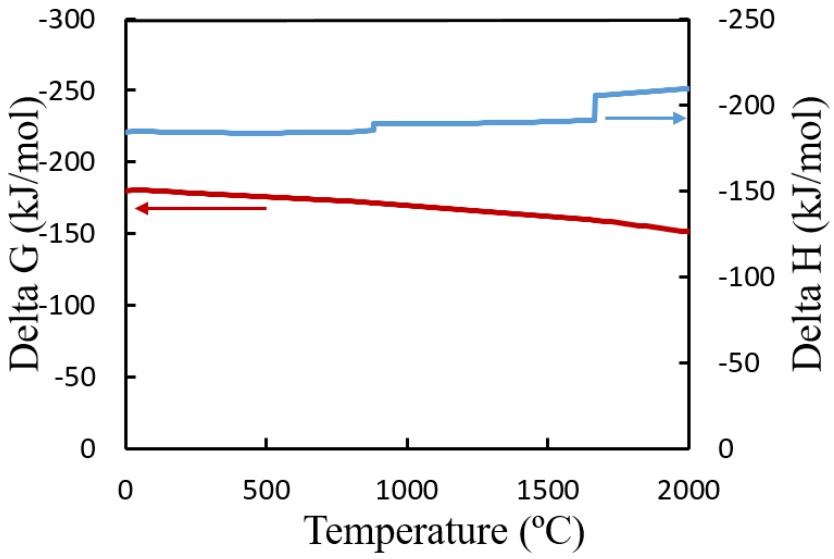

Figure 6.7. Change in the ΔG^{o} and ΔH^{o} of formation of TiC by temperature.

Table 6.2. EDS analysis of Fig. 6.6(e).

Point	1	2	3
Ti (at %)	0.38	54.11	91.23
C (at %)	99.62	45.89	8.77

The GIXRD results at the interface between the 2D C/C composite and Ti interlayer are provided in Fig. 6.8. The results indicate the Ti, Carbon, and TiC were detected in the GIXRD spectrum, which is in good accordance with the EDS analysis and thermodynamic expectation of formation of TiC phase.

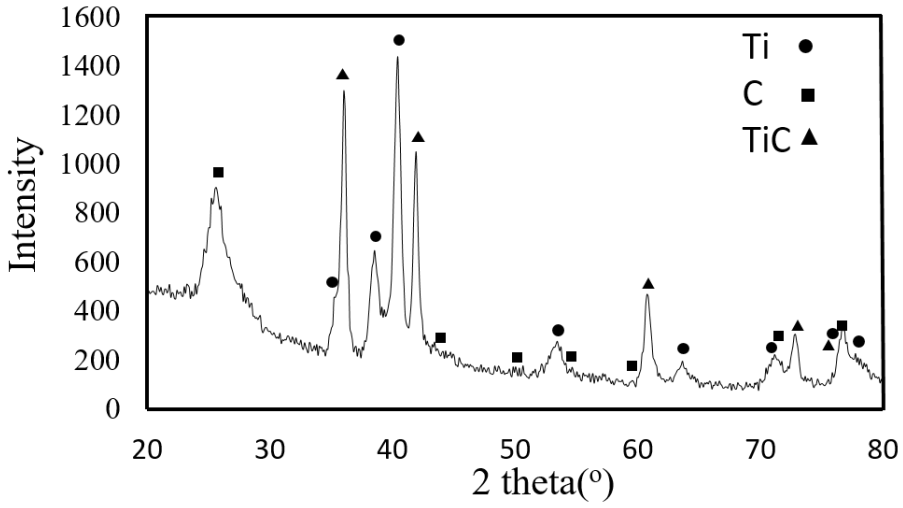

Figure 6.8. GIXRD at the interface of 2D C/C composite-Ti interlayer.

Considering the observed microstructure, GIXRD and EDS results, and thermodynamic considerations, two mechanisms can be considered as dominant mechanisms for joining at the interface between the Ti interlayer and 2D C/C composite. First, TiC phase was formed at the interface between Ti interlayer and 2D C/C composite due to solid-liquid reaction between Ti and the 2D C/C composite. Second, the melted metal was infiltrated into the porosities of the 2D C/C composite and pinned the interface of the joints. These two mechanisms contributed to both metallurgical and mechanical bonding. The Ti interlayer was melted as a result of the Joule heating caused by resistance welding, but the 2D C/C composite was not melted due to its high melting point. As a result, the formation of the TiC at the interface of the joint can be ascribed to the solid-liquid reaction between the solid carbon and Ti interlayer. Previous investigations proved that in the cases that the braze interlayers contained titanium, TiC phase was formed at the interface of the joints. They have shown that formation of the carbide layer at the interface of the joint decreases the interfacial tension and consequently improves the wettability of the molten braze materials on the C/C composite [33-38].

Regarding the interface between Ti and copper, for both joints using Ti sheet and powder interlayers, the interfaces between Ti and copper were intimate and no cracks and discontinuity were observed. The formation of defect-free joints at the interfaces between Cu and Ti interlayer can be attributed to the generation of adequate current density for melting this interface, as well as formation of the intermetallic phases between Ti and Cu. Fig 6.6 (c) and Fig. 6.9 show the SEM-BSE of the interface between Ti powder interlayer and copper, as well as elemental distribution map of copper and Ti. With considering the elemental map distribution of Cu and Ti, as well as observing the areas with different

contrast at the interface of Cu-Ti, formation of different intermetallic phases is expected. The binary diagram phase of Ti-Cu is provided in Fig. 6.10. From this diagram phase can be seen that the formation of a variety of intermetallics phase between Cu and Ti such as Ti2Cu, TiCu, Ti3Cu4, Ti2Cu3, TiCu2, TiCu4 is possible. EDS analysis was utilized for the selected areas in Fig. 6.9(a) to investigate the formation of intermetallic phases at the interface between Cu and Ti, and the results are provided in Table 6.3. Moreover, the interfacial phases at the interface of Cu-Ti was investigated by XRD (Fig. 6.11). According the EDS and XRD results, intermetallic phases including Ti2Cu, TiCu and TiCu2 were detected at the interface of Cu-Ti, which is in accordance with the intermetallic phases in the Ti-Cu binary diagram phase. In Fig. 6.9(a), point 3 contains 90.07% Ti and 9.93% Cu, and the point 6 contains 94.26 % Cu and 5.74% Ti. Therefore, the point 3 is solid solution of Cu in Ti and point 6 is solid solution of Ti in Cu.

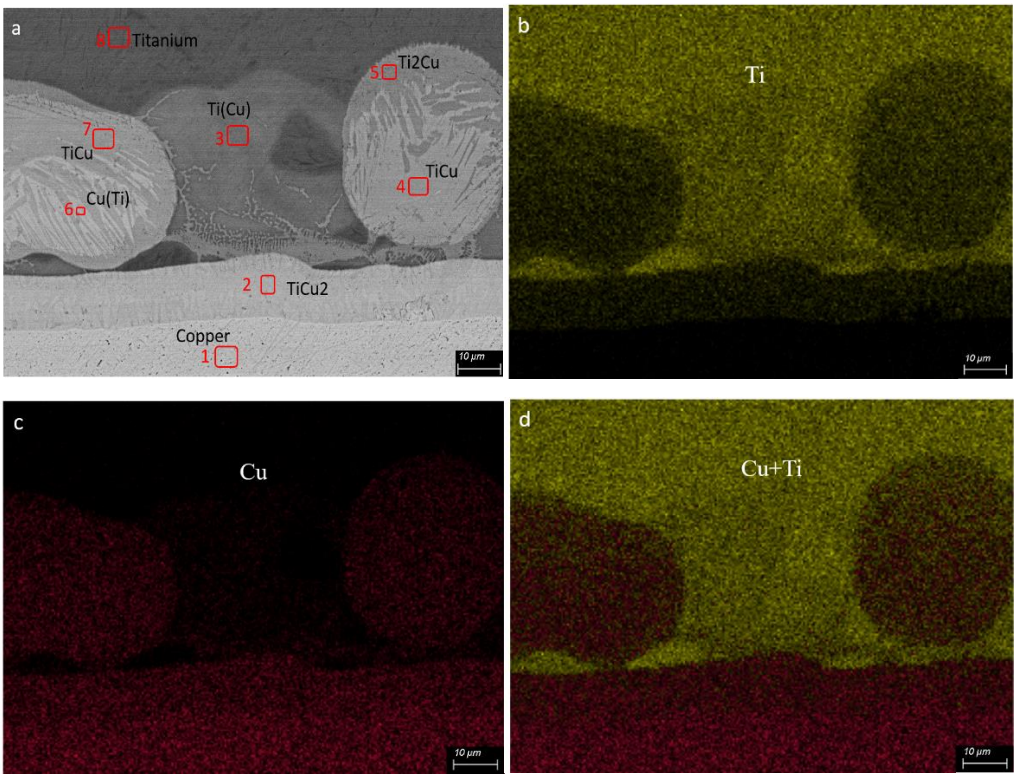

Figure 6.9. (a) interface between the Cu and Ti powder interlayer (b), (c) and (d) are the elemental map distribution of Ti, Cu and Cu+Ti respectively.

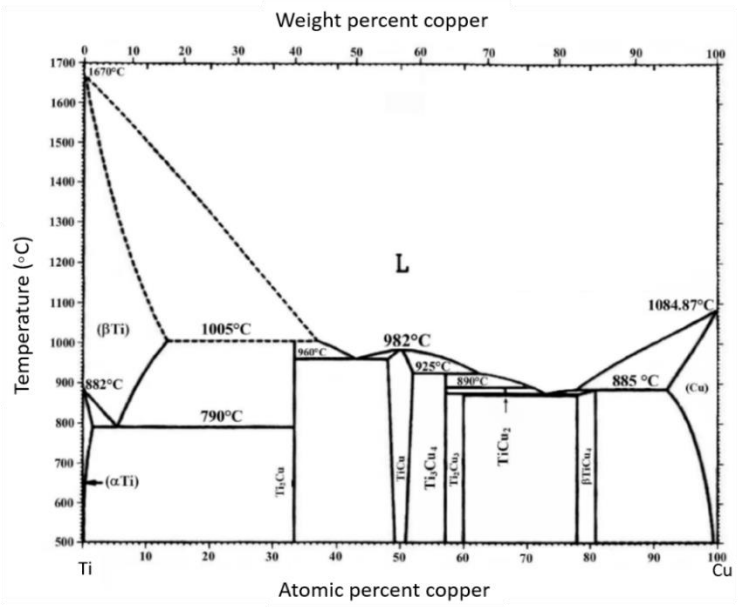

Figure 6.10. Binary diagram phase of Ti-Cu [93-97].

Table 6.3. EDS analysis of selected area in Fig. 6.9(a).

No	1	2	3	4	5	6	7	8
Composition	Cu	TiCu2	Ti(Cu)	TiCu	Ti2Cu	Cu(Ti)	TiCu	Ti
Ti (Atom%)	0	31.25	90.07	48.91	69.52	94.26	51.16	100
Cu (Atom%)	100	68.75	9.93	51.09	30.48	5.74	48.84	0

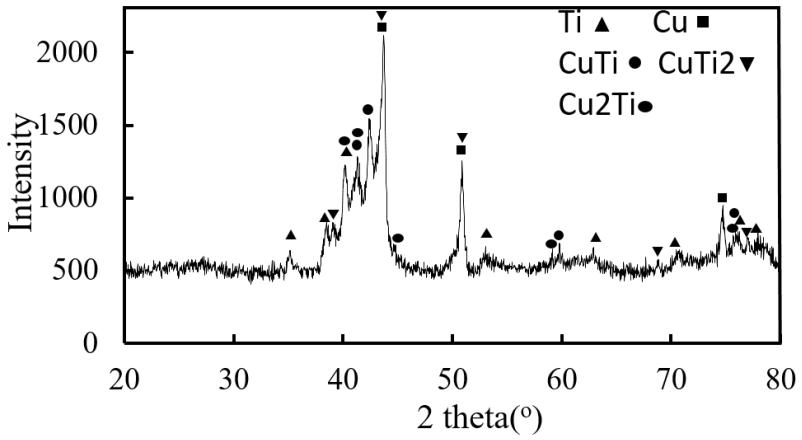

Figure 6.11. XRD at the interface between copper and Ti interlayer.

6.3.3 Mechanical properties of the joints

The shear strength, shear force and joining area of the joints with different Ti interlayers and welding currents are provided in Fig. 6.12. As can be seen, the shear strength and shear force of the joints with Ti powder interlayer are significantly higher than the shear strength of the joints by using the Ti thin sheet interlayer (Fig. 6.12(a,b)). The higher shear strength for the case of using Ti powder interlayer can be described by considering the microstructure of the interface of the joints and fracture surfaces. As can be seen in Fig. 6.4 and Fig. 6.5, a significant amount of cracks and defects were formed at the interface between the Ti sheet interlayer and 2D C/C composite. These cracks were formed as a result of distortion and deformation of the Ti sheet interlayer at high temperature and pressure. These cracks caused a decrease in the strength of the joints, whereas a defect-free interface between the 2D C/C composite and Ti interlayer was obtained for the joints with Ti powder interlayer. Fig. 6.13 shows typical fracture surfaces of the joints by using the Ti powder and thin sheet interlayer. As can be seen for all the joints, the fracture happened within the 2D C/C composite and fractured 2D C/C composite parts remained on the copper side, which reveals crack propagation occurred within the 2D C/C composite. Comparing the fracture surface of the joints reveals that in the case of using the Ti interlayer thin sheet, the fracture occurred within the 2D C/C composite and at near the interface of the joint (Fig. 6.13(a)). This observation is consistent with formed crack near the interface of the joints (Fig. 6.4 and Fig. 6.5). Therefore, after applying the load the cracks were propagated near the interface of the joints and caused deterioration of the joints (Fig. 6.13(a)). By contrast, in the case of using the Ti powder interlayer, the fracture occurred by the delamination of the 2D C/C composite (Fig. 6.13(b)). The shear strength of the joints for Ti powder interlayer is 8.73 MPa which is comparable to the interlaminar shear strength of the 2D C/C composite which is 8MPa. As can be seen in Fig. 6.6, in the case of the joints by using the Ti powder interlayer, the interface between the Ti powder interlayer and 2D C/C composite is intact and defect-free. Therefore, unlike the case of using the Ti sheet interlayer, there are no cracks near the interface and within the 2D C/C composite to cause fracture near the interface of the joints and fracture occurred by delamination of the 2D C/C composite (Fig. 6.13 (b)). As a result, it can be inferred that the strength of the 2D C/C composite- copper joints with Ti powder interlayer is higher than the interlaminar shear strength of the 2D C/C composite. Therefore, the shear strength of the joints produced using the Ti powder interlayer is not determined by the strength of the interfaces of joints, but by the 2D C/C composite. As a result, the effective shear strength of the joints cannot exceed the maximum interlaminar shear strength of the 2D C/C composite. In many literature, the failure of the joints within the C/C composite has been widely reported [2, 26, 28, 31, 34, 36, 68, 70, 83]. Moreover,

the shear fracture force of the joints using the Ti powder interlayer is significantly higher than the joints by using the Ti sheet interlayer (6.12(b)). As mentioned, the interface of the joints with Ti powder interlayer is defect-free and can withstand higher fracture force. Furthermore, as can be seen in Fig. 6.12(c) the joining area in the case of using the Ti powder interlayer is higher than the Ti sheet interlayer, which leads to withstanding higher fracture shear force.

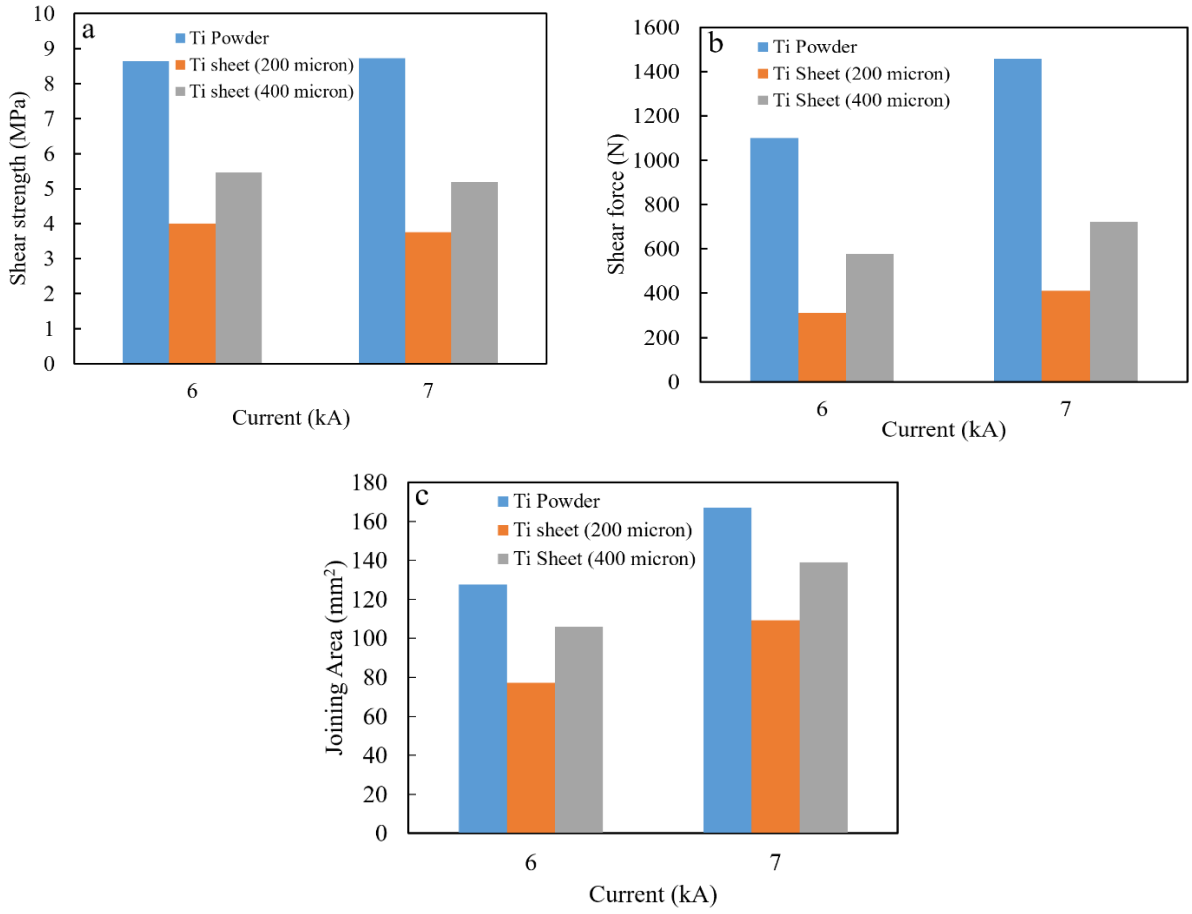

Figure 6.12. (a) Shear strength, (b) shear force and (c) joining area of 2D C/C composite-Cu joints with different interlayers at different currents.

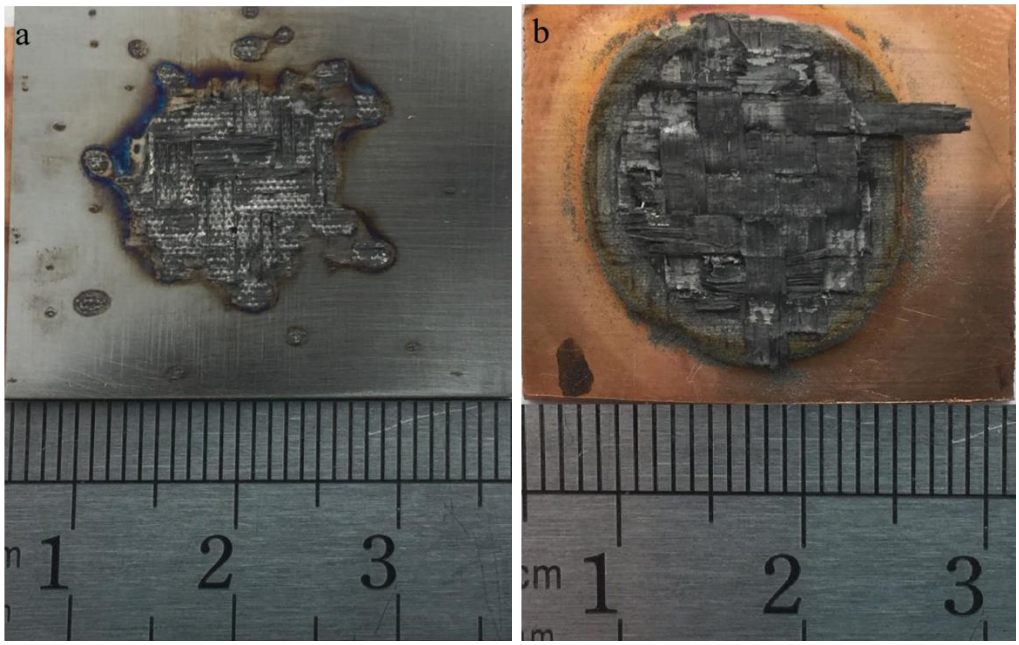

Figure 6.13. Typical fracture surface of the 2D C/C Composite-copper joints with (a) Ti sheet interlayer and (b) Ti powder interlayer.

6.4 Summary

This chapter introduced an innovative and user-friendly approach for dissimilar joining of the 2D C/C composite to copper by using the Ti sheet or powder interlayer and the following conclusions can be drawn:

1. In the case of the joints by using the Ti sheet interlayer, some cracks were formed at or near the interfaces, as a result of distortion and deformation of the Ti thin sheet at high temperature and pressure, whereas defect-free joints were obtained for the joint using the Ti powder interlayer.
2. The infiltration of the melted metal into the porosity of 2D C/C and solid-liquid reaction between the melted Ti and 2D C/C composite can be considered as the dominant mechanisms of joining at the interface between the Ti interlayer and 2D C/C composite. The Ti interlayer was melted by the heat produced by Joule heating during welding process and reacted with the carbon of 2D C/C composite to form a TiC thin layer at the interface of the 2D C/C composite and Ti interlayer. The 1 to 2 μm thin TiC layer improved the mechanical strength of the joints as a result of the formation of a chemical bonding between Ti interlayer and 2D C/C composite. Furthermore, the infiltrated Ti into the porosity of 2D C/C composite pinned the interface of

the joints, which was beneficial to the strength of the joints. Regarding the interface between the Cu and Ti interlayer, the bonding was obtained as a result of the formation of some intermetallic phases including TiCu2, TiCu and Ti2Cu.

3. In all shear tests, the fracture occurred within the 2D C/C composite. In the cases of using Ti sheet as interlayer, the strength of the joints was low because of the formation of cracks at or near the interface of the joints, whereas in the case of using Ti powder interlayer, the strength of the joints was 8.73 MPa, which is comparable to the interlaminar shear strength of the 2D C/C composite (8MPa). In the case of joining by using the Ti powder interlayer, the fracture occurred by delamination of the 2D C/C composite, which indicating that the joining between the 2D C/C and copper was mechanically stronger than the 2D C/C composite.

Chapter 7
Conclusion and future work

7.1 Conclusions

In this study, the feasibility of direct dissimilar joining of the C/C composites to Ti6Al4V and copper by reactive resistance spot welding technique, as an innovative joining technique, were investigated and the following conclusions were drawn:

Roles of porosity content and infiltrated structure

- It was found that the infiltrated structure plays a key role in the joining of the C/C composites to Ti6Al4V and copper. In the cases of using the 2D C/C composite with flat surface, well-bonded Ti6Al4V-2D C/C composite and copper-2D C/C composite joints were obtained as a result of the infiltration of the melted Ti into the porosity of the 2D C/C composite. On the other hand, regarding the joining of the flat surface 3D C/C composite to Ti6Al4V, the quality and strength of the joints were low as a result of the formation of cracks at the interface of the joints. Unlike the 2D C/C composite, the porosity content of the 3D C/C composite is low. Therefore, the melted Ti cannot be infiltrated into the 3D C/C composite, pin the interface of the joints and consequently contribute to the strength of the joints.
- In the case of joining between the 3D C/C composite and Ti6Al4V, it was necessary to manufacture rectangular grooves on the surface of the 3D C/C composite to facilitate the infiltration of the melted Ti into the 3D C/C composite and consequently obtain the desired strength. Using the interfacial groove-patterned structure caused decreasing the residual stresses at the interface of the joints, enlarging the joining area and strengthening of the joints by strong pinning effect.

Mechanisms of joining

C/C composite-Ti interface

- The solid-liquid reaction and infiltration of the melted metal into the porosity or fabricated grooves of the C/C composite can be considered as the dominant mechanisms of joining. Ti was melted as a result of Joule heat produced during resistance welding. The melted metal reacted with the carbon of the C/C composite to form a thin TiC layer with a thickness of 1 to 2 μm at the interface of the joint. This thin TiC layer improved the mechanical properties of the joint due to the formation of chemical bonding at the interface of the joints. Moreover, the

infiltration of the melted Ti into the porosity or grooves of the C/C composites increased the joining area and tightly pinned the C/C–Ti interface.

Cu-Ti interface

- In the case of the copper-2D C/C composite joints, the bonding at the interface between the Cu-Ti interlayer was obtained as a result of the formation of some intermetallic phases including TiCu2, TiCu and Ti2Cu.

Mechanical properties

- In the case of the 2D C/C composite-Ti6Al4V joints, the maximum strength of the joints was 7 MPa. In all shear tests, the failure occurred within the 2D C/C composite and not within the joints, demonstrating that the interfacial bonding between the 2D C/C and Ti6Al4V is mechanically stronger than the 2D C/C composite. Therefore, the effective shear strength of the joints cannot exceed the strength of the 2D C/C composite. By contrast, in the case of the joints by using the groove-patterned 3D C/C composite, a higher shear strength was obtained because of the higher mechanical properties of the 3D C/C composite. In the case of joining with the groove-patterned 3D C/C composite, by increasing the grooves depth from 1 to 3 mm and grooves width from 0.7 to 1 mm, the strength of the joint increased from 19.15 ± 4.81 to 46.14 ± 3.92 MPa.
- In the case of the copper-2D C/C composite joints, the strength of the joints by using Ti sheet as interlayer was low as a result of the formation of cracks at or near the interface of the joints. The origin of these cracks was deformation and distortion of the thin sheet Ti interlayer during joining process. By contrast, the strength of the joints in the case of using the Ti powder as interlayer, was 8.73 MPa, which is comparable with the interlaminar shear strength of the 2D C/C composite (8MPa). In the case of joining by using the Ti powder interlayer, the fracture occurred by the delamination of the 2D C/C composite which indicating that the joining between 2D C/C and copper was mechanically stronger than the 2D C/C composite.

7.2 Future work

In this study, for the first time, the feasibility of joining 2D and 3D C/C composite to Ti6Al4V as well as joining of 2D C/C composite to copper were studied. With considering the novelty of using reactive resistance spot welding for joining of the C/C composites, more research is required to

establish this technique as a promising technique for joining of C/C composites. Therefore, the following suggestions can be considered:

1) **Dissimilar joining of the groove-patterned 3D C/C composite to copper by reactive resistance spot welding.**

   As presented in chapter 6, the copper was successfully joined to 2D C/C composite as well as in chapter 5, the feasibility of joining 3D C/C composite to Ti6Al4V was proved. Therefore, in order to obtain high strength C/C composite-copper joints, the studying of joining of the 3D C/C composite to copper is suggested.

2) **Dissimilar joining of the groove-patterned chopped fiber C/C composite to Ti6Al4V and copper by reactive resistance spot welding**

   The chopped fiber C/C composite has lower price than 3D C/C composite and its strength is comparable to the 3D C/C composite. The porosity content of chopped fiber is low which leads to absence of the infiltration of the melted Ti into the chopped fiber C/C composite. Therefore, making a groove-pattern structure on the chopped fiber C/C composite can facilitate the infiltration of the Ti into the grooves and pin the interface of the joints.

3) **Measuring the strength of the joints at high temperature**

   With considering that in this research no interlayer (braze materials) with low melting point was used. It is expected, these joints have considerable strength at high temperature comparing to the conventional joints, which normally used brazed materials containing low melting temperature elements like Ag and copper. Therefore, the high temperature shear properties of the studied joints can be compared to the conventional braze joints.

References

[1] X.B. Zhou, H. Yang, F.Y. Chen, Y.H. Han, J. Lee, S.Y. Du, Q. Huang, Joining of carbon fiber reinforced carbon composites with Ti3SiC2 tape film by electric field assisted sintering technique, Carbon 102 (2016) 106-115.
[2] J.D.E. White, A.H. Simpson, A.S. Shteinberg, A.S. Mukasyana, Combustion joining of refractory materials: Carbon-carbon composites, J. Mater. Res. 23(1) (2008) 160-169.
[3] M.C. Wang, X.X. Hu, X.Q. Xu, Z.Q. Yun, J.C. Liu, H.Y. Du, A.R. Guo, A user-friendly heat-resistant modified polymer-based adhesive for joining and repair of carbon/carbon composites, Mater. Des. 86 (2015) 709-713.
[4] Y. Zeng, X. Xiong, G.D. Li, Z.K. Chen, W. Sun, D.N. Wang, Microstructure and ablation behavior of carbon/carbon composites infiltrated with Zr-Ti, Carbon 54 (2013) 300-309.
[5] E. Casal, M. Granda, J. Bermejo, J. Bonhomme, R. Menéndez, Influence of porosity on the apparent interlaminar shear strength of pitch-based unidirectional C–C composites, Carbon 39(1) (2001) 73-82.
[6] S. Li, X. Chen, Z. Chen, The effect of high temperature heat-treatment on the strength of C/C to C/C–SiC joints, Carbon 48(11) (2010) 3042-3049.
[7] T.S. Lin, M.X. Yang, P. He, C. Huang, F. Pan, Y.D. Huang, Effect of in situ synthesized TiB whisker on microstructure and mechanical properties of carbon-carbon composite and TiBw/Ti-6Al-4V composite joint, Mater. Des. 32(8-9) (2011) 4553-4558.
[8] J. Cao, H.Q. Wang, J.L. Qi, X.C. Lin, J.C. Feng, Combustion synthesis of TiAl intermetallics and their simultaneous joining to carbon/carbon composites, Scripta Mater. 65(3) (2011) 261-264.
[9] M.C. Wang, J.C. Liu, H.Y. Du, F. Hou, A.R. Guo, S. Liu, X. Dong, Joining of C/C composites by using B4C reinforced phosphate adhesive, Ceram. Int. 40(8) (2014) 11581-11591.
[10] J. Wang, K.Z. Li, X.R. Song, L.J. Guo, W. Li, Z.Q. Li, The study on joining carbon/carbon composites using Ti-Ni-Si compound, Materials Science and Engineering a-Structural Materials Properties Microstructure and Processing 547 (2012) 12-18.
[11] H.Q. Wang, J. Cao, J.C. Feng, Brazing mechanism and infiltration strengthening of CC composites to TiAl alloys joint, Scripta Mater. 63(8) (2010) 859-862.
[12] J. Lu, Q. He, Y. Wang, H. Li, Q. Fu, Preparation of co-deposited C/C-ZrC composites by CLVD process and its properties, J. Alloys Compd. 686 (2016) 823-830.
[13] F. Lamouroux, X. Bourrat, R. Naslain, J. Thebault, Silicon carbide infiltration of porous C□ C composites for improving oxidation resistance, Carbon 33(4) (1995) 525-535.
[14] J. Zhang, T.P. Wang, C.F. Liu, Y.M. He, Effect of brazing temperature on microstructure and mechanical properties of graphite/copper joints, Mater. Sci. Eng. A 594 (2014) 26-31.
[15] R. Fedele, A. Ciani, L. Galantucci, V. Casalegno, A. Ventrella, M. Ferraris, Characterization of innovative CFC/Cu joints by full-field measurements and finite elements, Mater. Sci. Eng. A 595 (2014) 306-317.
[16] R. Mitteau, P. Chappuis, L. Moncel, J. Schlosser, Evidence of damage in carbon fibre composite tiles joined to a metallic heat sink under high heat flux fatigue, J. Nucl. Mater. 258 (1998) 972-977.
[17] W. Guo, L. Wang, Y. Zhu, P.K. Chu, Microstructure and mechanical properties of C/C composite/TC4 joint with inactive AgCu filler metal, Ceram. Int. 41(5) (2015) 7021-7027.
[18] J. Cao, C. Li, J.L. Qi, Y.L. Shi, J.C. Feng, Combustion joining of carbon-carbon composites to TiAl intermetallics using a Ti-Al-C powder composite interlayer, Compos. Sci. Technol. 115 (2015) 72-79.
[19] Y.H. Zhou, D. Liu, H.W. Niu, X.G. Song, X.D. Yang, J.C. Feng, Vacuum brazing of C/C composite to TC4 alloy using nano-Al2O3 strengthened AgCuTi composite filler, Mater. Des. 93 (2016) 347-356.

[20] X.R. Song, H.J. Li, V. Casalegno, M. Salvo, M. Ferraris, X.R. Zeng, Microstructure and mechanical properties of C/C composite/Ti6Al4V joints with a Cu/TiCuZrNi composite brazing alloy, Ceram. Int. 42(5) (2016) 6347-6354.
[21] Y.Q. Qin, Z.S. Yu, Joining of C/C composite to TC4 using SiC particle-reinforced brazing alloy, Mater. Charact. 61(6) (2010) 635-639.
[22] V. Casalegno, M. Salvo, M. Ferraris, Surface modification of carbon/carbon composites to improve their wettability by copper, Carbon 50(6) (2012) 2296-2306.
[23] J.H.C. X.G. Song, S.P. Hu, J. Cao, J.C. Feng, D.Y. Tang, A novel metallization process for soldering graphite to copper at low temperature, Jurnal of Alloys and Compounds.
[24] Y.Q. Qin, J.C. Feng, Active brazing carbon/carbon composite to TC4 with Cu and Mo composite interlayers, Mater. Sci. Eng. A 525(1-2) (2009) 181-185.
[25] J. Schlosser, E. Martin, C. Henninger, J. Boscary, G. Camus, F. Escourbiac, D. Leguillon, M. Missirlian, R. Mitteau, CFC/Cu bond damage in actively cooled plasma facing components, Phys. Scr. 2007(T128) (2007) 204.
[26] J.S. Zhang, R.Y. Luo, C.L. Yang, A multi-wall carbon nanotube-reinforced high-temperature resistant adhesive for bonding carbon/carbon composites, Carbon 50(13) (2012) 4922-4925.
[27] J.T. Xiong, J.L. Li, F.S. Zhan, X. Lin, W.D. Huang, Direct joining of 2D carbon/carbon composites to Ti-6Al-4V alloy with a rectangular wave interface, Mater. Sci. Eng. A 488(1-2) (2008) 205-213.
[28] K.X. Zhang, L.H. Xia, F.Q. Zhang, L.L. He, Active Brazing of C/C Composite to Copper by AgCuTi Filler Metal, Metall. Mater. Trans. A 47A(5) (2016) 2162-2176.
[29] W. Guo, T. Gao, X. Cui, Y. Zhu, P.K. Chu, Interfacial reactions and zigzag groove strengthening of C/C composite and Rene N5 single crystal brazed joint, Ceram. Int. 41(9) (2015) 11605-11610.
[30] Y. Shen, Z. Li, C. Hao, J. Zhang, A novel approach to brazing C/C composite to Ni-based superalloy using alumina interlayer, J. Eur. Ceram. Soc. 32(8) (2012) 1769-1774.
[31] Y.-C. Lin, A.A. Nepapushev, P.J. McGinn, A.S. Rogachev, A.S. Mukasyan, Combustion joinining of carbon/carbon composites by a reactive mixture of titanium and mechanically activated nickel/aluminum powders, Ceramics International 39(7) (2013) 7499-7505.
[32] A.S. Mukasyan, J.D.E. White, Combustion joining of refractory materials, International Journal of Self-Propagating High-Temperature Synthesis 16(3) (2007) 154-168.
[33] Y. Qin, J. Feng, Microstructure and mechanical properties of C/C composite/TC4 joint using AgCuTi filler metal, Materials Science and Engineering: A 454 (2007) 322-327.
[34] M. Salvo, V. Casalegno, Y. Vitupier, L. Cornillon, L. Pambaguian, M. Ferraris, Study of joining of carbon/carbon composites for ultra stable structures, J. Eur. Ceram. Soc. 30(7) (2010) 1751-1759.
[35] D. Liu, Y. Zhou, X. Song, W. Huo, J. Feng, Interfacial microstructure and performance of nano-diamond film/Ti-6Al-4V joint brazed with AgCuTi alloy, Diamond and Related Materials 68 (2016) 42-50.
[36] M. Singh, T.P. Shpargel, G.N. Morscher, R. Asthana, Active metal brazing and characterization of brazed joints in titanium to carbon–carbon composites, Materials Science and Engineering: A 412(1-2) (2005) 123-128.
[37] M. Singh, R. Asthana, Characterization of brazed joints of CC composite to Cu-clad-Molybdenum, Composites Science and Technology 68(14) (2008) 3010-3019.
[38] P. Appendino, M. Ferraris, V. Casalegno, M. Salvo, M. Merola, M. Grattarola, Direct joining of CFC to copper, J. Nucl. Mater. 329 (2004) 1563-1566.
[39] F.T. Lan, K.Z. Li, H.J. Li, L.J. Guo, Y.G. He, L.L. Zhang, High-temperature property of carbon/carbon composite joints bonded with ternary Ti-Si-C compound, J. Alloys Compd. 480(2) (2009) 747-749.
[40] J.T. Xiong, J.L. Li, F.S. Zhang, W.D. Huang, Joining of 3D C/SiC composites to niobium alloy, Scripta Mater. 55(2) (2006) 151-154.

[41] X.R. Song, H.J. Li, X.R. Zeng, Brazing of C/C composites to Ti6Al4V using multiwall carbon nanotubes reinforced TiCuZrNi brazing alloy, J. Alloys Compd. 664 (2016) 175-180.
[42] J. Li, J.-F. Yang, J.-L. Chen, High heat load properties of actively cooled W/CuCrZr mock-ups by cladding and diffusion bonding with a two-step process, J. Nucl. Mater. 418(1) (2011) 110-114.
[43] D. Jiang, J. Long, M. Cai, Y. Lin, P. Fan, H. Zhang, M. Zhong, Femtosecond laser fabricated micro/nano interface structures toward enhanced bonding strength and heat transfer capability of W/Cu joining, Mater. Des. 114 (2017) 185-193.
[44] Y. Zhang, G. Zou, L. Liu, A. Wu, Z. Sun, Y. Zhou, Vacuum brazing of alumina to stainless steel using femtosecond laser patterned periodic surface structure, Materials Science and Engineering: A 662 (2016) 178-184.
[45] A. Mukasyan, J.D. White, Combustion joining of refractory materials, Int. J. Self-Propag. High-Temp Synth. 16(3) (2007) 154-168.
[46] Y.-C. Lin, P.J. McGinn, A.S. Mukasyan, High temperature rapid reactive joining of dissimilar materials: Silicon carbide to an aluminum alloy, J. Eur. Ceram. Soc. 32(14) (2012) 3809-3818.
[47] Z. Li, G. Feng, S. Wang, S. Feng, High-efficiency Joining of C f/Al Composites and TiAl Alloys under the Heat Effect of Laser-ignited Self-propagating High-temperature Synthesis, Journal of Materials Science & Technology 32(11) (2016) 1111-1116.
[48] B.H. Rabin, Joining of Silicon Carbide/Silicon Carbide Composites and Dense Silicon Carbide Using Combustion Reactions in the Titanium–Carbon–Nickel System, J. Am. Ceram. Soc. 75(1) (1992) 131-135.
[49] J. Feng, J. Cao, Z. Li, Microstructure evolution and reaction mechanism during reactive joining of TiAl intermetallic to TiC cermet using Ti–Al–C–Ni interlayer, J. Alloys Compd. 436(1) (2007) 298-302.
[50] R. Rosa, P. Veronesi, S. Han, V. Casalegno, M. Salvo, E. Colombini, C. Leonelli, M. Ferraris, Microwave assisted combustion synthesis in the system Ti–Si–C for the joining of SiC: Experimental and numerical simulation results, J. Eur. Ceram. Soc. 33(10) (2013) 1707-1719.
[51] R. Rosa, E. Colombini, P. Veronesi, G. Poli, C. Leonelli, Microwave ignited combustion synthesis as a joining technique for dissimilar materials, J. Mater. Eng. Perform. 21(5) (2012) 725-732.
[52] J. Cao, C. Li, J. Qi, Y. Shi, J. Feng, Combustion joining of carbon–carbon composites to TiAl intermetallics using a Ti–Al–C powder composite interlayer, Compos. Sci. Technol. 115 (2015) 72-79.
[53] A.A. Shokati, N. Parvin, N. Sabzianpour, M. Shokati, A. Hemmati, In situ synthesis of NiAl–NbB 2 composite powder through combustion synthesis, J. Alloys Compd. 549 (2013) 141-146.
[54] A.A. Shokati, N. Parvin, M. Shokati, Combustion synthesis of NiAl matrix composite powder reinforced by TiB 2 and TiN particulates from Ni–Al–Ti–BN reaction system, J. Alloys Compd. 585 (2014) 637-643.
[55] J.D.E. White, A.S. Mukasyan, M.L. La Forest, A.H. Simpson, Novel apparatus for joining of carbon-carbon composites, Rev. Sci. Instrum. 78(1) (2007).
[56] G.-j. Feng, Z.-r. Li, S.-c. Feng, Z.-k. Shen, Effect of Ti–Al content on microstructure and mechanical properties of Cf/Al and TiAl joint by laser ignited self-propagating high-temperature synthesis, Transactions of Nonferrous Metals Society of China 25(5) (2015) 1468-1477.
[57] M. Petrantoni, C. Rossi, L. Salvagnac, V. Conédéra, A. Estève, C. Tenailleau, P. Alphonse, Y.J. Chabal, Multilayered Al/CuO thermite formation by reactive magnetron sputtering: Nano versus micro, J. Appl. Phys. 108(8) (2010) 084323.
[58] Timothy P. Weihs (June 12, 2015). Brazing Dissimilar Metals with a Novel Composite Foil. Retrieved from http://energy.gov/sites/prod/files/2015/06/f24/lm098_weihs_2015_o.pdf.
[59] F.L. Zhao, Q.G. Fu, L. Wang, X.Y. Nan, Improving mechanical strength of Ti-Ni-Si joints for joining carbon/carbon composites by thermal cycling treatment, Mater. Sci. Eng. A 663 (2016) 56-63.

[60] J.P. Zhang, Q.G. Fu, J.L. Qu, R.M. Yuan, H.J. Li, Blasting treatment and chemical vapor deposition of SiC nanowires to enhance the thermal shock resistance of SiC coating for carbon/carbon composites in combustion environment, J. Alloys Compd. 666 (2016) 77-83.
[61] G. Kou, L.-j. Guo, Z.-q. Li, J. Peng, J. Tian, C.-x. Huo, Microstructure and flexural properties of C/C-Cu composites strengthened with in-situ grown carbon nanotubes, J. Alloys Compd. 694 (2017) 1054-1060.
[62] L. Li, H. Li, X. Yin, Y. Chu, X. Chen, Q. Fu, Oxidation protection and behavior of in-situ zirconium diboride–silicon carbide coating for carbon/carbon composites, J. Alloys Compd. 645 (2015) 164-170.
[63] M. Ferraris, A. Ventrella, M. Salvo, M. Avalle, F. Pavia, E. Martin, Comparison of shear strength tests on AV119 epoxy-joined carbon/carbon composites, Composites Part B: Engineering 41(2) (2010) 182-191.
[64] M. Singh, G.N. Morscher, T.P. Shpargel, R. Asthana, Active metal brazing of titanium to high-conductivity carbon-based sandwich structures, Mater. Sci. Eng. A 498(1-2) (2008) 31-36.
[65] <A simple test to determine the effectiveness of different braze.pdf>.
[66] Y.X. Shen, Z.L. Li, C.Y. Hao, J.S. Zhang, Joining C/C composite to copper using active Cu-3.5Si braze, J. Nucl. Mater. 421(1-3) (2012) 28-31.
[67] M. Singh, R. Asthana, Characterization of brazed joints of C-C composite to Cu-clad-Molybdenum, Compos. Sci. Technol. 68(14) (2008) 3010-3019.
[68] G.N. Morscher, M. Singh, T. Shpargel, R. Asthana, A simple test to determine the effectiveness of different braze compositions for joining Ti-tubes to C/C composite plates, Mater. Sci. Eng. A 418(1-2) (2006) 19-24.
[69] F. Lan, K.-z. Li, H. Li, Q. Fu, X. Lin, Vitreous joining of SiC-coated carbon/carbon composites, Mater. Lett. 62(15) (2008) 2347-2350.
[70] V. Casalegno, T. Koppitz, G. Pintsuk, M. Salvo, S. Rizzo, S. Perero, M. Ferraris, Proposal for a modified non-active brazing alloy for joining CFC composites to copper, Compos. Part B-Eng. 56 (2014) 882-888.
[71] P. Appendino, M. Ferraris, V. Casalegno, M. Salvo, M. Merola, M. Grattarola, Proposal for a new technique to join CFC composites to copper, J. Nucl. Mater. 348(1) (2006) 102-107.
[72] M. Barlak, J. Piekoszewski, Z. Werner, J. Stanislawski, E. Skladnik-Sadowska, K. Borkowska, M. Miskiewicz, A. Kolitsch, R. Grötzschel, W. Starosta, Wettability improvement of carbon ceramic materials by mono and multi energy plasma pulses, Surf. Coat. Technol. 203(17) (2009) 2536-2540.
[73] V. Casalegno, M. Salvo, S. Murdaca, M. Ferraris, One-step brazing process for CFC monoblock joints and mechanical testing, J. Nucl. Mater. 393(2) (2009) 300-305.
[74] B. Schedler, T. Friedrich, H. Traxler, E. Eidenberger, C. Scheu, H. Clemens, R. Pippan, F. Escourbiac, Examination of C/C flat tile mock-ups with hypervapotron cooling after high heat flux testing, Fusion Eng. Des. 82(3) (2007) 299-305.
[75] Y. Shen, Z. Li, C. Hao, J. Zhang, Joining C/C composite to copper using active Cu–3.5 Si braze, J. Nucl. Mater. 421(1) (2012) 28-31.
[76] B. Schedler, T. Huber, T. Friedrich, E. Eidenberger, M. Kapp, C. Scheu, R. Pippan, H. Clemens, Characteristics of an optimized active metal cast joint between copper and C/C, Phys. Scr. 2007(T128) (2007) 200.
[77] J. Li, R. Luo, Y. Bi, Q. Xiang, C. Lin, Y. Zhang, N. An, The preparation and performance of short carbon fiber reinforced adhesive for bonding carbon/carbon composites, Carbon 46(14) (2008) 1957-1965.
[78] M.C. Wang, R. Miao, J.K. He, X.Q. Xu, J.C. Liu, H.Y. Du, Silicon Carbide whiskers reinforced polymer-based adhesive for joining C/C composites, Mater. Des. 99 (2016) 293-302.

[79] Y.W. Mao, S. Yu, Y.Z. Zhang, B.B. Guo, Z.B. Ma, Q.R. Deng, Microstructure analysis of graphite/Cu joints brazed with (Cu-50TiH(2)) + B composite filler, Fusion Eng. Des. 100 (2015) 152-158.
[80] M.W. Chase, Jr., NIST-JANAF Thermochemical Tables, 4th ed., J. Phys. Chem. Ref. Data, Monograph No. 9, 1998.
[81] J. Wang, K. Li, H. Li, W. Li, Z. Li, L. Guo, Partial transient liquid phase bonding of carbon/carbon composites using Ti–Ni–Al 2 O 3–Si compound as interlayer, J. Alloys Compd. 550 (2013) 57-62.
[82] Z. Wang, G. Wang, M. Li, J. Lin, Q. Ma, A. Zhang, Z. Zhong, J. Qi, J. Feng, Three-dimensional graphene-reinforced Cu foam interlayer for brazing C/C composites and Nb, Carbon 118 (2017) 723-730.
[83] F.T. Lan, K.Z. Li, H.J. Li, Y.G. He, X.T. Shen, W.F. Cao, Joining of carbon/carbon composites for nuclear applications, J. Mater. Sci. 44(14) (2009) 3747-3750.
[84] M.C. Wang, M.M. Zhuang, X. Tao, X.Q. Xu, H.T. Geng, J.C. Liu, High Temperature Bonding Effect of the Room-Temperature-Curing Phosphate Adhesive for C/C Composites, Key Eng. Mater., Trans Tech Publ, 2016, pp. 179-183.
[85] M. Wang, J. Liu, A. Guo, L. Zhao, G. Tian, S. Shen, S. Liu, Preparation and Performance of the Room-Temperature-Cured Heat-Resistant Phosphate Adhesive for C/C Composites Bonding, International Journal of Applied Ceramic Technology 12(4) (2015) 837-845.
[86] M. Wang, J. Liu, H. Du, A. Guo, X. Tao, X. Dong, H. Geng, A SiC whisker reinforced high-temperature resistant phosphate adhesive for bonding carbon/carbon composites, J. Alloys Compd. 633 (2015) 145-152.
[87] X. Shi, X. Jin, H. Lin, J. Jing, L. Li, C. Wang, Joining of SiC nanowires-toughened SiC coated C/C composites and nickel based superalloy (GH3044) using Ni71CrSi interlayer, J. Alloys Compd. 693 (2017) 837-842.
[88] L.M. Evans, L. Margetts, V. Casalegno, F. Leonard, T. Lowe, P. Lee, M. Schmidt, P. Mummery, Thermal characterisation of ceramic/metal joining techniques for fusion applications using X-ray tomography, Fusion Eng. Des. 89(6) (2014) 826-836.
[89] G. Pintsuk, V. Casalegno, M. Ferraris, T. Koppitz, M. Salvo, Thermal fatigue characterization of CFC divertor modules using a one step brazing process, J. Nucl. Mater. 426(1) (2012) 78-84.
[90] P. Appendino, V. Casalegno, M. Ferraris, M. Grattarola, M. Merola, M. Salvo, Joining of C/C composites to copper, Fusion Eng. Des. 66 (2003) 225-229.
[91] M. Salvo, V. Casalegno, S. Rizzo, F. Smeacetto, M. Ferraris, M. Merola, One-step brazing process to join CFC composites to copper and copper alloy, J. Nucl. Mater. 374(1) (2008) 69-74.
[92] M. Singh, R. Asthana, T. Shpargel, Brazing of carbon–carbon composites to Cu-clad molybdenum for thermal management applications, Materials Science and Engineering: A 452 (2007) 699-704.
[93] A. Dziadoń, M. Konieczny, M. Gajewski, M. Iwan, Z. Rzączyńska, Microstructure evolution at the Cu-Ti interface during high temperature synthesis of copper-intermetallic phases layered composite, Archives of metallurgy and materials 54(2) (2009) 455-466.
[94] M. Bateni, S. Mirdamadi, F. Ashrafizadeh, J. Szpunar, R. Drew, Formation of Ti–Cu intermetallic coatings on copper substrate, Mater. Manuf. Processes 16(2) (2001) 219-228.
[95] M. Bateni, F. Ashrafizadeh, J. Szpunar, R. Drew, Improving the tribological behavior of copper through novel Ti–Cu intermetallic coatings, Wear 253(5) (2002) 626-639.
[96] J. Murray, The Cu− Ti (Copper-Titanium) system, Journal of Phase Equilibria 4(1) (1983) 81-95.
[97] J.L. Murray, Binary Alloy Phase Diagrams, 2nd Edition, Vol. 2, ASM International, Materials Park, OH, USA, 1990, p. 1494.